**Ricardo André Baptista Pereira da Costa**

Mestre em Física

# The role of succinate dehydrogenase in the *Drosophila melanogaster* intestinal stem cells and tissue homeostasis

Dissertação para obtenção do Grau de Doutor em Bioengenharia (MIT-Portugal)

Orientador: António Coelho Jacinto, Professor Catedrático Convidado, CEDOC – FCM/UNL
Co-orientador: Manuel Nunes da Ponte, Professor Catedrático, FCT/UNL

Júri:

Presidente: Prof. Doutor José Paulo Barbosa Mota
Arguentes: Doutora Catarina de Cértima Fernandes Homem
Doutora Zita Carvalho dos Santos

Vogais: Prof. Doutor António Alfredo Coelho Jacinto
Prof. Doutor Cláudio Emanuel Moreira Gomes
Doutor Miguel Jorge Zuzarte de Mendonça Godinho Ferreira
Doutora Rita Oliveira Teodoro

FACULDADE DE CIÊNCIAS E TECNOLOGIA
UNIVERSIDADE NOVA DE LISBOA

**Setembro, 2017**

**Ricardo André Baptista Pereira da Costa**

# The role of succinate dehydrogenase in the *Drosophila melanogaster* intestinal stem cells and tissue homeostasis

Submitted to the graduate degree program in Bioengineering and the Graduate Faculty of the Nova University of Lisbon in partial fulfillment of the requirements for the degree of Doctor of Philosophy.

Orientador: Prof. António Coelho Jacinto, CEDOC/NMS-UNL
Co-orientador: Prof. Manuel Nunes da Ponte, FCT-UNL

**September, 2017**




FACULDADE DE CIÊNCIAS E TECNOLOGIA
UNIVERSIDADE NOVA DE LISBOA

**The role of succinate dehydrogenase in the *Drosophila melanogaster* intestinal stem cells and tissue homeostasis**

# Preface

In 2011, as a recent physics postgraduate with no background in biology, I wanted to engage in a biotechnological field and joined the MIT-Portugal Program in Bioengineering. During the first semester of classes, I developed a strong interest in fundamental biology and decided I wanted to work with stem cells in *Drosophila*. Later in 2012 I have decided to join the Laboratory of Dr. Leanne Jones (UCLA) and while waiting for my visa approval, I was kindly invited by a member of my thesis committee, Dr. Miguel Godinho Ferreira, to rotate in his laboratory working on a project with zebrafish to gain more experience in a biology laboratory setting.

I finally joined the Dr. Jones Lab at UCLA in April 2013, on a 2-year term, where I started a project to study micro-RNAs in adult stem cells, which after 7 months we have decided to abandon due to unforeseen events, and I then started the project described in this thesis. After the end of my stay at UCLA, in April 2015, my adviser Professor António Jacinto accepted me in his lab at CEDOC/NMS to continue my project. During that period, as my scholarship ended, I had the pleasure to tutor school students in mathematics and physics until recently. In the meanwhile, in 2016, I initiated a fruitful collaboration with the Environmental and Biological Mass Spectrometry Group at Faculdade de Ciências da Universidade de Lisboa, where I learned to use gas chromatography—mass spectrometry to quantify metabolites in my biological samples, and finalized my project.

**Declaration:**

The experiments described in this thesis were performed in the Jones Laboratory at University of California, Los Angeles; the Tissue Morphogenesis and Repair Lab at CEDOC/NMS, Universidade Nova de Lisboa; and at the Environmental and Biological Mass Spectrometry Group at the Departamento de Química e Bioquímica, DQB, of Faculdade de Ciências da Universidade de Lisboa. All the experimental work was performed by me, with the exception of 2 groups of samples in the screen presented in part 1 of the Results and Discussion chapter — the lines 106700 KK and 106095 KK — that were dissected and immuno-stained by R. Demarco at the Jones Lab, UCLA.

# Acknowledgements

I would like to express my strong gratitude to Professor Leanne Jones for accepting me in her laboratory at UCLA. Dr. Jones took many chances with me, I was a student with a limited background in biology and as we learned that I could only stay at UCLA for 2 years, Dr. Jones maintained her support and showed extraordinary commitment. I am also very grateful to have worked with the other members of the Jones laboratory, from whom I have learned so much. Particularly, I would like to express my special gratitude to Rafael Demarco for enthusiastic mentorship, support and impromptu biology lessons; and also to Pedro Resende for his support and introducing me to the lab and the city of Los Angeles. I also feel thankful to have had the opportunity to learn from the other talented members of the MCDB department, namely the scientists at the Walker Lab, who I thank for valuable scientific and technical feedback and reagents.

I am greatly indebted to Prof. António Jacinto for accepting me in his laboratory and providing me with everything I needed to complete my doctoral work. I also need to express my heart-warmed appreciation to the other past and present members of the AJ Lab for a warm welcome, kindness and valuable feedback.

I am also thankful to the GEMAB group at FCUL namely Dr. Ana Marques, for teaching me how to use the GC-MS equipment and particularly grateful to Professor Carlos Borges for his openness in accepting me in his laboratory and trusting me with the equipment.

I would also like to extend my gratitude to all the coordinators and members of the MIT-Portugal Program, namely to José Silva Lopes and Fátima Silva Lopes for being very helpful with all the administrative needs, and to all the different universities, institutes, laboratories, and companies that we have interacted with along the way. I am also very grateful to have had the company and support of my colleagues in the doctoral program, as well as peers from other programs, namely the BEB PhD programme in Coimbra.

I would like to thank the members of my thesis committee, Prof. Manel Nunes da Ponte, Dr. Rita Teodoro and Dr. Miguel Godinho Ferreira for spending their valuable time in the process, and the enthusiastic support from Miguel in giving me my first insights into the biology of aging. I would also like to acknowledge the financial support from Fundação para a Ciência e a Tecnologia.

And finally, a very special gratitude to my family and all my friends and loved ones for support and encouragement during these years, to whom I dedicate this thesis.

# Abstract

Adult stem cells maintain tissue homeostasis and act in response to challenges such as infection or mechanical damage. The fruit fly *Drosophila melanogaster* has emerged as a powerful model to study adult stem cells due to its conserved pathways and the existence of different stem cell systems, particularly a stem cell niche in the intestine. Intestinal stem cells (ISCs) have a major role in maintaining tissue homeostasis and improvements in their function result in refined tissue function in aged or damaged organs. Metabolism plays an important role in regulating stem cell activity, influencing cellular events such as differentiation and proliferation. However, several aspects remain unraveled, particularly the role of different subunits of the mitochondrial electron transport chain (ETC) — end players in the oxidative phosphorylation process.

Given the importance of metabolism in regulating stem cell activity, we hypothesized that ETC subunits also have a role in regulating ISC activity and tissue homeostasis. To test our hypothesis, we performed a candidate screen to knock down individual subunits of the ETC specifically in ISCs and their direct progeny — enteroblasts — in the adult fly and studied their requirements for normal cell division, differentiation, survival and impact in surrounding differentiated cells. Subunits of the ETC complex II, which converts succinate to fumarate in the Krebs cycle, particularly subunit D (SdhD), emerged from the screen as strong candidates required for normal ISC activity.

Knockdown of SdhD in ISCs resulted in inhibition of cell division, hypertrophy with polyploidy, and ultimately, cell death. At a tissue level, evidence of a differentiation bias towards secretory enteroendocrine cells in lieu of absorptive enterocytes was observed upon SdhD knockdown in progenitor cells. Further experiments showed that knockdown of SdhD causes succinate to accumulate, possibly due to a decrease in the function of succinate dehydrogenase activity. Succinate is a known ligand for the GPR91 receptor in mammals which is known to be involved in cellular hypertrophy and death via apoptosis. Further studies need to be performed to determine the existence of a succinate receptor in *Drosophila*.

This work has unveiled a direct relationship between inhibition of complex II subunits and stem cell hypertrophy and death, with succinate as a possible intermediate, and provides a suitable model for the study of the molecular pathways underlying cellular

hypertrophy and death in metabolic-deficiency backgrounds. These insights may contribute to the understanding of hypertrophic pathologies, or proliferative diseases, such as cancer.

**Keywords:** stem cells, intestine, metabolism, hypertrophy, cell division, cellular death, homeostasis

# Resumo

As células estaminais existem em organismos adultos onde possuem um importante papel na manutenção da homeostase e na resposta a danos no tecido. A mosca-da-fruta *Drosophila melanogaster* destaca-se como um modelo animal no estudo de células estaminais, graças aos seus diferentes mecanismos moleculares conservados entre espécies e à presença de células estaminais adultas, nomeadamente de um nicho de células estaminais no intestino. As células estaminais intestinais (ISCs, na sigla inglesa) desempenham um papel crucial na regulação da homeostase no tecido, e vários estudos demonstram que melhorias na sua função celular resultam em melhorias na capacidade dos tecidos num contexto de envelhecimento ou detioração de tecidos. O metabolismo desempenha um papel crucial na regulação do comportamento e actividade de células estaminais através de moléculas metabólicas intermediárias e produtos de reacção, que controlam como estas se diferenciam ou dividem. No entanto, ainda existem vários aspectos a serem estudados, nomeadamente o papel de diferentes subunidades dos complexos da cadeia de respiração mitocondrial (ETC, na sigla inglesa).

Dada a importância do metabolismo na regulação da actividade de células estaminais, levantámos a hipótese de que subunidades da ETC desempenham um papel na regulação do comportamento das ISCs, com um impacto na homeostase no tecido. Para testar esta hipótese, induzimos subexpressão de diferentes subunidades da ETC em células progenitoras no intestino (incluindo ISCs) por vias de interferência de RNA, e avaliámos os efeitos no comportamento de células progenitoras e o consequente papel no tecido intestinal. Subunidades do complexo II, nomeadamente a succinato dehidrogenase, subunidade D (SdhD) destacou-se entre as várias, por ser requerida em ISCs.

Subexpressão de SdhD inibe a replicação de células estaminais, induz poliploidia, hipertrofia e por fim, morte celular. A nível de impacto no tecido intestinal, as células progenitoras sofrem uma mudança de comportamento, notando-se uma preferência na diferenciação em células enteroendócrinas em vez de enterócitos.

Análises quantitativas indicaram que subexpressão da SdhD causa uma acumulação de succinato no tecido. O succinato é um activador conhecido do receptor acoplado à proteína G 91 (GPR91), que foi em estudos prévios associado a hipertrofia e apoptose.

Os resultados obtidos neste trabalho contribuíram para um melhor entendimento relativamente aos mecanismos de regulação da actividade celular por processos

metabólicos, demonstrando que a *Drosophila melanogaster* é um modelo importante para o seu estudo. Uma melhor compreensão acerca dos processos de regulação de hipertrofia e replicação celular poderá ter um impacto positivo no desenvolvimento de terapias para doenças relacionadas com hipertrofia, ou com replicação celular, como o cancro.

**Termos chave:** células estaminais intestinais, metabolismo, hipertrofia, morte celular, divisão celular, homeostase

# Table of contents

# List of Figures

# List of Tables

# List of Abbreviations

| | |
|---|---|
| **β-Gal** | β-galactosidase |
| **DAPI** | 4',6-diamidino-2-phenylindole |
| **EB** | Enteroblast |
| **EC** | Enterocyte |
| **EE** | Enteroendocrine cell |
| **EGFR** | Epidermal growth factor receptor |
| **EM** | Electron microscopy |
| **ETC** | Electron transport chain |
| **EtOH** | Ethanol |
| **Esg** | Escargot |
| **FAD** | Flavin adenine dinucleotide |
| **FOV** | Field of view |
| **GFP** | Green fluorescent protein |
| **GTP** | Guanosine triphosphate |
| **ISC** | Intestinal stem cell |
| **JNK** | c-Jun N-terminal kinase |
| **MAPKs** | Mitogen-activated protein kinases |
| **MPCs** | Mitochondrial pyruvate carriers |
| **NAD** | Nicotinamide adenine dinucleotide |
| **OXPHOS** | Oxidative phosphorylation |
| **qRT-PCR** | Quantitative real-time reverse transcription-polymerase chain reaction |
| **Pros** | Prospero |
| **Rpr** | Reaper |
| **RNA** | Ribonucleic acid |
| **RNAi** | RNA-interference |
| **ROS** | Reactive oxigen species |
| **SdhA** | Succinate dehydrogenase, subunit A |
| **SdhC** | Succinate dehydrogenase, subunit C |
| **SdhD** | Succinate dehydrogenase, subunit D |
| **SEM** | Standard error of the mean |
| **Su(H)** | Suppressor of hairless |
| **TCA** | Tricarboxylic acid cycle |
| **Tub** | Tubulin |
| **UAS** | Upstream activating sequence |
| **YFP** | Yellow fluorescent protein |

# Introduction

**Introductory remarks**

In part 1 of his chapter, I introduce the different types of stem cells and their role in development and tissue maintenance. In the second part, I describe the intestine of the fruit-fly *Drosophila melanogaster* as an adult stem cell niche model and the conserved mechanisms that regulate homeostasis and stress responses. In part 3, I present the basis of metabolic regulation of stem cells, explore the existing gaps in the field, and describe the workplan to answer some of the pending questions.

# 1- Stem cells: role in development and tissue repair

Stem cells are characterized by their ability to divide through mitosis to produce more stem cells (self-renewal) and differentiate to a specific cell lineage. These traits allow them to build new tissue and organs during development where a great number of new cells is required, and to provide tissue homeostasis or regeneration during adulthood [1][2].

Stem cells are divided into three main categories: embryonic stem cells (ESCs), adult stem cells (ASCs; also referred to as somatic stem cells), and induced pluripotent stem cells (iPSCs). Early embryonic stem cells in the morula are totipotent, as they can give rise to all cell types in the body, including the extraembryonic, or placental cells. Upon formation of the blastocyst, the inner mass cells are considered to be pluripotent, as they generate the 3 types of embryonic germ layers: ectoderm, mesoderm and endoderm. During development, these cells become more restricted in their ability to differentiate into multiple lineages. In adults, where stem cells are only capable of forming a limited number of cell types, they are considered to be multipotent or unipotent [3][4][5]. ASCs are found in different tissues of adult organisms across species. The most studied in mammals are hematopoietic stem cells (HSCs) and mesenchymal stem cells (MSCs), which have a lower self-renewal potential than ESCs [6]. Germline stem cells are usually considered to be ASCs. The third category of stem cells, iPSCs, is obtained from mature adult cells, normally fibroblasts, that were artificially reprogrammed in vitro to an ESC-like state mainly through overexpression of core stemness regulators [7], which are detailed below.

**Embryonic stem cells**

ESCs were first isolated in 1981 from the inner cell mass of early embryos and blastocysts of mice [8][9]. These cells have the ability to proliferate indefinitely in vitro while remaining pluripotent, rapid proliferation and high telomerase activity [10]. These cells can be differentiated in vitro into a variety of specific cell types such as neural [11], cardiac [12]

or intestinal lineages [13]. As such, ESCs have a high therapeutic potential to repopulate and repair damaged or degenerating tissues.

**Induced pluripotent stem cells**

iPSCs are generated from differentiated cells by expressing core transcription factors that are required for maintenance of pluripotency and proliferation of ESCs. In their 2006 groundbreaking study, Yamanaka and colleagues reprogrammed murine fibroblasts to iPSCs by retroviral-mediated expression of the 'stemness'-associated factors OCT4 (octamer-binding transcription factor 4), SOX2 (SRY (sex-determining region Y)-box 2), KLF4 (Kruppel-like factor 4), and C-MYC [14]. In 2007, Yu and colleagues generated mice iPSCs by expressing a different set of factors, OCT4, SOX2, NANOG, and LIN28, using a lentiviral system [15]. Following these accomplishments, researchers were also able to generate iPSCs derived from human somatic cells [16]. iPSCs exhibit many traits similar to ESCs, such as morphology, cell-surface markers, telomerase activity and epigenetic marks, but they differ in global gene expression [7].

**Adult stem cells**

Most adult tissues contain reservoirs of stem cells used to replenish differentiated cells that are lost upon tissue injury, infection or normal cell turnover. Upon stress, differentiated cells send a variety of signals to stem cells to regulate their replication and differentiation dynamics [2][17]. In some organisms, upon injury, fully differentiated cells can also de-differentiate to stem cells in order to fulfill the requirements of stem cell population to provide the tissue with newly formed cells [1]. In the absence of injury, ACSs continue to generate new cells to replace those that have worn out, in order to maintain tissue homeostasis. While many of the pathways responsible for ASC activation are shared with those in pluripotent stem cells during development, the dynamics of cell communication and proliferation are distinct, as are the types of cells involved. Studies in mice and humans have shown the existence of different ASC types across the organism, including in the bone marrow [18], skeletal muscle [19], skin epithelia [20], intestine [21], heart [22][23], brain [24][25], and lungs [6][26]. These cells are used sparingly and are generally tucked away in protected niches [6]. They are also scarce, and with the relative exception of HSCs, are difficult to isolate.

HSCs produce all the different cells present in the mammalian blood, including platelets, red blood cells and white blood cells. These cells and their progenitors can be collected from umbilical cord blood or peripheral blood, and isolated by their cell-surface markers such as CD34. In contrast, MSCs generate various mesodermal cell lineages,

including myocytes, chondroblasts, fibroblasts, osteoblasts and adipocytes. MSCs are usually isolated from bone marrow and umbilical cord blood and display a different expression profile of cell surface markers than that of HSCs [7].

**The stem cell nice**

ASCs are often tucked away in niches, physically protected from potential damage, either mechanical or from pathogens. The stem cell niche also comprises a pool of intricate signals occurring between the stem cells and their environment, that are required for proper tissue homeostasis and response to damage. In the niche, ASCs are largely quiescent, i.e., they display low proliferation and differentiation rates. The germline of *Drosophila* was one of the first stem cell niches to be characterized [27]. In mammals, the bone marrow is an example of a niche, where HSCs reside [6]. The concept of the niche is better perceived in part 2 of this chapter in the context of the *Drosophila* intestinal epithelium.

**Applications**

Due to their potential to self-renew, possibility of in vivo growth and patient specificity, stem cells have a notable potential for regenerative medicine. Animal models and clinical studies have shown that transplantation of stem cells from diverse origins can successfully treat many acute and chronic diseases. Bone marrow transplantation is the most common example, used to treat aplastic anemia, leukemias, immune deficiency and hemoglobin disorders. The potential for stem cell therapy extends to many disorders, including myocardial infarction, Parkinson disease, myelin disease and liver failure [6][28]. iPSCs present a high potential for transplantation treatments as they have the same genetic signature as other cells in the patient, greatly reducing chances of immune rejections, and can be genetically corrected [16].

To fully explore the therapeutic potential of stem cells it is essential to understand the mechanisms that regulate their activity. Dissecting the mechanisms of proliferation is also of great importance for the development of targeted therapies against tumor progression, as cancer cells share many common replication pathways with stem cells [29][30]. The mechanisms responsible for stem cell division and differentiation are largely conserved among species, and as such, several animal models are used to study stem cell-mediated development, regeneration and homeostasis, as described below.

**Non-mammalian models of development and regeneration**

Stem cell research is not limited to mice and humans, and several other animals such as the chick, amphibians, fish or the fruit-fly have provided the community with important

insights about morphological patterning during development and stem cell activation in adults. Amphibians such as urodeles (salamanders or axolotls) or anurans (frogs or toads) have high regeneration potential and have been studied as models for limb repair. As tadpoles, anurans are able to regenerate limbs and tails but this capacity to regenerate rapidly declines during metamorphosis [5]. Zebrafish has emerged as a powerful model organism to study vertebrate development and regeneration [17][31]. Zebrafish is able to regenerate retina, heart and the fin, which has been extensively used a model for regeneration. ASCs have also been characterized in the intestine and bone marrow. Regeneration in zebrafish may rely on stem cell activation, or dedifferentiation of surrounding cells. Zebrafish offers several advantages such a short generation time, live imaging and fast regeneration of the caudal fin upon amputation [5][31]. The chicken embryo, possibly the oldest system used to study vertebrate development — dating back to Aristotle around the year 350 BCE — has contributed substantially to the understanding of human development and disease [32]. The chicken embryo is an attractive model due to being phylogenetically closer to mammals than zebrafish, having a convenient size, being stationary, having a short incubation time, and the egg being nutritionally self-sufficient [33][34].

**The fruit-fly *Drosophila melanogaster* as a model for adult stem cells**

The fruit-fly *Drosophila melanogaster* has been extensively used as a model to study development and ASCs [27]. It offers several advantages such as having a fully-sequenced genome, short reproductive cycle, relatively low maintenance and large availability of genetic tools such as collections of transgenes and mutated alleles, drivers (promoters) of gene expression that cell type — and temporal — specific, RNAi-interference (RNAi) constructs, and different types of fluorescent reporters [35]. Furthermore, *Drosophila* shares several conserved pathways with humans, including those involved in metabolism and also regulation of stem cells [36].

The adult intestine of the fruit-fly *Drosophila melanogaster* contains a stem cell niche and has emerged as an important model in the study of ASCs, allowing for a better understanding of regulatory mechanisms both during homeostatic and stress-response conditions [37][38][39][40]. The following section explores the intestinal stem cell niche of the fruit fly, comparing differences to the mammalian intestine and the several conserved pathways responsible for regulation of stem cells.

# 2- The intestine of *Drosophila melanogaster*

The intestine absorbs ingested water and food and provides a barrier against harmful agents, such as bacteria and toxins from the environment. To maintain these roles, it must be highly adaptive in response to both environmental cues and intrinsic signals.

**Morphology**

The intestine of *Drosophila* comprises three main morphologically distinct sections: the foregut, the midgut, and the hindgut [41]. The foregut is located at the most anterior part of the intestine and stores food and regulates its flow into the midgut for further processing. The midgut, of endodermal origin, corresponds to the small intestine in humans and is responsible for food digestion and nutrient absorption. In similarity with the mammalian small intestine, the midgut is highly compartmentalized and can be divided according to differences in gene expression, pH, metabolism, enzymes and immunity. It is surrounded by a network of tubules known as trachea that deliver oxygen to its cells and by longitudinal and circular muscle that mediate intestinal peristalsis. The midgut comprises a simple linear epithelium, in contrast to the small intestine of mammals that contains several invaginations named Crypts of Lieberkühn, that harbor stem cells at its bottom part. The hindgut, of ectodermal origin, is located at the posterior-most part of the intestine and corresponds to the large intestine in humans [41][42]. The focus of this work is on the midgut part of the intestine, where a stem cell nice exists and has been used as a model to dissect pathways involved in somatic stem cell behavior [37][38][39][40].

**Composition**

The midgut of *Drosophila* is composed of several absorptive enterocytes (ECs), which are terminally-differentiated, large polyploid cells. ECs contain a brush border consisting of microvilli on its apical side (depicted in **Figure 1 A**, in blue), that increase its surface area to aid nutrient absorption, in similarity with mammalian ECs [41]. Enteroendocrine cells (EEs), present in both *Drosophila* and mammalian intestine, are fully differentiated diploid cells that are responsible for segregating regulatory peptides. These peptide hormones are responsible for regulation of appetite, gastrointestinal motility and secretion, and have sequence and functional homology to the ones in mammals [42][43]. EEs express the homeodomain transcription factor Prospero (Pros) and are uniquely identified using anti-Prospero antibodies in immunofluorescent imaging. The tubular epithelium is surrounded by thebasal membrane (BM) -- an extracellular collagenous matrix that is also present in mammals. Visceral muscle layers (VM) reside underneath the BM [40].

Intestinal stem cells (ISCs; **Figure 1 A**, in green) are responsible for generation of new cells in the midgut. These diploid cells reside near the BM and commonly form pairs with their daughter cells, the enteroblasts (EBs; in cyan) which express the transcription factor Suppressor of hairless (Su(H)) [37][38]. ISCs and EBs are collectively referred to as "progenitor cells". ISCs are tucked away in their niche, where they are separated from the lumen where potential damaging factors exist. At this location, ISCs receive signals both from muscle cells below and from the other cell types around.

The mammalian small intestine, in contrast to the linear epithelium of the *Drosophila* midgut, has several epithelial protrusions called villi that greatly increase its absorptive surface area. These are maintained by stem cells identified by their cell-surface markers Bmi1 (B lymphoma Mo-MLV insertion region 1 homolog) and Lgr5 (Leucine-rich repeat-containing G-protein coupled receptor 5) [41].

**Homeostasis/differentiation**

To maintain homeostasis upon loss of differentiated cells due to injury or normal cell turnover, ISCs divide to replenish tissue. ISCs can divide symmetrically to proliferate, generating a new identical ISC, or asymmetrically to generate an ISC and a newly formed EB. EBs are transient cells that do not divide, and eventually differentiate to either ECs or EEs [41]. EBs are formed as small, diploid cells and while differentiating into ECs may go through endoreduplication and appear larger [44].

The Notch pathway is a major regulator of progenitor cell maintenance and differentiation in different organisms and systems, including the fly and mammalian intestines. In *Drosophila*, ISCs express the Delta ligand which binds the cell-surface Notch receptor in EBs and activates the Su(H) factor that identifies them in the midgut (**Figure 1 B**). Both progenitor cell types express the transcription factor Escargot (Esg), a homologue of the mammalian Snail family, that acts as an inhibitor of differentiation [45]. The differentiation choice to either ECs or EEs is controlled by the intensity of Delta-Notch signaling between ISCs and EBs: higher levels of Notch signaling lead EBs to differentiate into ECs, while lower Notch activity causes them to differentiate into EEs [45]. It has also been observed the existence of a subset of ISCs that accumulate Pros in a polar manner inside the cell and, upon division, Pros remains in one of the new cells that will become an EE [42][46].

Notch genes encode transmembrane receptors that regulate a broad spectrum of cell fate decisions and differentiation processes during development. Binding of one of the four Notch receptors with Notch ligands (Delta or Serrate in *Drosophila*) results in proteolytic cleavage of the receptor, releasing the free Notch intracellular domain ($N^{intra}$) that

translocates into the nucleus, where it binds to different transcription factors (including Su(H) (the homologue of mammalian CBF1) to activate the expression of target genes [47][48][49]. In the mammalian intestine, Notch is essential to maintain the stem cell crypt compartment in its undifferentiated, proliferative state and also controls absorptive versus secretory fate decisions. In *Drosophila,* Delta–Notch signaling also promotes the mitotic-to-endocycle switch during differentiation to ECs [50]. In EBs, Esg positively regulates Notch activity via its target Amun. Notch-RNAi in progenitor cells causes Esg-positive tumors and elevated numbers of EEs [45]. Loss of Notch function within ISCs may block differentiation in EBs, leading to over-proliferation of ISCs [38]. In contrast to the mammalian intestine, where Notch favors proliferation of stem cells, in *Drosophila* is required for differentiation. However, in both *Drosophila* and mammals, Notch activation favors differentiation towards an enterocyte fate at the expense of secretory cells [40][51].

In the mammalian intestine, $Bmi1^{+}$ stem cells divide asymmetrically to generate one cell of the same type and a new $Lgr5^{+}$ stem cell, which in turn divides asymmetrically to yield one cell of the same type and a transient amplifying (TA) cell that divides a limited number of times and finally differentiates into one of the 4 fully-differentiated cell types: enterocytes, enteroendocrine cells, Paneth cells, or mucous-secreting goblet cells. The intestinal crypts harbor stem cells and TA cells. TA cells divide 4–5 times before they terminally differentiate into the specialized intestinal epithelial cell types, that then localize to the tip of the villus, with the exception of the Paneth cells that remain at the bottom of the crypts. When the cells at the tip of the villi undergo apoptosis, they are shed into the lumen. Paneth cells are responsible for innate immunity and antibacterial responses, as they secrete bactericidal peptides and lysozymes [47]. In analogy to Esg expression in progenitor cells of flies, expression of Snai1—a member of the mammalian Snail family—was found in ISCs and TA cells of mice [52].

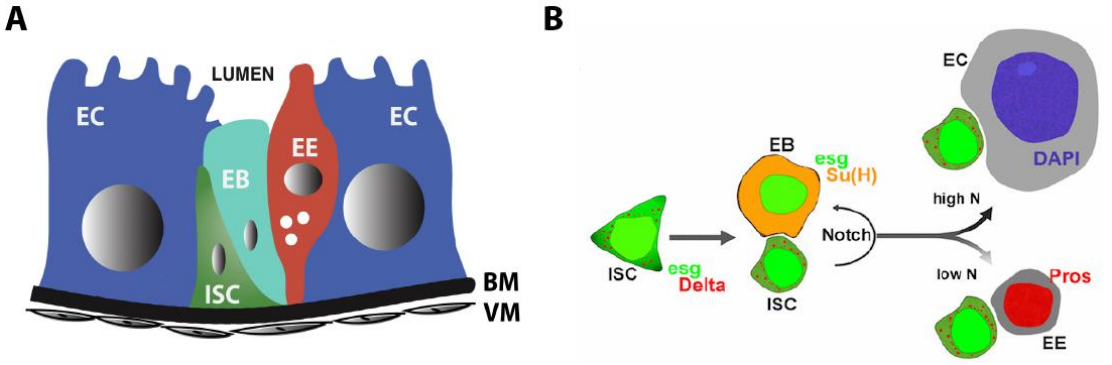


**Figure 1: Stem cell niche morphology and cell lineage specification in the midgut of *Drosophila melanogaster***
**A.** Cross-sectional representation of the cellular organization in the mono-layered intestinal epithelium of *Drosophila*. Intestinal stem cells (ISCs, in green) are located near the basal membrane (BM) and do not share an interface with the lumen. Enteroblasts (EBs, in cyan) are transitory daughter cells of ISCs that differentiate into the other cell types. EBs may assume different shapes and sizes while differentiating. Enteroendocrine cells (EEs, in red) are small diploid cells that segregate peptides and hormones to aid digestion. Enterocytes (ECs) are large polyploid cells responsible for nutrient absorption that have microvilli to increase the area of contact with the lumen. All cells lay on the BM that is surrounded by visceral muscle (VM) that regulates the movement of food. Image adapted from Dutta et al [53]. **B**. Lineage specification in the midgut. ISCs divide either asymmetrically to originate a new ISC and a daughter EB, or symmetrically to generate two identical ISCs. ISCs express Delta, which binds the Notch receptors in EBs (in orange), and activates the Suppressor of hairless (Su(H)) transcription factor in these cells. ISCs and EBs are commonly found in pairs and are collectively referred to as progenitor cells. They both express the transcription factor Escargot (Esg, in green). EBs differentiate into either ECs or EEs depending on the intensity of the Delta-Notch (N) signaling originating from the ISC-EB interface: higher levels of Notch signaling cause EBs to differentiate to ECs, while low Notch signaling promotes differentiation to EEs. The fluorescent stain DAPI marks the nuclei of all cells, which are considerably larger in ECs (in blue). EEs are marked by expression of the transcription factor Prospero (Pros). Image obtained from Loza-Coll et al. [45].

## Aging in the intestine of *Drosophila melanogaster*

During aging, there is a loss of tissue homeostasis, causing ISCs to divide more often, and a widespread accumulation of cells that express both markers of progenitor ($Esg^+$) and differentiated cells, suggesting a compromised ability for terminal differentiation. These cells form stacks of double and triple layers as opposed to the single layer found in healthy intestines and show reduced barrier permeability [54][55][56]. Examples of these intestines are found later in sections 1.1 and 2.2 of the Results and Discussion chapter.

## Mechanisms of stem cell modulation

Cells in the intestine are constantly challenged by exposure to bacteria and other damaging factors. Exposure to stressors such as potent oxidants such as hydrogen peroxide or paraquat, or bleomycin—a DNA-damaging peptide that induces strand breaks—triggers intestinal stem cell proliferation in response to enterocyte death [42][57]. Upon sensing damage, these cells initiate a series of signals to stimulate ISC division and EB differentiation in order to restore tissue structure and function. When severely damaged, ECs enter an

apoptotic program and are excised to the lumen, in similarity with the mammalian case. The rates of progenitor cell division and differentiation are adjusted in response to EC and EE turnover through a combination of positive and negative feedback loops initiated by these cells [42]. Several conserved pathways are involved in autocrine or paracrine signaling occurring between progenitor and differentiated cells in the niche, which are described below.

**JAK/STAT** (Janus kinase/signal transducers and activators of transcription) is a pathway activated by a variety of ligands that is involved in proliferation, differentiation and apoptosis, during development, homeostasis or stress-responses. In the midgut of *Drosophila*, Jak-Stat is activated by the cytokines of the Unpaired family Upd, Upd2 and Upd3. Upon stress, ECs release these cytokines to promote ISC proliferation and EB differentiation, via stimulation of Delta-Notch signaling [58]. Unpaired ligands bind the Domeless receptor, phosphorylating Hopscotch, a type of Janus kinase, promoting translocation of the Stat92E transcription factor to the nucleus, to activate its target genes [59]. In the mammalian intestine JAK-STAT plays a similar role [58].

***Wnt*** signaling (Wingless, or Wg, in *Drosophila)* is a conserved pathway that plays key roles both during development and in maintenance of different adult tissues [60]. Endogenous Wg ligands are expressed at low levels in ISCs of *Drosophila* and act to promote self-renewal in these cells [61]. Wg is also expressed in the visceral muscle [61] and EBs upon injury [62] to promote ISC division. Conversely, Wg signaling from the visceral muscle inhibits Upd2 and Upd3 expression in ECs suppressing ISC activity via inhibition of the JAK-STAT pathway, suggesting a dual role part of a tightly regulated network [63]. In the mammalian small intestine, *Wnt* is expressed in the crypt to promote stem cell renewal and control differentiation [64]. Wnt/Wg signaling works by binding of the Wnt/Wg ligand to its coreceptors, Frizzled2 and LRP (Arrow in *Drosophila*), to initiate a sequence of events that leads to Dishevelled–mediated inactivation of a protein destruction complex that allows stabilized β-catenin (Armadillo in *Drosophila*) to translocate to the nucleus, binding to the transcription factor T-cell factor that promotes the activation or repression of genes related to proliferation, apoptosis and cell fate [65][60]. Notch also acts downstream of the Wg pathway to control maintenance and differentiation of *Drosophila* intestinal progenitor cells [61].

**JNKs** (c-Jun N-terminal kinases) are part of a conserved mitogen-activated protein kinase (MAPK) cascade with important roles in development, wound healing, and stress-responses [66][67][68]. In *Drosophila*, the JNK Basket (Bsk) is phosphorylated by the JNK kinase (JNKK) Hemipterous (Hep). Bsk then phosphorylates different transcription factors,

including Foxo (Forkhead Box O transcription factor), inducing changes in gene expression related to growth, proliferation and differentiation. Upon stress, JNK mediates the transcription of damage-repair genes such as *thor* and small heat shock proteins. In the midgut, JNK is activated in ECs and EEs. ECs with dysfunctional tricellular junctions signal to ISCs to promote proliferation and regeneration [69]. JNK pathways have a dual-role in promoting apoptosis or inducing stem cell proliferation, depending on the type of activated transcription factors [54]. JNKs are also present in the mammalian intestine, where it modulates Wnt signaling [68][41][67].

The epidermal growth factor receptor (**EGFR**) is activated by ligands produced in the intestinal epithelium upon damage or stress, promoting ISC proliferation. The EGFR ligand Vein is expressed in the visceral muscle to promote ISC maintenance and proliferation. ISCs also express two different EGFR ligands, Spitz and Keren, that act as autocrine signals to maintain these cells [70]. Upon damage, the EGFR receptor induces activation of the RAS GTPase and MAPK, which phosphorylates the transcriptional repressor Cic (Capicua), activating expression of cell cycle regulator genes *Pointed*, *Ets21C*, *Cdc25* and cyc*E* (Cyclin E) [71]. Mammal ISCs also require EGFR signaling for proper function [41].

**IGF** (insulin-like growth factor; InR in *Drosophila*) signaling is a conserved pathway involved in cell growth and proliferation. In the *Drosophila* midgut, muscle cells and EBs express insulin-like peptides named Dilps that induce ISC proliferation [72]. Dilps activate InR that signals through Chico, a homolog of the mammalian insulin receptor substrates 1–4 (IRS 1–4), activating PI3K (phosphatidylinositol 3'-kinase), leading to phosphorylation of Akt (protein kinase B), which inhibits the transcription factor Foxo and activates TOR (target of rapamycin) protein kinases, that promote growth and proliferation [73][74]. Insulin signaling may also stimulate cell proliferation via activation of the RAS/MAPK pathway [75].

**Hedgehog** (Hh) signaling is another conserved pathway involved in cell growth and proliferation. In the midgut of *Drosophila* Hh is activated in injured EBs and promotes the expression of Upd2 to activate the JAK-STAT pathway that promotes ISC proliferation. Hh is also active in the mammalian intestine where it promotes differentiation via inhibition of Wnt signaling [76].

**Hippo** is a conserved pathway initially identified in *Drosophila* that controls organ size by restraining stem cell proliferation and inducing apoptosis in specific cells. It is a complex signaling network with over 30 components. The core of the Hippo pathway is a kinase cascade leading from activation of the tumor suppressor Hippo (Mst1/2 in mammals) that phosphorylate Warts (Lats1/2 in mammals) to inhibit the activity of the transcriptional co-

activator Yorkie (YAP and TAZ in mammals). When active, Yorkie translocates to the nucleus to bind the transcription factor Scalloped (TEAD family in mammals) to induce expression of a wide range of genes involved in autocrine or paracrine cell proliferation and survival responses, such as *diap1* (*Drosophila* inhibitor of apoptosis), *cycE*, *Upd1/2/3* and *Vein* [77][78][79]. Stress-induced Hippo pathway inactivation in ECs of *Drosophila* results in increased stem cell proliferation via expression of Upd JAK/STAT ligands. In ISCs, Hippo inactivation or Yki overexpression results in increased proliferation [51]. In the mouse intestine, overexpression of YAP also leads to activation of progenitor cell proliferation [80]

The pathways here described act synergistically to maintain homeostasis in the *Drosophila* midgut. As an example, inactivation of either EGFR, Wg or JAK/STAT results in progressive ISC loss over time, while simultaneous disruption of these 3 pathways leads to total loss of ISCs. However EGFR over-activation can partially replace Wg or JAKSTAT, and vice versa [70]. Upon stress, JNK and EGFR signaling act simultaneously to initiate ISC proliferation, via activation of Sox21a (a member of the conserved Sox family of transcription factors) in these cells [81].

In summary, the physical location of the different cell types in the intestine and the intricate signaling that occurs between them constitute the intestinal stem cell niche. This presents a powerful model for the study of stem cells in a tissue context, owing to its conserved signaling pathways, availability of genetic tools, and morphological simplicity. The following sections explore the importance of metabolism in regulating stem cell activity in different systems.

# 3- Role of metabolism in stem cell activity

## 3.1- Energy production in Metazoa

Metabolism transforms nutrients into usable forms of energy and provides substrates for synthesis of new molecules. In the cytoplasm, glucose is broken down into pyruvate via glycolysis, reducing nicotinamide adenine dinucleotide ($NAD^+$) to NADH and producing adenosine triphosphate (ATP) from adenosine diphosphate (ADP). Pyruvate obtained from glycolysis is then transported into the mitochondria via mitochondrial pyruvate carriers (MPCs), where it is converted to acetyl-CoA by pyruvate dehydrogenase that enters the Citric Acid Cycle (also Krebs Cycle, or TCA (tricarboxylic acid) cycle). Under limiting oxygen conditions, pyruvate from glycolysis is instead reduced to lactate by lactate dehydrogenase, regenerating NADH back to $NAD^+$ to reenter glycolysis. This fermentation process is less efficient than aerobic respiration (described below), as for each molecule of glucose, aerobic respiration generates 36 molecules of ATP while anaerobic glycolysis generates only 2 molecules [82]. This process, however, can produce ATP at a faster rate than aerobic respiration [82][83].

Cells also produce ATP via protein catabolism. In this process, the α-amino group of amino acids is removed, and the resulting carbon skeleton is converted into different metabolic intermediates depending on the amino acid. These intermediates include pyruvate, acetyl-CoA, acetoacetyl-CoA, or the TCA cycle intermediates α-ketoglutarate, succinyl CoA, fumarate, and oxaloacetate and can be used to form fatty acids, ketone bodies, or glucose [86]. Amino acids that are converted to acetyl-CoA or acetoacetyl-CoA are termed *ketogenic* amino acids since they can give rise to ketone bodies or fatty acids. Amino acids that yield pyruvate, α-ketoglutarate, succinyl CoA, fumarate, or oxaloacetate are termed *glucogenic* amino acids [86][87].

Lipids are broke down in the cytoplasm into glycerol and fatty acids in a process called lipolysis. Fatty acids are then broke down in the mitochondria in the beta-oxidation pathway to generate acetyl-CoA that enters the Krebs cycle, and NADH and $FADH_2$ that are used by the electron transport chain (ETC) to generate ATP [88]. Acetyl-CoA is also produced by oxidation of fatty acids in the mitochondria via beta-oxidation, yielding NADH and flavin adenine dinucleotide in the reduced form ($FADH_2$) [84][85].

In aerobic respiration, acetyl-CoA generated from the different aforementioned processes enters the Krebs cycle in the mitochondrial matrix, where it undergoes several transformations to yield NADH and ATP (**Figure 2**).

The ETC occurs in the inner mitochondrial membrane and oxidizes NADH and succinate from the Krebs cycle, building up a proton gradient across the inner mitochondrial membrane, which is ultimately used to generate ATP from ADP (adenosine diphosphate) (**Figure 2**). This highly conserved process is termed oxidative phosphorylation (OXPHOS) [85].

The ETC comprises 5 complexes. Complexes I - IV are responsible for the transport of electrons to the corresponding reducing sites or the transfer of $H^+$ protons across the membrane, while complex V (ATP synthase) uses the potential created by the proton gradient to generate ATP, channeling $H^+$ back into the mitochondrial matrix. ATP is then transported to the cytosol to be used by the cell as energy [85].

Complex I (NADH:ubiquinone oxidoreductase) is the largest complex in the ETC and contains 44 subunits which are encoded by both mitochondrial and nuclear genome [89]. These subunits are assembled by 4 assembly factor proteins in humans, and at least 1 in *Drosophila* [90]. Complex I oxidizes NADH from the Krebs cycle to $NAD^+$ with removal of 2 electrons. These electrons are transported to a ubiquinone (coenzyme $Q_{10}$, Q, **Figure 2**) binding site, where it is reduced to ubiquinol ($QH_2$). The electron flow within the complex is thought to cause conformational changes in its proteins, causing them to pump the hydrogen protons originating from NADH to the inter-membrane space [91].

Complex II (succinate dehydrogenase, SDH) participates both in the Krebs cycle and in the ETC [85]. It is composed of 4 subunits—SdhA, SdhB, SdhC and SdhD. The subunit A is responsible for the enzymatic activity that leads to the conversion of succinate to fumarate via reduction of the flavin adenine dinucleotide (FAD) cofactor to $FADH_2$ in the Krebs cycle. The remaining subunits—SdhB, SdhC and SdhD—channel the resulting electrons via iron-sulfur clusters to the ubiquinone binding site, where it is reduced to ubiquinol, as part of the ETC. While SdhA and SdhB are lipophobic components, SdhC and SdhD are lipophilic subunits that keep the complex attached to the mitochondrial inner membrane [92].

Complex III (coenzyme Q:cytochrome c – oxidoreductase) is composed of 11 subunits; it accepts electrons from ubiquinol — which was reduced at complexes I and II — and regenerates it back to ubiquinone. The electrons obtained from the oxidation of ubiquinol are then transferred to the carrier cytochrome c, in a process that is coupled to the pumping of $H^+$ protons from the matrix to the intermembrane space. Complex IV (cytochrome c oxidase) is composed of 14 subunits, both nuclear—and mitochondrial—

encoded. This complex oxidizes cytochrome c (reduced at complex III) and transfers the resulting electrons to reduce molecular oxygen ($O_2$) in the mitochondrial matrix, generating water. Finally, complex V (ATP synthase) uses the electrochemical potential generated from the proton gradient to add an inorganic phosphate group to ADP to form ATP, through a rotational motor mechanism. This process requires that protons that built up in the intermembrane space are transported back to the matrix, completing the process [85].

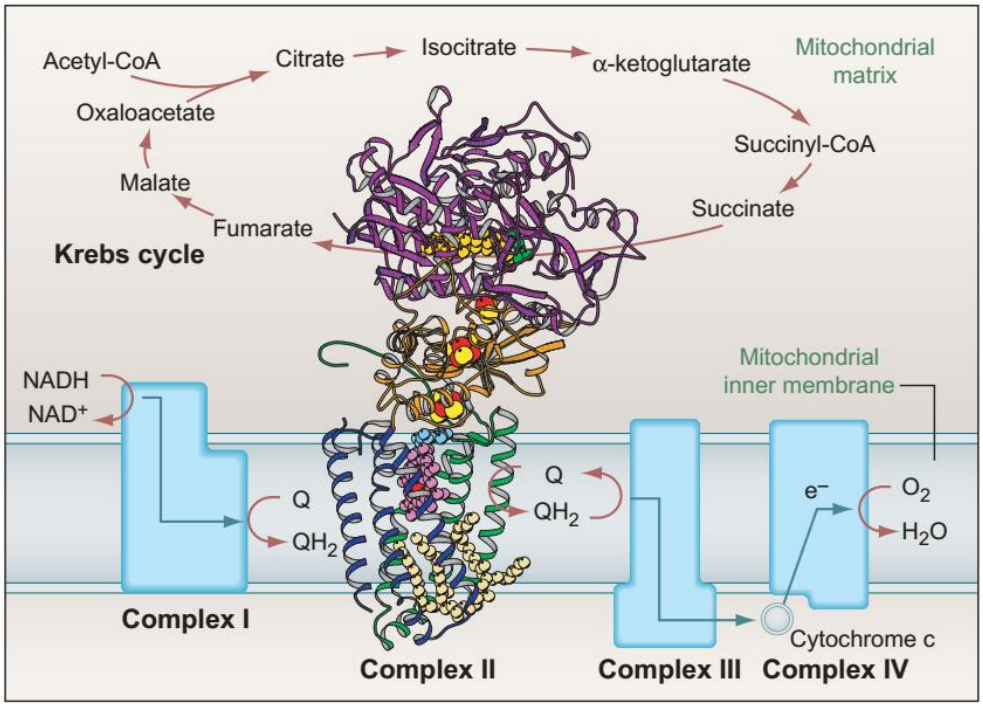


**Figure 2: Krebs cycle and the electron transport chain**
The Krebs cycle takes place in the mitochondrial matrix and oxidizes acetyl-CoA in a series of steps to produce NADH and $FADH_2$ that are used by the electron transport chain (ETC). The ETC takes place in the inner mitochondrial membrane (IMM) and is composed of 5 complexes: complex I oxidizes NADH from the Krebs cycle to $NAD^+$, coupled to a reduction of ubiquinone (Q) to ubiquinol ($QH_2$); complex II is composed of 4 subunits (with their protein structure detailed in the picture) and participates in both the Krebs cycle and the ETC; it oxidizes succinate to fumarate in the Krebs cycle, and the resulting electrons reduce ubiquinone to ubiquinol in the IMM as part of the ETC. Ubiquinol is then oxidized in complex III, which is coupled to a reduction of cytochrome c. Cytochrome c is then oxidized in complex IV and the resulting electrons reduce molecular oxygen ($O_2$) to water ($H_2O$). Finally, complex V (ATP synthase; not shown) generates ATP using the potential from the proton gradient generated across the IMM from the successive oxidations in the previous steps, completing the process. Image source: L. Hederstedt [92].

## 3.2- Metabolic regulation of stem cell activity

This section covers the differences in mitochondrial dynamics and metabolic requirements between stem cells and their differentiated counterparts, describing how changes in metabolic pathways may strongly influence stem cell behavior.

Besides playing a fundamental role in energy production through oxidative phosphorylation (OXPHOS) or amino acid or fatty acid catabolism, mitochondria play important roles in cell signaling by metabolic intermediates, reactive oxygen species (ROS), calcium homeostasis, and apoptosis [93].

**Mitochondria structure in different cell types**

Several studies have established correlations between cell potency (or stemness) and the structure of their mitochondria. Electron microscopy studies reveal that while somatic cells such as fibroblasts show mature, elongated mitochondria, with numerous cristae and an electron-dense matrix, ESCs or iPSCs contained fewer, immature, and globular mitochondria. [94][95][96][97]. Accordingly, during differentiation of ESCs and iPSCs, the mitochondria of these cells change to a more mature morphology and replicate to higher numbers [95]. These data suggest that stem cells rely less on OXPHOS for obtaining their energy.

**Metabolic shifting between stemness states**

In addition to the increase in mitochondrial biogenesis and structural differences, studies in different cell populations indicate that while differentiated cells mainly depend on OXPHOS as the primary source of energy production, stem cells traditionally rely largely on glycolysis as their main source of NADH and ATP. Accordingly, differentiation of ESCs and iPSCs is generally associated with a metabolic shift from a predominant glycolysis-based metabolism in these cells toward an increased OXPHOS-based metabolism in differentiated cells. The general preference of stem cells for glycolysis may be due to the hypoxic environment in the niche in which they normally exist [93][98][99].

With low oxygen availability, cells must rely on anaerobic glycolysis, which can be triggered by the hypoxia-inducible factor 1-alpha (Hif1-α). In fact, hypoxia sustains the self-renewal state of cultured ESCs and prevents their spontaneous differentiation [100]. This metabolic state usually results in increased lactate production [101]. Mouse HSCs exhibit a significantly higher utilization of glycolysis and lower reliance on OXPHOS. These cells also present a lower oxygen consumption and a strong expression Hif1-α, when compared to

other cells types in the bone marrow [102]. The preferential use of anaerobic glycolysis by HSCs is mediated by a pyruvate dehydrogenase kinase (PdK)-dependent mechanism, which in normal conditions suppresses the activity of pyruvate dehydrogenase in the mitochondria, and consequently inhibits OXPHOS. Importantly, PdK-mutant HSCs display lower lactate dehydrogenase activity and reduced self-renewal potential, while maintaining normal differentiation capacity, indicating that inhibition of OXPHOS is required for stem cell self-renewal [103].

Conversely, differentiated somatic cell lines display increased oxygen consumption rates and intracellular ATP content while secreting less lactate, suggesting a preference for OXPHOS [96]. Furthermore, differentiation of ESCs and iPSCs is associated with increased intracellular ATP levels and lower lactate production, while nuclear reprograming to iPSCs is coupled with a shift to glycolysis, and stimulation of glycolysis improves reprogramming efficiency, while inhibition of glycolysis decreases it [104].

Stem cells not only have different metabolic requirements when compared to their differentiated progeny, but also exhibit strong shifts in behavior when changes in distinct metabolic pathways are induced. Stimulation of mitochondrial biogenesis with S-nitrosoacetylpenicillamine (SNAP) in ESCs reduces the expression of pluripotency markers and triggers differentiation [97][105][106]. Similarly, overexpression of PGC-1α (peroxisome proliferator-activated receptor (PPAR) gamma coactivator-1α) — an important endogenous promoter of mitochondrial biogenesis — in mouse iPSCs triggers their differentiation into adipocytes [107].

Conversely, inhibiting mitochondrial function promotes pluripotency and prevents differentiation. Mitochondrial uncoupling by CCCP (carbonyl cyanide m-chlorophenylhydrazone) in ESCs increases the expression of the stemness factors NANOG, SOX2, and OCT4 and represses differentiation [108]. Schell and colleagues report that inhibition of MPCs (mitochondrial pyruvate carriers) in mouse intestinal stem cells and in vitro intestinal cell bodies, stimulates proliferation and population growth. These effects are coupled with decreased oxygen consumption and reduced citrate levels, confirming lower OXPHOS activity. The authors also show that endogenous MPC expression increases following differentiation of ISCs [109].

ESCs and iPSCs are more sensitive to inhibition of glycolysis than inhibition of OXPHOS for maintenance of normal ATP levels, while the opposite effect is observed in differentiated cells [101]. Despite these results, stem cells still rely on OXPHOS at a certain

level. Upon OXPHOS inhibition, ESCs and iPSCs still show reduced ATP levels, suggesting that OXPHOS also contributes to energy production in these cells [101][110].

The reports here described reveal that stem cells rely largely on anaerobic glycolysis while differentiated cells rely mainly on OXPHOS, and inhibition of OXPHOS is required to maintain a stem cell state. Despite that behavior, most cells are metabolically plastic and they shift between metabolic states when needed [98]. In the following section, similar behaviors are described specifically in the intestinal stem cell niche of *Drosophila melanogaster*.

## 3.3- Metabolism in the *Drosophila* intestinal progenitor cells

In similarity with the stem cell types described in the previous section, metabolism also plays an important role in the maintenance of intestinal progenitor cells of *Drosophila*, with consequences at a tissue level and animal lifespan. These cells are dependent on metabolism in similar ways as the different types of mammalian stem cells and also present fewer mitochondria than differentiated cells in the same tissue [111].

Schell and colleagues, in the study cited in the previous section using mice intestinal stem cells [109], also explore the role of mitochondrial pyruvate carriers (MPCs) in ISCs of *Drosophila*. The authors show that ISCs express lower levels of MPCs compared to the other differentiated cell types in the intestine, and that inhibition of MPCs causes ISCs to over-proliferate, while overexpression of MPC suppresses their ability to proliferate. These results reinforce the correlation between decreased OXPHOS and increased proliferation, while demonstrating a parallel between mammalian and *Drosophila* intestinal stem cells, in terms of metabolic-dependent behavior.

M. Rera and colleagues, exploring the role of the conserved mitochondrial biogenesis regulator dPGC-1 in progenitor cells of *Drosophila*, show that dPGC-1 overexpression raises mitochondrial content and increases the activity of the Krebs cycle enzyme citrate synthase and expression of ETC complexes I, III, IV and V. This is accompanied by delayed aging phenotypes in the intestine, such as restriction of progenitor cell over-proliferation and maintenance of intestinal barrier integrity, resulting in longer lifespan of the fly [112]. This work reinforces the correlation between increased aerobic respiration and lower stem cell activity, and reveals the importance of proper intestinal progenitor cell function to maintain tissue homeostasis, positively impacting the lifespan of the organism.

Singh et al. show that ISCs rely heavily on lipolysis–beta oxidation, while no evidence of activity of these pathways was found in differentiated cells in the intestine. Furthermore, attenuation of the lipolysis pathway leads to ISC death by necrosis [113]. Beta oxidation has previously been shown to be important for adult neural stem cell maintenance in mice [114][115].

The aforementioned reports indicate that intestinal progenitor cells in *Drosophila*, in similarity with the different mammalian stem cell types presented in the previous section, rely less on OXPHOS than their differentiated counterparts. Despite that, they still depend upon mitochondria for maintenance. Accordingly, ablation of the mitochondrial autophagy (mitophagy) genes *pink* and *parkin* resulting in altered mitochondrial ultrastructure, induces a senescence-like state in ISCs, blocking the over-proliferative condition normally observed

during aging [111]. Interestingly, while blocking pyruvate uptake by MPC inhibition induces ISC over-proliferation, blocking beta oxidation results in necrotic ISC death, indicating that these cells might rely on lipolysis-beta oxidation as a energy source to some level, although probably not predominantly, since these cells present fewer mitochondria, and the products of beta oxidation (acetyl-CoA, NADH and $FADH_2$) require mitochondria to be oxidized in the Krebs cycle and the ETC. While these sections showed the general role of glycolysis, beta oxidation and OXPHOS in stem cells, the following section focuses on the particular role of different complexes of the ETC and its subunits.

## 3.4- Implications of the electron transport chain in cell maintenance and organismal longevity

As described in the previous sections, stem cells are sensitive to ablations of different OXPHOS components which commonly correlate with increased proliferation. Inhibition of ETC complexes or particular subunits commonly results in similar effects.

Reprogramming of somatic cells into iPSCs is accompanied by a downregulation of several subunits of ETC complexes I and II [104]. In ESCs, inhibition of complex III with antimycin A, results in increased expression of stemness genes such as NANOG and OCT4, and reduced expression of genes that promote differentiation [110]. In ESCs and iPSCs, inhibition of complex V with oligomycin, decreases ATP levels only by less than 5%, suggesting that these cells rely only marginally on OXPHOS, or that upon OXPHOS inhibition they are able to shift their metabolism to keep up with energetic demands [101]. In mice, keratinocyte-specific knockout of mitochondrial transcriptional factor A (TFAM), a key activator of transcription in mitochondria, causes a reduction in the activity of complexes I, III, IV, and V, but not complex II or citrate synthase, which are not encoded by mitochondrial DNA [116]. Accordingly, TFAM-deficient cells exhibit significantly lower oxygen consumption, and lower levels of ROS [117]. At a functional level, these cells display impaired differentiation, increased proliferation, and no evidence of apoptosis, reinforcing the connection between decreased OXPHOS activity and increased proliferation / impaired differentiation. Due to the broad number of genes affected by this knockout, it is not clear whether the phenotypes arise from inhibition of a particular respiratory complex, or from a general downregulation of the aerobic respiration machinery.

In intestinal progenitor cells of *Drosophila,* expression of NDI1 — the yeast equivalent of ETC complex I (NADH dehydrogenase) — results in increased non-endogenous NADH oxidation and inhibits ISC over-proliferation in older flies, while lessening the number of cells expressing both markers of differentiated and progenitor cells, which are normal aging phenotypes, causing an extension in the lifespan of the fly [56]. These phenotypes are coupled with a reduction in the levels of activated (phosphorylated) AMPK (5’ adenosine monophosphate-activated protein kinase, that senses high AMP/ATP ratios that occur in low energy conditions), independent of insulin signaling. This work shows that ETC activity, at least NADH dehydrogenase, also has an impact in ISCs, and reinforces the correlation between increased OXPHOS activity and decreased proliferation.

Conversely, there are instances where inhibition of ETC components is detrimental to stem cell activity. In *Drosophila,* Mandal et al. demonstrate that low ATP resulting from a mutation in complex IV subunit Va (CoVa) causes cell cycle arrest in the late G1 phase in cells

of the developing eye disc [118][119]. The authors show that the lower ATP are sufficient to sustain survival and differentiation but not to progress through the cell cycle. The cell cycle-arrest phenotype is caused AMPK phosphorylation due to a higher AMP/ATP ratio, that leads to activation of the tumor-suppressor p53 and subsequent degradation of the G1-S transition protein Cyclin E, ultimately causing arrest in G1. Furthermore, the authors show that mutations in the PDSW subunit of Complex I and mitochondrial ribosomal proteins mRpL4 and mRpL17 also cause cell cycle arrest in the same cells. These data oppose the reports previously described, by coupling downregulation of OXPHOS to inhibition of proliferation. This raises the question why inhibition of OXPHOS components in the cells of the *Drosophila* developing eye causes cell cycle arrest, while in other stem cells types it induces proliferation. It appears to be a cell type-dependent effect since inhibition of different components (CoVa, PDSW, mRpL4 and mRpL17) result in a similar phenotype. Since the authors describe an ATP-dependent mechanism, it does not appear to be any specific mechanism related to the mutations, but rather a special requirement in these cells for the wild type gene in ATP production. Perhaps cells in the developing eye of *Drosophila* are unable to counteract the low ATP levels by increasing anaerobic respiration, or do not receive enough nutrients to maintain their ATP levels from anaerobic respiration (since this process is less efficient) or lipolysis – beta oxidation. A different report shows that oxygen deprivation or cyanide treatment (which inhibits cytochrome c oxidase of complex IV in the ETC) coupled with a slight reduction in ATP levels cause cell cycle arrest in *Drosophila* embryos [120]. However, the phenotype was not rescued by addition of ATP into the embryo, which suggests a different mechanism than the one in the eye disc.

Copeland and colleagues [121] unraveled the importance of individual subunits of the ETC for the lifespan of *Drosophila*. In a knockdown screen, the authors show that while ubiquitous knockdown of specific subunits of the ETC via RNAi (RNA-interference) results in lethality or premature death, knocking down different subunits of the same complexes increases longevity in the fruit fly. The ATP levels and fertility rates of these long-lived flies remain unchanged in some of the cases, indicating that the lifespan extension is not caused by a general slow-down of biological processes, and suggesting that their cells are able to counteract the specific subunit knockdown by shifting metabolism from OXPHOS. It remains to be determined what are the specific mechanisms underlying the observed lifespan extension.

In summary, different cell types have different metabolic requirements, although in general stem cells rely little on OXPHOS. In parallel, inhibition of OXPHOS generally leads to increased stem cell proliferation. ISCs seem to follow this aspect, since inhibition of MPC

resulting in downregulated OXPHOS activity leads to increased proliferation; while increased mitochondrial or NADH dehydrogenase activity lead to decreased proliferation in older flies.

# 4- Aims and outline of the thesis:

The reports presented in this chapter show that in general, a depletion of aerobic respiration, rather than deleterious, is essential for stem cell division. This has a few exceptions that appear to be specific of the cell type.

Despite the efforts in understanding the role of the ETC in stem cell maintenance, several questions related to how different complexes and subunits regulate distinct stem cell types still remain. Are different subunits/complexes required in a specific cell type in the same manner? Do different cell types have distinct requirements for a specific subunit/complex? Through which mechanisms?

In addition, due to a previous lack of tools with cell-type specificity for ISCs or EBs, some studies did not differentiate between these 2 cell types and as such they were treated equally [56][112]. Consequently, there is currently a gap in knowledge regarding how metabolism regulates these two cell types differently.

This work aimed at filling the gap in understanding the role of individual ETC complex subunits in intestinal progenitor cell maintenance — both in ISCs and EBs — and how it affects tissue homeostasis. Given the role of different subunits in the organism in mediating lifespan and the tight relationship between lifespan and intestinal stem cell regulation, we hypothesized that different ETC subunits may have distinct roles in regulating intestinal progenitor cells in *Drosophila*, with a consequent impact in tissue homeostasis.

To test this hypothesis, we performed a candidate screen by knocking down several subunits of the ETC in intestinal progenitor cells and assess their requirements for cell division, differentiation and consequently, proper tissue homeostasis.

## Thesis outline:

**Screen for the requirement of different ETC subunits in progenitor cells**

To identify ETC subunits that are required for normal function in intestinal progenitor cells, we performed a candidate screen to knock down individual subunits specifically in these cells. Their abundance in the tissue was compared to controls as a readout of survival, self-renewal and differentiation rates. Succinate dehydrogenase subunit D (SdhD) of Complex II was identified as a strong candidate, that upon knockdown caused a significant reduction in the number of progenitor cells.

**The requirements for SdhD in progenitor cell maintenance**

In this section, I explore the requirements for SdhD in each type of progenitor cells (ISCs and EBs) by knocking down SdhD in these cell types individually and characterize its phenotypes in terms of survival and self-renewal potential, assessing differences between the two cell types.

**The requirements for SdhD in progenitor cell differentiation**

In this part, I explore how knocking down SdhD in progenitor cells affects the differentiation choice towards an enterocyte or enteroendocrine fate, by counting the number of differentiated cell types upon SdhD knockdown in progenitor cells, and performing lineage-tracing analysis.

**Mechanisms originating from SdhD knockdown**

Finally, I present possible mechanisms originating from SdhD knockdown, particularly its effects in the accumulation of succinate, and its possible consequences as a signaling molecule.

# Materials and methods

## Fly husbandry and stocks

Flies were raised in vials containing standard cornmeal/molasses/agar medium (in weight/volume: 1% agar, 3% brewer's yeast, 1.9% sucrose, 3.8% dextrose, and 9.1% cornmeal). In experiments using RU486 (mifepristone; described below), an ethanol solution of the compound was mixed in warm, liquid media at a concentration of 10 μg/ml (0.023 mM) and let cool down at room temperature. As control, the same volume of ethanol with no solute was mixed in the media. RU486 was purchased from Cayman Chemicals, cat. #10006317.

As the homeostatic balance in the fruit-fly intestine is highly dependent on age, sexual activity, mating status, and nutritional and environmental conditions, we used special precautions to minimize such variations [122]. All flies used for the experiments were mated females that were kept in vials with no more than 20 individuals and turned onto fresh food vials every 2-3 days. All crosses using RNAi lines were performed at 18 °C, to prevent any 'leakage' expression during development; the progeny was kept at 18 °C until 2-3 days after eclosion and then switched to 25 °C, or 29 °C for flies containing a temperature-sensitive construct ($Gal80^{TS}$, described below), and maintained on a 12-hour light-dark cycle.

All stocks contained a CyO balancer on the second chromosome (II) and a TM3 (third multiple) or TM6 balancer on the third (III), which have several inversions to suppress meiotic recombination. Throughout the text, these are omitted for simplicity.

**The GAL4-UAS system**

The GAL4-UAS system allows expression of genes of interest in specific cell types, via the *Saccharomyces cerevisiae* transcriptional activator GAL4 and the Upstream Activating Sequences (UAS) transcription promoter element. GAL4 binds to UAS genomic sequences, which in turn promotes the expression of a responder gene of choice [123][35]. To achieve this, flies carrying a promoter for a gene specific for cell type (ex.: *esg* for progenitor cells) that initiates GAL4 expression (the duo is termed *driver*) are crossed to flies that carry a UAS sequence promoting a responder gene (ex.: UAS-GFP (Green fluorescent protein)). In this example, expression of GAL4 in progenitor cells promoted by *esg* activates the UAS element which induces expression of GPF in these cells. Uses other than GFP reporters include RNA-interference, fluorescent probes, or overexpression of endogenous genes, among others.

A chimeric version of GAL4 containing a progesterone receptor-ligand-binding domain allows activation of GAL4 only upon binding of the antiprogestin RU486, which can be added to the meal preparation to timely activate GAL4 expression, a system that is

named P{Switch} [124]. As an example, to avoid expression during development, the flies are kept on normal food and upon reaching adulthood are shifted to RU486-containing food. A different method to achieve time-sensitive expression is to co-express the temperature-sensitive GAL4-inhibitor GAL80 from yeast, also termed Gal80$^{TS}$. When flies are incubated at 18 °C, GAL80 inhibits GAL4 activity; however, when the incubation temperature is raised to 29 °C, GAL80 is degraded and Gal4 becomes active [35][125].

**Drivers of gene expression in progenitor cells**

The *Su(H)-LacZ; 5961-Gal4$^{GS}$,esg-GFP$^{NLS}$* line was used to drive *Gal4* expression in progenitor cells (ISCs and EBs). The *5961-Gal4$^{GS}$* construct originated from a large screen consisting of insertions of enhancer-trap P{Switch} elements throughout the genome [126]. With this construct, GAL4 expression was observed in progenitor cells upon RU486 feeding [127]. This line contains a *LacZ* gene originally from *Escherichia coli* that encodes β-galactosidase (β-Gal) and is expressed under the control of *Su(H)* to mark EBs, using anti-β-Gal antibodies. The *esg-GFP$^{NLS}$* reporter expresses a nuclear-localizing GFP in progenitor cells, independent of GAL4 activity. The *5961$^{GS}$* line was a gift from B. Ohlstein and *esg-GFP$^{NLS}$* a gift from L. Cooley; these two constructs were previously recombined by other members of the Jones laboratory at University of California, Los Angeles to generate the aforementioned line. Throughout the text, this line is simply referred to as *5961-Gal4$^{GS}$*.

The *Su(H)-LacZ; esg-Gal4,UAS-GFP,tub-Gal80$^{TS}$* line (referred to simply as *esg-Gal4*) was also used to drive expression in progenitor cells. Both GFP (via GAL4-UAS) and GAL4 are expressed in progenitor cells under the control of *esg.* When flies are incubated at 18 °C, expression of GAL4 is inhibited by the ubiquitously-expressed GAL80 (under the control of *tubulin*), but becomes active when flies are switched to 29 °C, enabling expression of the genes downstream of UAS. The original *esg-Gal4,UAS-GFP,tub-Gal80$^{TS}$* [128] stock was a gift from B. Edgar (Huntsman Cancer Institute, Salt Lake City, USA) and was combined with the *Su(H)-LacZ* line (1$^{st}$ chromosome).

**ISC-specific driver**

The *esg-Gal4,Su(H)-Gal80,UAS-2xYFP; tub-Gal80$^{TS}$* driver was used to drive GAL4 expression specifically in ISCs [129]. This line works similarly to the *esg-Gal4* driver (above) but contains a *Su(H)-Gal80* sequence to express GAL80 in EBs, which blocks GAL4 expression in these cells, restricting GAL4 expression to only ISCs. It also expresses 2 copies of YFP (yellow fluorescent protein) in ISCs that can be marked using anti-GFP antibodies, as these are also specific for YFP. GAL80 is expressed under the control of tubulin to inhibit GAL4

expression during development. This driver was a gift from S. Hou (Center for Cancer Research, National Cancer Institute, Frederick, USA).

**Enteroblast-specific driver**

The *Su(H)-Gal4,UAS-GFP; tubGal80$^{TS}$* line drives expression of GAL4 and GFP in EBs under the control of *Su(H)* [45]. The *tubGal80$^{TS}$* construct allows temporal-specific control of GAL4 expression. This line was a gift from S. Hou (Center for Cancer Research, National Cancer Institute, Frederick, USA).

**Other drivers**

The RU486-sensitive, EC-specific, 5966-Gal4$^{GS}$ driver (referred to as 5966$^{GS}$) originated from the same screen as the *5961$^{GS}$* [127] and was provided by H. Jasper (Buck Institute for Research on Aging, Novato, USA). The *tub-Gal4, Gal80$^{TS}$* was originally developed by Lee and colleagues [130] and drives ubiquitous expression of GAL4.

The lineage-tracing tool *esg-Gal4,tub-Gal80$^{TS}$,UAS-GFP; UAS-flp,act>CD2>Gal4*, termed esg-FlipOut expresses the recombinase Flippase (Flp) in progenitor cells under the control of *esg-Gal4* (and *Gal80$^{TS}$*) which promotes the excision of the CD2 stop codon, allowing expression of *Gal4* under the control of the ubiquitously expressed Actin (Act) to also mark daughter cells with GFP [58][131]. This line was a gift from B. Edgar (Huntsman Cancer Institute, Salt Lake City, USA).

**RNAi lines**

The RNAi lines used in the initial screening were a gift from David Walker (UCLA, Los Angeles, USA) and were originally obtained from the Vienna Drosophila Resource Center (VDRC) [132]. These lines are listed on **Table 1** in section 1 of the Results and discussion chapter. The 2 other RNAi lines targeting SdhD were 10219R-1 (SdhDNIG.10219R), obtained from NIG-Fly Stock Center [133] and 26776 GD from VDRC. The RNAi line against super oxide dismutase 2 (SOD2-RNAi) was acquired from the Bloomington stock center (Indiana University, Bloomington, USA; stock #24484).

**Other stocks**

The *pKC43* line (obtained from VDRC) was used as control for all the KK type VDRC lines, as it contains the equivalent vector that was used to host the RNAi sequences, that lands in the same genomic regions [134]. In this line, the vector contains no RNAi sequence, offering a genetic background identical to that of the RNAi line. For RNAi lines other than the KK collection, the *w$^{1118}$* line was used as control to match their genetic background.

The line for overexpression of the pro-apoptotic genes *reaper (rpr) and head involution defective (hid), UAS-rpr,UAS-hid,* was a gift from E. Rulifson. The Apoliner reporter was a gift from M. Resnik (UCLA, Los Angeles, USA). The Mito-roGFP probe was a gift from R. Demarco (UCLA, Los Angeles, USA).

## Immuno-fluorescence

Samples were prepared following standard procedures [135]. Intestine were dissected whole in phosphate-buffered saline (PBS) solution, fixed in 4 % paraformaldehyde (PFA) for 40 minutes, washed 3X for 10 minutes in PBST (0.1% Triton X in PBS), blocked in 0.3% bovine serum albumin (BSA) in PBST for 30 minutes, incubated in primary antibodies for 4 hours, washed 3X in PBST, incubated in secondary antibodies for 2 hours, washed 3X in PBST and finally incubated for 10 minutes in Vectashield + DAPI (Vector Laboratories, Burlingame, USA). The samples were then mounted on slides in the same media.

### Antibodies

The following primary antibodies were used: mouse anti-Prospero (at a concentration of 1:100), mouse anti-*Snakeskin* (SSK, 1:10) and mouse Anti-Armadillo (1:10), obtained from the Developmental Studies Hybridoma Bank, created by the NICHD of the NIH and maintained at The University of Iowa, Department of Biology, Iowa City, IA 52242. Rabbit anti-phosphohistone H3 (pHH3) from EMD Millipore, Darmstadt, Germany. Rabbit anti-GFP (1:5000) from Molecular Probes, Eugene, USA. Chicken anti-β-Gal (1:100) and chicken anti-GFP (1:200) from Aves Labs, Tigard, USA. The chicken anti-GFP antibody was observed to recognize YFP molecule expressed in the ISC-specific driver *esg-Gal4,Su(H)-Gal80,UAS-2xYFP; tub-GAL80$^{TS}$*. Cell membranes were stained with anti-Armadillo antibodies (the *Drosophila* homologue of beta-catenin) at a concentration of 1:10. Rabbit anti-cleaved-Caspase 3 was obtained from Cell Signaling, Danvers, USA (item #9664).

The secondary antibodies used were the following: Alexa Fluor anti-rabbit 488, anti-chicken 488, anti-mouse 568, anti-mouse 594, anti-mouse 633 and anti-rabbit 647, obtained from Molecular Probes and diluted 1:500 in PBST+BSA.

## qRT-PCR

The enterocyte-specific 5966$^{GS}$ driver was used, since enterocytes constitute most of cell mass in the midgut and only whole midguts were used for mRNA extraction. Adult flies were raised in standard conditions on food containing RU486 or only ethanol for 2 days and

70 intestines on each group were dissected whole and immediately frozen at -80 °C. The samples were prepared according to manufacturer instructions and previous reports [45]: a premix of Trizol (Life Technologies, #15596026) was prepared using the following amounts (per sample): 100 µl of Trizol, 100 ng of tRNA (in water containing diethyl pyrocarbonate (DEPC) to inactivate RNase enzymes), 0.2 µl linear polyacrylamide (LPA; Sigma-Aldrich 56575). A 100 µl of this premix was added to each sample. The suspension was frozen in liquid nitrogen and thawed in water at 37 °C, and repeated 5 times. The suspension was vortexed for 5 minutes at room temperature and left settling for 30 seconds. The procedure was repeated 5 times and then left settling again for 5 minutes. 20 µl of chloroform were added, followed by 15 seconds of vigorous shaking. The tubes were then centrifuged at 10,000 RPM for 15 minutes at 4 °C. 60 microliters of isopropanol were then added to a clean tube and the previous aqueous solution was added on top. The tubes were shaken, vortexed and left settling for 10 minutes at room temperature. The tubes were then centrifuged for 15 minutes at 13,000 RPM and the supernatant was removed. Five hundred microliters of 70 % ethanol in water was added to the remaining pellet and left at -80 °C for 30 minutes. Tubes were again centrifuged, the supernatant removed, and the pellet allowed to air-dry for 5 minutes, and finally re-dissolved it in DEPC water solution.

The samples were then treated with DNase by mixing 1 µl of buffer with 1.5 µl DNase (Promega, cat#M610A) and 1.5 µg of RNA in DEPC water was added to a final volume of 10 µl. The mixture was incubated for 30 minutes at 37 °C, after which 1 µl of stop solution was added and incubated for 10 minutes at 65 °C. For the reverse transcriptase (RT) reaction, 7.33 µl of RNA in solution were mixed with 4 µl of RT mix (iScript kit, Bio-Rad, #170- 8841) and water was added to a final volume of 20 µl. A no-RT reaction was run in parallel to the control. The reaction ran for 5 minutes at 25 °C, followed by 30 minutes at 42 °C and finally 5 minutes at 85 °C.

For qPCR reactions, forward and reverse primers were equally combined in the same aliquot at a concentration of 4 µM in water. For each well were added 10 µl of SYBR Green (Bio-Rad, #1725-264), 2.5 µl of 0.5 µM oligonucleotides solution, 6.5 µl of water and 1 µl of cDNA solution. Dilutions were performed in the ratios of 1:1, 1:5, 1:25 and 1:125. Plates were strongly vortexed and then centrifuged to settle down the solution. The samples were run in triplicate. Thermocycler settings: 30 minutes at 95 °C, and 40 cycles of 5 min at 95 °C, plus 30 min at 62 °C. Equipment: CFX96/C1000 Touch system (Bio-Rad).

Primers used: SdhD (CG10219) Forward: ACTCCCCTGAAGAGCTACTCC, Reverse: ACGGGCGCTACAATCTTGG; PTPMT1 (CG10371) Fwd: CGTTTCCTTCTACCCCACCC, Rev: CCCAGTATCACATGCTCATCG; RP49 Fwd: ATCGTGAAGAAGCGCACCAA;

Rev: TGTCGATACCCTTGGGCTTG. All primers were manufactured by IdT Technologies, Iowa, USA.

## Assessment of oxidative state using the mito-roGFP probe

The genetically-encoded Mito-roGFP reporter was used to quantify the ratio of oxidative/reductive potential within progenitor cells. This construct consists of a modified GFP protein containing two cysteines that, upon oxidation, form a disulfide bond between the both, shifting the excitation wavelength of GFP [136]. The ratio of oxidized/reduced GFP can then be determined by exciting the protein under a confocal microscope using two different excitation wavelengths – 405 nm for the oxidized molecule and 476 nm for the reduced - and acquiring the corresponding green signal for each of the excitation wavelengths. The ratio between intensity of emission in the green spectrum for each of the excitation wavelengths is a read-out of the oxidative environment within the cell. In an oxidizing environment, the ratio of the oxidation/reduction is higher than that in normal conditions. This specific probe localizes to the mitochondria.

The intestines were quickly dissected in PBS on ice. Samples for reduced or oxidized controls were incubated in the reducing agent DTT (1,4-Dithiothreitol; 10 mM; Sigma D0632) or the oxidizer Diamide (1 mM; Sigma D3648), respectively, for 30 minutes. Both samples were dissolved in a solution of PLP cofactor (Pyridoxal 5'-phosphate; Sigma P9255)and then moved to a solution containing NEM (N-Ethylmaleimide; Sigma E1271) and 4% PFA fixatives in PLP for 30 minutes and subject to a standard immunostaining protocol, while protecting from light. Positive controls were confirmed to be oxidized or reduced by exhibiting a strong signal in the corresponding channels. Anti-armadillo antibodies were used to stain cell membranes.

## Imaging and cell counting

This work focused on the P3-P4 region of the *Drosophila* midgut (previously described in a characterization of the intestinal morphology and function [122]), as it is the region where most of the research in progenitor cells in the intestine of *Drosophila* cited in this thesis is focused on. Intestines were observed under a Zeiss LSM 710 Laser Scanning confocal microscope, using 40X or 63X objectives and scanned as z-stacks of approximately 1 µm thickness each, capturing all ISCs, EBs, EEs and ECs in the field of view (FOV). Z-stacks were converted to maximum intensity projections using an automated plug-in running on the Fiji software (ImageJ) [137]. Maximum intensity projections were then imported into Cell Profiler [138] where the cells were automatically counted, according to their fluorophore

color and size. The number of cells of interest per FOV was normalized to the total number of cells in the same FOV (marked by the nuclear stain DAPI). Statistical analyses were performed using the GraphPad Prism version 5.03, GraphPad Software. The significance in cell counting experiments was determined using a two-tailed, unpaired Student's t-test and expressed as p values.

## Apoptag kit for detection of apoptosis (TUNEL assay)

The test used to detect apoptosis is based on the TUNEL assay (Terminal deoxynucleotidyl transferase (TdT) dUTP Nick-End Labeling) which detects fragmented DNA ends characteristic of apoptotic cells, by addition of modified nucleotides that can be detected with antibodies [139][140]. The DNA strand breaks are detected by enzymatically labeling the free 3'-OH termini — that are found in apoptotic cells — with modified digoxigenin(DIG)-nucleotides, by catalytic action of the terminal deoxynucleotidyl transferase (TdT) enzyme. Anti-DIG antibodies conjugated to a peroxidase reporter are then used to label DIG-nucleotides.

The Apoptag kit (red) was purchased from Chemicon International (Temecula, USA #S7165), the anti-DIG-POD from Roche (# 11 207 733 910) and Tyramide Signal Amplification (TSA) fluorescence kits from PerkinElmer.

The protocol was performed according to manufacturer instructions: intestines were dissected in PBS on ice, fixed in 2% paraformaldehyde in PLP for 30 minutes, rinsed in PBST, incubated 2x 10 minutes in PBST + Na-deoxycholate (0.3%), rinsed twice in PBST, rinsed twice in equilibrium buffer and incubated for 2 minutes at room temperature in the same buffer. Samples were then incubated in reaction buffer with DNA-polymerase TdT enzyme (in a 7:3 ratio for 1 hour at 37 °C, rinsed with stop/wash solution and incubated for 10 minutes in the same solution, rinsed and washed in PBST and blocked in TNB blocking buffer (0.1M Tris-HCl, pH 7.5, 0.15M NaCl, 0.5 % blocking reagent) for 30 minutes, incubated in sheep anti-DIG-POD antibody in TNB overnight at 4 °C, washed with PBT, incubated in a solution of TSA-cyanine 3 diluted 1:50 in amplification diluent for 30 minutes at room temperature and finally washed in PBST and mounted in Vectashield.

## Quantification of succinate by GC-MS

Gas chromatography – mass spectrometry (GC-MS) is a standard analytical method for precise detection, identification, and quantification of different molecules. A chromatographic column offers a high separation rate between different analytes in the

sample (mobile phase) dependent on their interaction with the column (stationary phase) and on the temperature at which the column is. Following separation, analytes then enter the mass spectrometer where they are bombarded by electrons and split into several ionic components, to finally reach a detector that determines their mass-to-charge ratio (charge is usually +1 or -1) and abundance. Analysis of the mass of the split components allows for identification of the original compound by comparison of the obtained spectra with that of an empirical library of known compounds, or alternatively, predicted theoretical spectra. GC-MS offers a strong advantage that in a ~30-minute run is able to detect and quantify several compounds, in contrast to colorimetric assays that normally only allow for the quantification of one single analyte at a time [141].

Gas chromatography requires analyzed molecules to be volatile, so they can enter the column in the gaseous phase. Succinic acid (succinate at biological pH) is not readily volatile and therefore needs to be derivatized. The derivatization of succinic acid consists in replacing the hydrogens in its hydroxyl groups (-OH) with a trimethylsilyl group (-3($CH_3$)Si) (**Figure 3**). This is achieved by combining N-Methyl-N-(trimethylsilyl) trifluoroacetamide (MSTFA, Sigma #M7891) with the sample in a reaction termed “silylation” (named after its silicone-containing group), resulting in succinic acid bis(trimethylsilyl) ester (abbreviated as succinic acid 2TMS). Derivatization eliminates the strong interactions between the hydroxyl groups of neighboring molecules, resulting in increased volatility and thermal stability, which provides a better separation between different molecules and a more precise quantification [142].

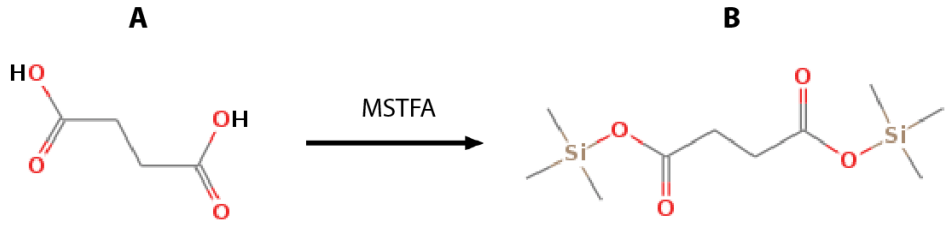


**Figure 3: Derivatization of succinic acid**
Derivatization of succinic acid (**A**) by reacting with MSTFA (N-Methyl-N-(trimethylsilyl) trifluoroacetamide), in which the hydrogen atoms in the hydroxyl group (-OH) are replaced by a trimethylsilyl group (–Si($CH_3$)$_3$), obtaining its silylated derivative, succinic acid bis(trimethylsilyl) ester (abbreviated as succinic acid 2TMS) (**B**). Images obtained from the NIST online library [143].

### Extraction of fruit-fly samples for succinate quantification

Control (pKC43) and SdhD-RNAi (101739 KK) flies were crossed to the ubiquitous *tub-Gal4,Gal80$^{TS}$* driver, that expresses Gal4 under the control of *tubulin* and *Gal80$^{TS}$*. Parental flies were crossed at 18 °C and progeny was switched to 29 °C 2-3 days after eclosion and incubated for 13 days before extraction.

The extraction process was based on previous reports [144][145]. 15 flies on each group, with 3 biological replicates, were anesthetized using $CO_2$, placed in a 1.5 mL Eppendorf tube, immediately washed twice in cold 1X PBS, and soaked in 500 µL 90% methanol in water at -20 °C. Flies were then homogenized manually using a small plastic pestle, snap-frozen in liquid nitrogen and thawed twice, and incubated for 1 h at -20 °C. Tubes were then centrifuged at 10,000 rpm for 10 min, the supernatant was extracted to a new tube and a second extraction was performed using 60 % methanol at -20 °C. The supernatants were combined and lyophilized at -50 °C under vacuum. To the dry extracts was added 30 µl of acetonitrile (ACN) solvent and 90 µL MSTFA and incubated at room temperature for 2 hours. ACN was chosen for its ability to dissolve succinic acid.

**GC-MS equipment and parameters**

The experiments were performed on a Thermo Scientific ITQ 900 Trace GC Ultra device equipped with a DB5 column, using analytical-grade Helium as a carrier gas. The software Thermo Xcalibur was used for acquisition and the Thermo Xcalibur Qual Browser 2.2 with a set of NIST MS libraries (NIST v7, Mass Spectrometry Data Center, National Institute of Standards and Technology, Gaithersburg, USA ) was used for compound identification.

The following sampling parameters were used: 3 plunger strokes, pre-injection of 5.0 µL and needle wash with 40 µL ACN. 1 µL of sample was delivered to the injector at 250 °C. Oven: Initial temperature of 60 °C for 1 min and increase 10 °C/min up to 250 °C, resulting in a run time of about 20 min; Helium flow of 1 mL/min; transfer line at 290 °C; solvent delay of 8.50 min; ion source at 230 °C; MS oven at 150 °C; mass range of 50 to 600 m/z.

Succinic acid (purchased from Sigma, #S9512) was derivatized to succinic acid 2TMS and used as a standard to provide a location reference in the chromatogram and to confirm its mass spectra. Control and SdhD-RNAi samples were analyzed in random order, with 3 ACN cleaning cycles and 1 ACN+MSTFA cycle as cleaning/negative control in between.

Succinic acid 2TMS in samples was identified in the same region in the chromatogram as the standard sample (at a retention time of 14.04 minutes). Peak detection and calculation of area were performed automatically by the Thermo Xcalibur Qual Browser v.

2.2 software, using absolute intensity values. Ares of the peaks (in arbitrary units) corresponding to the amounts of succinate in control and RNAi groups were then exported to the Graphpad Prism software (v5.03) for statistical analysis.

# Results and discussion

# I - Screen for electron transport chain subunits with an impact in progenitor cell activity

| Complex | Symbol | Name of target | Annotation | VDRC stock ID |
|---|---|---|---|---|

To assess the requirement for individual subunits of the ETC in intestinal progenitor cells (ISCs and EBs), we performed a candidate screen that consisted in knocking down different ETC subunits specifically in progenitor cells by means of RNAi. The abundance of progenitor cells in the tissue after RNAi expression was used as a read-out of the screen to determine changes in survival, proliferation or differentiation rates.

Specific genes were chosen for their importance in terms of structural roles (such as complex I assembly factor, CIA30), enzymatic activity (SdhA) or direct electron transport function (Cyt-C1L) according to published reports cited in Flybase [146]. These lines also target genes that, upon ubiquitous constitutive knockdown, resulted in lethality or changes in the lifespan of flies in the study by Copeland and colleagues mentioned in the Introduction chapter [121] (section 3.4). These RNAi lines and corresponding genes are listed in **Table 1**.

Activation of RNAi expression specifically in intestinal progenitor cells was induced by the driver *Su(H)-LacZ; 5961-Gal4$^{GS}$,esg-GFP$^{NLS}$* (*5961$^{GS}$*), which is activated by the drug RU486 (referred to as RU from hereon now) that is dissolved in ethanol (EtOH) and added to the fly meal. As schematized in **Figure 4**, female flies containing the UAS-RNAi sequence for each of the genes of interest were crossed with males carrying the *5961$^{GS}$* line containing an *esg-GFP$^{NLS}$* reporter that expresses GFP localizing to the nuclei of progenitor cells, to identify these cells. Fly crosses were set up on vials containing normal food (no RU or ethanol), and were kept at 18 °C to minimize any possible 'leakage' of RNAi expression during development. Upon reaching adulthood, 2-3 days after eclosion, flies were separated into two groups: one in vials containing food where a solution of RU in ethanol was added (to activate RNAi expression), and the second where only ethanol was added to the food, as isogenic controls with no RNAi expression. Flies were left on each type of food for 8 days at 25 °C, at which point the intestines were dissected, prepared for immunofluorescence and scanned under a fluorescence microscope, obtaining several sections to cover all ISCs, EBs, ECs and EEs, and processed as z-stack projections.

**Table 1: List of RNAi lines selected for the candidate screen**

| | | | | |
|---|---|---|---|---|
| Complex I | CIA30 | Complex I intermediate-associated protein, 30 kDa (assembly factor) | CG7598 | 14859 GD |
| | ND-B12 | NADH dehydrogenase (ubiquinone) B12 subunit | CG10320 | 104890 KK |
| | ND-13A | NADH dehydrogenase (ubiquinone) 13 kDa A subunit | CG8680 | 102017 KK |
| | ND-PDSW | NADH dehydrogenase (ubiquinone) PDSW subunit | CG8844 | 106095 KK |
| | ND-ACP | NADH dehydrogenase (ubiquinone) acyl carrier protein | CG9160 | 107907 KK |
| | ND-18 | NADH dehydrogenase (ubiquinone) 18 kDa subunit | CG12203 | 101489 KK |
| | ND-B14 | NADH dehydrogenase (ubiquinone) B14 subunit | CG7712 | 100616 KK |
| Complex II | SdhAL | Succinate dehydrogenase, subunit A (flavoprotein)-like | CG5718 | 100071 KK |
| | | | | 42443 GD |
| | SdhC | Succinate dehydrogenase, subunit C | CG6666 | 6031 GD |
| | SdhD | Succinate dehydrogenase, subunit D | CG10219 | 101739 KK |
| Complex III | UQCR-C2 | Ubiquinol-cytochrome c reductase core protein 2 | CG4169 | 100818 KK |
| | Cyt-C1L | Cytochrome c1-like | CG14508 | 106229 KK |
| | UQCR-Q | Ubiquinol-cytochrome c reductase ubiquinone-binding protein | CG7580 | 101371 KK |
| Complex IV | COX7C | Cytochrome c oxidase subunit 7C | CG2249 | 104970 KK |
| | COX4L | Cytochrome c oxidase subunit 4-like | CG10396 | 106700 KK |
| | COX6B | Cytochrome c oxidase subunit 6B | CG14235 | 20702 GD |
| | COX4 | Cytochrome c oxidase subunit 4 | CG10664 | 3923 GD |

♀ UAS-RNAi line x ♂ *5961$^{GS}$* progenitor-cell

Maximum-intensity projections of immunofluorescence images were loaded into the Cell Profiler software [138] to automatically identify and count the population of progenitor cells (GFP-positive) and the number of total cells in the field of view (marked by the nuclear

18 °C

**Figure 4: Candidate screen workflow diagram**

To knock down individual subunits of the ETC in progenitor cells (ISCs and EBs), females containing each RNAi construct were crossed with males carrying the progenitor cell-specific driver *Su(H)-LacZ; 5961$^{GS}$,esg-GFP* and incubated at 18 °C, to minimize any possible RNAi leaking during development. Upon reaching adulthood (2-3 days after eclosion), progeny were separated into vials containing food mixed with an ethanol solution of the drug RU486 to induce RNAi expression, and vials containing only food with the vehicle ethanol, as control. Both groups were then incubated at 25 °C for 8 days, after which the intestines were dissected for immunofluorescence, scanned under the microscope and the numbers of cells were counted.

stain DAPI). The abundance of progenitor cells in the region of interest (corresponding to 1 field of view) was obtained as the number of progenitor cells divided by the total number of cells (DAPI-positive). Data for each intestine were plotted as a circle (control) or a square (RNAi) and grouped for each RNAi line (**Figure 5**).

The RNAi line producing the most significant phenotype was subunit D of complex II (SdhD), that caused a substantial decrease in the abundance of progenitor cells. Knockdown of subunit C of complex II (SdhC) also resulted in a significant decrease in the population of progenitor cells, albeit more modest, which suggests a complex II-specific role that will be discussed later in section 4.3. Knockdown of SdhA with 2 different RNAi lines, however, resulted in a modest, non-significant increase in the number of these cells. In the study by Copeland and colleagues [121], ubiquitous knockdown of SdhA (42443 GD line) during development and adulthood increased lifespan up to about 27%, while knockdown of SdhC was semi-lethal (resulted in low numbers of adult progeny), and knockdown of SdhD was lethal (no adult progeny). These data show an interesting correlation between the resulting abundance of progenitor cells in our screen and lethality/lifespan in the aforementioned study.

In complex I, RNAi against CIA30 resulted in an increase in the number of progenitor cells. In the Copeland study, knockdown of ND-B12, ND-13A, ND-PDSW and ND-ACP resulted in lethality and ND-18 was semi-lethal, correlating again with a (small) decrease in the abundance of progenitor cells in our screen. RNAi against PDSW of complex I, previously mentioned in section 3.4 as its mutant allele causing cell cycle arrest in the developing eye of *Drosophila*, showed only a small, non-significant reduction in the number of progenitor cells when compared to controls, suggesting that PDSW is not required in progenitor cells, or alternatively, that RNAi knockdown did not lower its levels as much as the mutation, eliciting only a mild effect.

In complex III, expression of UQCR-C2 RNAi resulted in a mild, non-significant reduction in the abundance of progenitor cells, and in the Copeland study resulted in reduced lifespan to about 58% of controls. In the same study, expression of RNAi against COX7C of complex IV resulted in a 57.1% increase in lifespan, while in the present screen it did not result in any significant changes.

There seems to be a general correlation between reduction in the abundance of intestinal progenitor cells and lethality upon expression of different subunits, suggesting that intestinal progenitor cells are sensitive to knockdown of ETC subunits in a similar manner to other cells during development.

Overall, the average number of normalized progenitor cells in EtOH controls shows a strong variance between different RNAi lines. We attribute this to differences in genetic backgrounds despite the GD and KK collections being supposedly isogenic; or, an example of the sensitivity of intestinal homeostasis that could shift upon very small environmental changes. Furthermore, the datapoints for each group show a strong variance between them, which is more visible in complex I. The focus of this project was on SdhD of complex II as it showed a strong significance and more solid data.

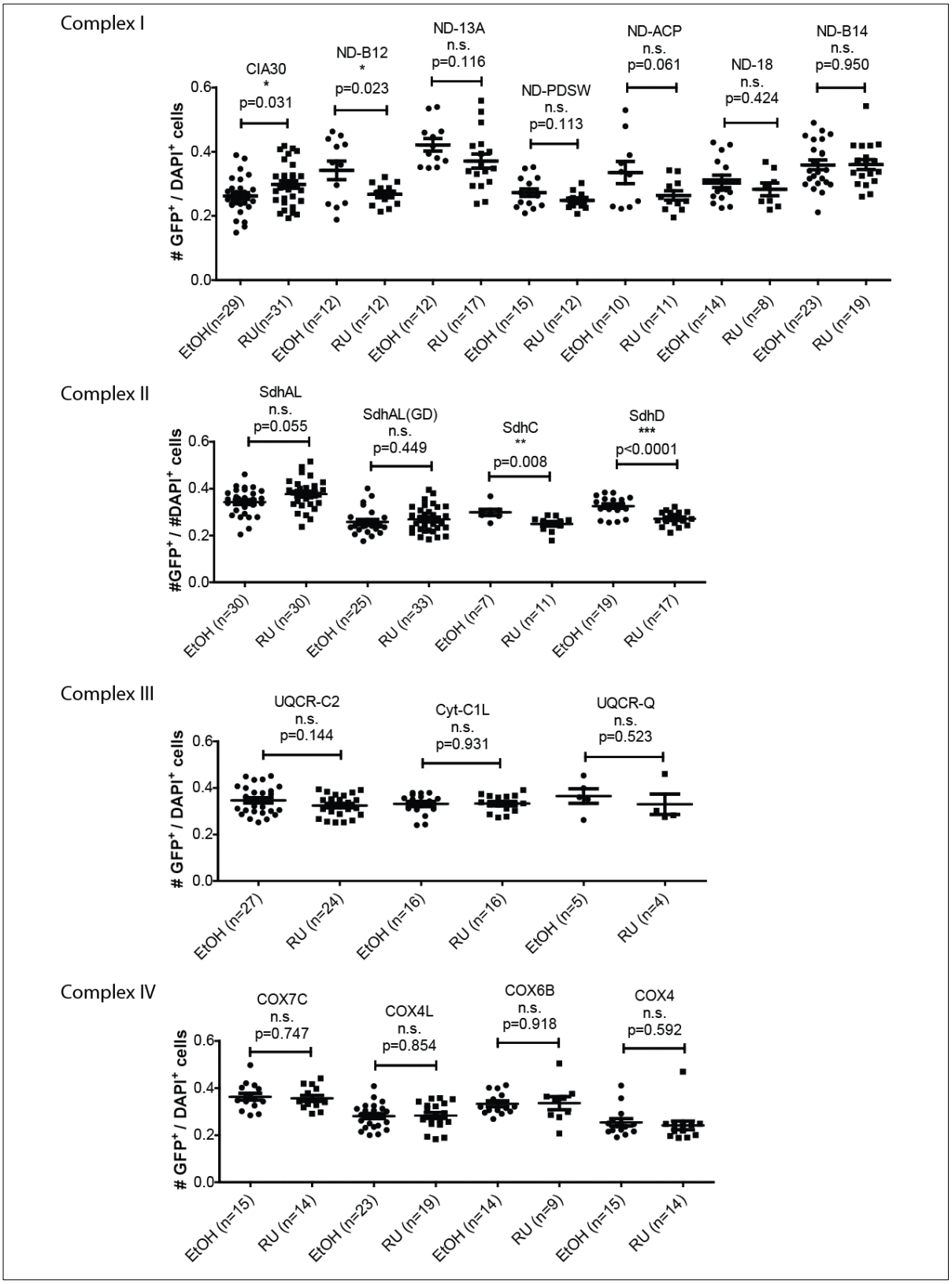


**Figure 5: Results of candidate screen for regulators of progenitor cell activity**

Number of progenitor cells (GFP-) adjusted to the total number of cells ($DAPI^+$) obtained in the same field of view, plotted for each ETC subunit as control (EtOH, circles) vs RNAi (RU, squares). Horizontal lines in plots represent means of the obtained values, with standard error of the mean (SEM). *n* refers to the number of individuals in each group. RNAi of SdhD of Complex II resulted in the most significant phenotype, causing a reduction in the number of progenitor cells, which was also observed at a smaller scale with SdhC knockdown. Unpaired two-tailed Student's *t*-test. n.s.: non-significant difference ($p>0.05$); *: $p\leq0.05$; **: $p<0.01$; ***: $p<0.001$.

## 1.1- Knockdown of succinate dehydrogenase subunit D in progenitor cells causes a decrease in its population

The immunostaining images below (**Figure 6**) show the effects of SdhD-RNAi for 8 days in progenitor cells of the intestine (marked with GFP, in green; isolated in the panels in the middle, in grey), representative of the quantifications in **Figure 5**. These data show a reduced abundance of progenitor cells in the SdhD-RNAi group (lower panels) when compared to controls (upper panels). The DAPI channels showing the nuclei of all cell types are isolated in the panels on the right.

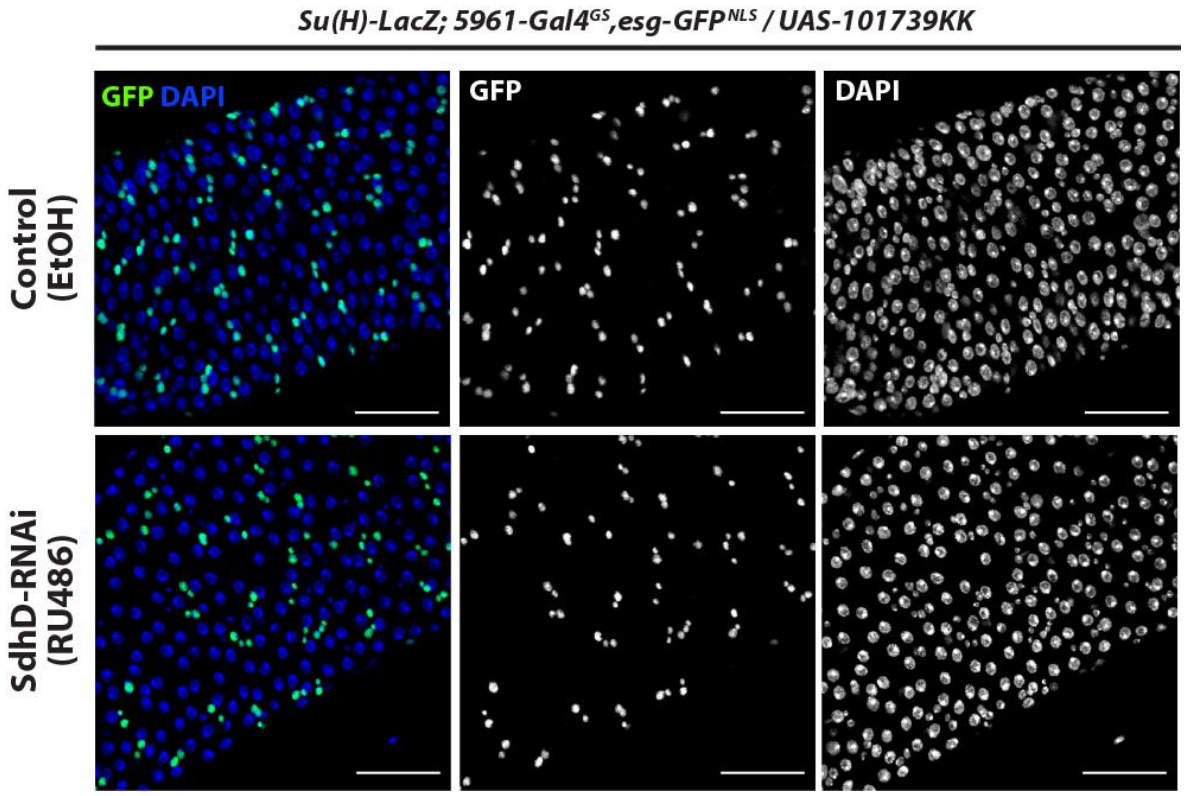


**Figure 6: Effects of SdhD knockdown in progenitor cells using the *5961$^{GS}$* driver**
Immunofluorescence images acquired perpendicularly to the intestinal axis, processed to maximum z stack projections, depicting representative examples of control (EtOH, upper panels) vs SdhD knockdown (RU, lower panels) after 8 days of RNAi expression in progenitor cells, using the 5961$^{GS}$ driver. Progenitor cells are shown in the left panels in green, marked by an *esg-GFP$^{NLS}$* reporter and isolated in greyscale the panels in the middle. Cell nuclei were stained with DAPI (isolated in panels on the right). SdhD knockdown produced a decrease in the number of progenitor cells, as shown here and quantified in the graph in Figure 5. Scale bars = 50 µm. n=19 in the EtOH group and n=17 in the RU (SdhD-RNAi) group.

To validate the SdhD-knockdown phenotype observed in the screen, we repeated the experiments using the progenitor cell-specific *Su(H)-LacZ; esg-Gal4,UAS-GFP,tub-Gal80$^{TS}$* driver (referred to simply as *esg-Gal4*; described in the Materials and Methods section) that in similarity with the *5961$^{GS}$* driver, activates expression of GAL4 in both ISCs and EBs. This line also contains a *Su(H)-LacZ* reporter that induces LacZ expression in EBs, allowing for

individual identification of both cell types. Flies were kept at 18 °C during development to repress RNAi expression, and were switched to 29 °C 2-3 days after eclosion, to induce SdhD-RNAi.

Knockdown of SdhD in progenitor cells using the *esg-Gal4* driver causes a sharp decrease in their population at day 6 (**Figure 7 A**, quantified in **B**), as revealed by GFP staining (in green on the left panels; isolated in greyscale in the middle panels). These results are in accordance with the data shown for the $5961^{GS}$ driver in the screen; in the present case, however, the phenotype is stronger, which is attributed to a stronger expression of the *esg-Gal4* driver as previously observed [45][147]. With the *Su(H)-LacZ* reporter and antibodies against β-Gal (the product of LacZ; isolated in greyscale in the panels on the right), ISCs and EBs were identified separately and their numbers were assessed. The abundance of both ISCs and EBs was significantly reduced, as shown in the graphics. These results were partially validated using other two different RNAi lines against SdhD (26776 GD and 10219R-1; **Supplemental Figure 1**). Although the number of ISCs is only slightly, non-significantly reduced with the two different SdhD-RNAi lines, the number of EBs is significantly reduced as in the case of the 101739KK RNAi line described here. The occurrence of progenitor cell pairs appears to be reduced in the 3 cases, which is attributed to loss of EBs. Differences in phenotype strength between the different RNAi lines against SdhD are attributed to variations in RNAi effectiveness of each line.

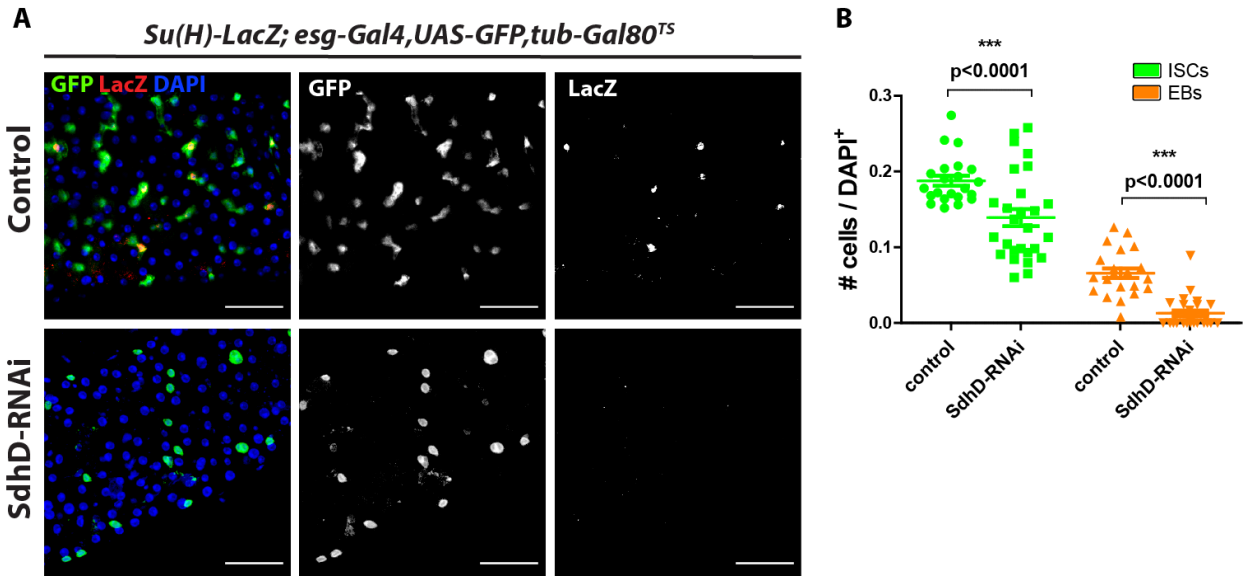


**Figure 7: Effects of SdhD knockdown in progenitor cells using the *esg-gal4* driver**
**A.** Knockdown of SdhD in progenitor cells (marked with GFP) using the progenitor cell-specific *esg-Gal4* driver, crossed to the 101739KK SdhD-RNAi line (lower panel), or pKC43 empty-vector control (upper panel). A visible reduction in the number of progenitor cells (isolated in the panels in the middle) is observed after 6 days of RNAi expression, when compared to controls. LacZ staining reveals that the number of EBs is strongly reduced (panels on the right) in SdhD-RNAi individuals (lower right panels). **B.** The number of ISCs per field of view was quantified by subtracting the number of $LacZ^+$ cells (EBs) from the number of $GFP^+$ cells (ISCs+EBs), and was

divided by the total number of cells in the same field of view and plotted in the graphic (in green), showing a significant reduction in their abundance. The numbers of EBs are also significantly reduced, as seen in the orange plots. n=24 in control group and n=30 in SdhD-RNAi. Lines represent mean with SEM. Unpaired two-tailed Student's *t*-test. Scale bars = 50 µm.

### 2.1.2 Depletion of progenitor cells using the *esg-Gal4* driver occurs in a gradual manner

To characterize the effects of SdhD depletion in progenitor cells over time, SdhD-RNAi was expressed in these cells using the *esg-Gal4* driver and intestines were analyzed after 15 and 30 days. Inhibition of SdhD for 15 days further reduced the abundance of progenitor cells (**Figure 8 A'**, quantified in **A''**) when compared to day 6 (**Figure 7 A** in the previous section, lower panels), and eventually reached zero in most samples at day 30 (**B',** quantified in **B''**). In contrast, control flies display increasing numbers of GFP-positive cells at day 15 (**A**) and 30 (**B**) (quantified in **A''** and **B''**), as a normal aging phenotype (as described in part 2 of the Introduction chapter). SdhD-RNAi progenitor cells at day 15 (**A'**) appear to be shrunk, which will be discussed in section 2.3. It has previously been shown that intestines maintain their population of differentiated cells (EEs and ECs) for at least 20 days following complete ablation of progenitor cells, suggesting that maintenance of differentiated cells is possible without progenitor cells, at least in unchallenged conditions [148].

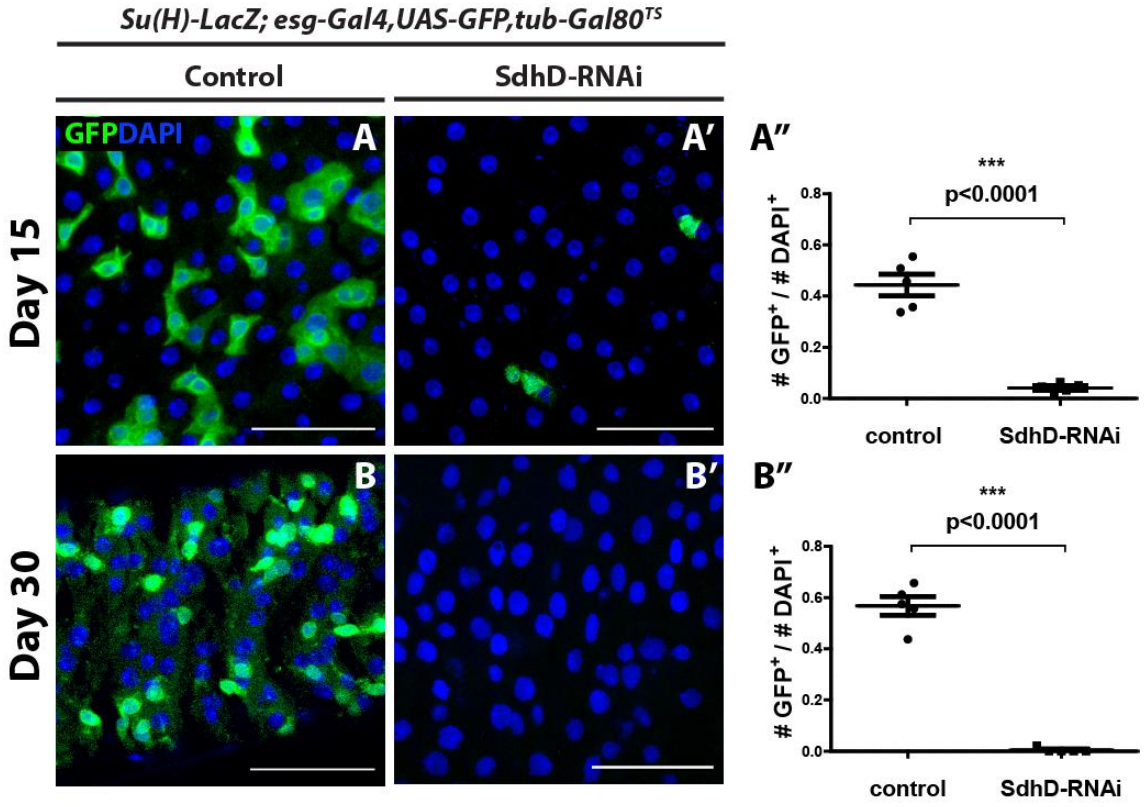


**Figure 8: Progression of the SdhD knockdown phenotype using the *esg-gal4 driver***
Representative images indicating a progression of the SdhD knockdown phenotype in progenitor cells after 15 and 30 days of RNAi induction. The number of progenitor cells drastically decreased in the SdhD-RNAi group at day 15 (A') when compared to controls (A; quantified in A''), reaching eventually zero in most samples at day 30 (B vs B'; quantified in B''). In controls, the opposite effect is observed, where the number of GFP-positive cells increased (A vs B; quantified in A'' and B'', in the plots on the left), which is a normal occurrence during aging. Furthermore, the cells in the SdhD-RNAi group at day 15 exhibit morphological changes, such as shrinking.

Sample sizes: day 15: n=5 in controls and n=5 in SdhD-RNAi; day 30: n=6 in controls and n=11 in SdhD-RNAi. Scale bars = 50 µm.

## 1.2- qRT-PCR quantification confirms downregulation of SdhD transcripts upon RNAi expression

To confirm the effectiveness of the SdhD-RNAi line (ID 101739 KK, VDRC), the levels of SdhD mRNA in flies expressing SdhD knockdown versus controls were assessed via qRT-PCR (quantitative real-time reverse transcription-polymerase chain reaction). The RNAi line was crossed to the EC-specific driver *5966-Gal4$^{GS}$*, the adult flies were left on RU/ethanol-containing food for 2 days and whole guts were processed for analysis. This specific driver was chosen because ECs comprise most of the cells in the gut, allowing whole-gut mRNA extractions for quantification. RNAi was induced for 2 days which was considered to be enough for RNAi expression and activity, while minimizing other possible phenotypes at the intracellular level.

The housekeeping gene *ribosomal protein 49* (RP49) was used as a normalization standard, as previously described [51][71][149]. VDRC reports that the 101739 KK RNAi line has a theoretical off-target — the PTPMT1 (protein tyrosine phosphatase, mitochondrial 1) transcript [132]. For this reason, mRNA levels of this gene were also quantified to determine whether unintentional PTPMT1 knockdown occurred.

qRT-PCR quantification confirmed that mRNA levels of SdhD were lowered in intestines of flies expressing SdhD-RNAi to levels about half of the ones in controls (**Figure 9**, bars on the left), showing that the 101739 KK line is effective in knocking down SdhD.

Levels of the predicted off-target gene PTPMT1, on the other hand, were increased upon activation of the RNAi line (**Figure 9**, black (control) and grey (RNAi) bars to the right), showing that the RNAi expression with the 101739 KK line did not lower its levels. PTPMT1 is a protein that localizes to the mitochondria and was previously found to have a role in modulating mitochondrial membrane morphology and respiration in mice, as well as upregulation of SdhA activity in zebrafish [150][151]. This role of PTPMT1 in upregulating SdhA activity could explain why SdhD-RNAi lead to upregulation of this gene. Conceivably, suppression of SdhD in ECs could cause a decrease in enzymatic activity of SdhA, as previously observed in other systems [152][153], which could induce an increase in PTPMT1 levels as a response to reestablish SdhA function. These mechanisms were not assessed in this study.

These data indicate that the 101739KK RNAi acts effectively to downregulate the levels of SdhD without decreasing the levels of the predicted PTPMT1 transcript.

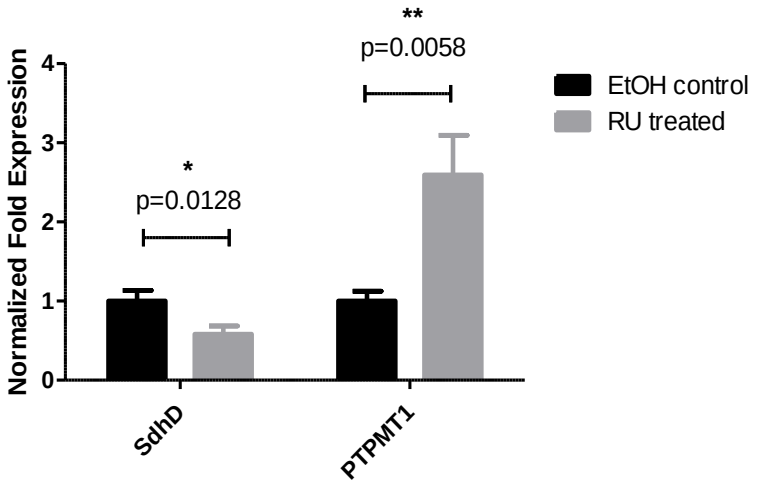


**Figure 9: Levels of SdhD and PTPMT1 mRNA upon RNA-interference against SdhD**
Quantification of SdhD levels in whole intestines upon SdhD knockdown in ECs using the $5966^{GS}$ driver crossed to the 101739 KK RNAi line to target SdhD. The levels of SdhD mRNA (bars on the left) are lowered upon SdhD-RNAi (RU-treated flies; grey bar) when compared to controls (ethanol-treated flies; black bar). The levels of the predicted off-target gene PTPMT1 (bars on the right) are strongly increased upon SdhD-RNAi (grey bar) when compared to controls (black bar). Values are normalized to RP49 (ribosomal protein 49) transcript levels in EtOH controls. Horizontal lines represent SEM. n=3 replicates for each group of 70 intestines. Unpaired two-tailed Student's *t*-test.

**Remarks:**

These sections introduced SdhD as a strong candidate required to maintain normal numbers of both ISCs and EBs. It was also shown that the *esg-gal4* driver induces a stronger phenotype than the $5961^{GS}$, and that the SdhD-RNAi phenotype when using *esg-gal4* is progressive, resulting in a total loss of progenitor cells in the region of interest after 30 days. These experiments focused on the requirement for SdhD simultaneously in ISCs and EBs and did not explore the effects in each cell type individually. In the following chapters, the requirements of SdhD for ISCs and EBs separately are covered, using drivers of expression specific for each cell type.

# II – Effects of SdhD knockdown in ISCs and EBs

## 2.1- SdhD is required in intestinal stem cells, but not enteroblasts, to maintain progenitor cell population

### 2.1.1 Knockdown of SdhD specifically in ISCs causes a depletion in the population of both ISCs and EBs

The results presented in the previous sections revealed that knockdown of SdhD in progenitor cells (in ISCs and EBs simultaneously) causes a reduction in the population of both cell types. To assess the cell-type specificity of SdhD knockdown, the ISC-specific driver *esg-Gal4,Su(H)-Gal80,UAS-2xYFP; tub-Gal80$^{TS}$* (described in the Materials and methods chapter) was used to knock down SdhD in exclusively ISCs and the resulting abundance of both ISCs and EBs was assessed. RNAi expression was activated by shifting the flies from 18 °C to 29 °C after they reached adulthood — 2-3 days after eclosion — and intestine were dissected after 7 days.

Knockdown of SdhD in ISCs resulted in a significant decrease in their population (**Figure 10 A**, quantified in **A''**, in green). To assess the population of EBs in the absence of a *Su(H)-LacZ* reporter in this line, these cells were identified as being YFP-negative (that marks only ISCs), Prospero-negative (that marks EEs) and not delimited by the EC-specific membrane stain Snakeskin (SSK) [69]. A detailed example of an EB is shown in the **A'** insets in a control intestine, in an ISC-EB pair where the ISC is marked by YFP (in green) and the EB is pointed by the arrow, as a small, Prospero-negative, YFP-negative cell; the SdhD-RNAi example shows an ISC-EE pair, where the EE is marked by Pros (in red). Determining the abundance of EBs revealed that knockdown of SdhD exclusively in ISCs resulted in a significant decrease in the population of EBs (quantified in **A''**, in orange). The size of ISCs and ECs appear to be increased in SdhD-RNAi flies, which will be discussed in section 2.4.

These results are in line with the ones described in 1.1 for both progenitor cell types and indicate that SdhD is required in ISCs to maintain the abundance of both ISCs and EBs at normal levels. At a functional level, possible reasons for progenitor cell depletion include reduced division rates, cellular death or forced differentiation to other cell types. In the following sections, these parameters are discussed in the context of SdhD knockdown in ISCs. In the case of EB loss, a possible explanation is a reduction in the number of ISCs leading to failure in replenishing the pool of EBs population via asymmetrical division, while existing EBs normally differentiate to either EEs or ECs. In Section III it is confirmed via a lineage-tracing experiment that differentiation still occurs upon SDhD knockdown in progenitor cells. The following section explores the requirements for SdhD specifically in EBs.

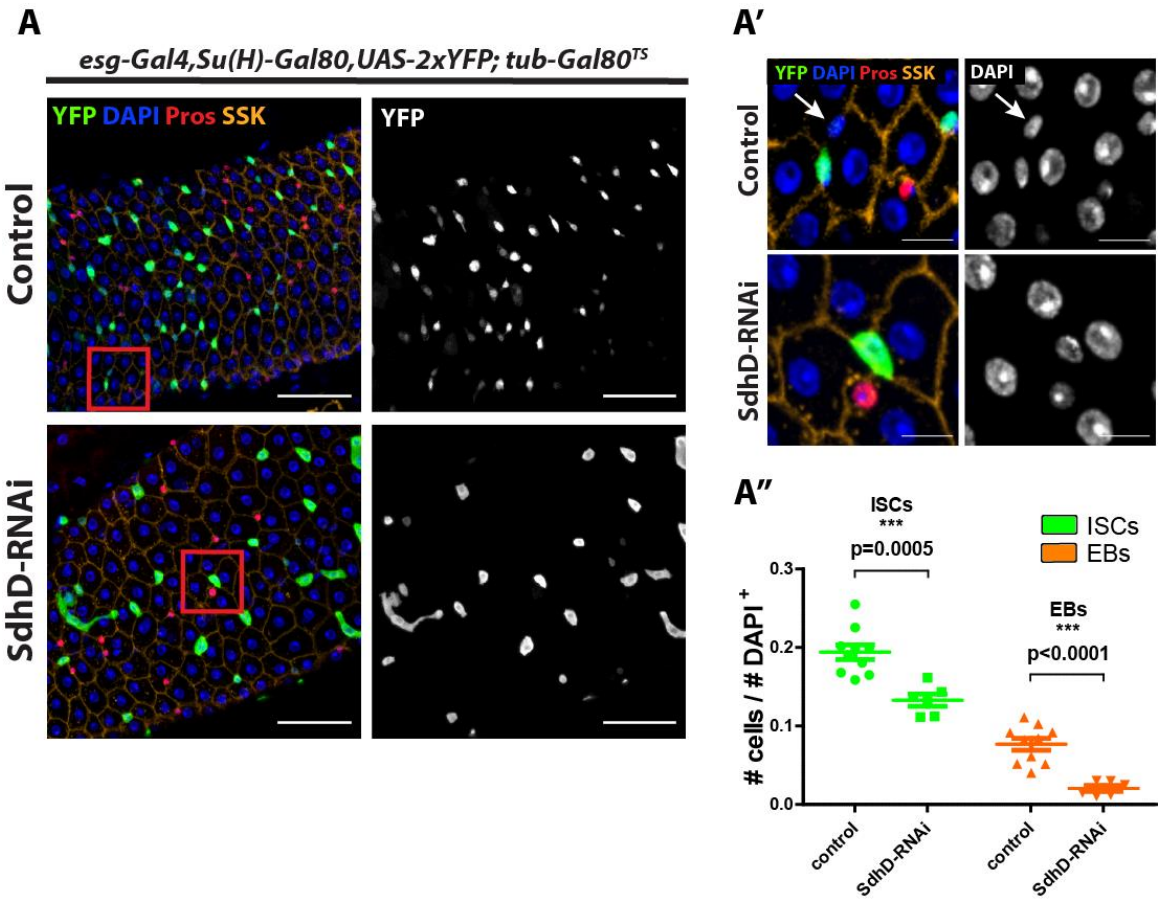


**Figure 10: Effects of ISC-specific SdhD-knockdown in progenitor cells**

**A.** Representative images in the midgut upon knockdown of SdhD (lower panels) in ISCs (marked in green (YFP); isolated in panels on the right), showing a decrease in their population, when compared to controls (upper panels), after 7 days of RNAi expression. EBs were identified as cells that are YFP-negative, Prospero (red)-negative and are not delimited by the EC-membrane marker Snakeskin (SSK, in orange). An example of an EB is pointed by the arrows in upper panels in the insets in **A´** (obtained from the red squares in A), in a ISC-EB pair. The lower panels (SdhD-RNAi) show an ISC-EE pair (Pros-positive) and no EBs. Scale bars in A = 50 µm. Scale bars of insets = 10 µm. **A''**. Abundance of ISCs (in green) and EBs (orange) in control and SdhD-RNAi midguts, demonstrating a significant decrease in the population of both cell types upon SdhD knockdown in ISCs. Horizontal lines represent mean with SEM. n=10 in controls and n=6 in SdhD-RNAi group. Unpaired two-tailed Student's *t*-test.

### 2.1.2 Knockdown of SdhD in enteroblasts does not affect their population numbers

In the previous section it was shown that knockdown of SdhD specifically in ISCs caused a decrease in the population of both ISCs and EBs, demonstrating a role for ISCs in the depletion of the EB population. To assess the effects of SdhD knockdown in EBs, SdhD was knocked down specifically in these cells using the driver *SuH-Gal4,UAS-GFP; Gal80$^{TS}$* [45]. In similarity with the previous experiments, flies were incubated at 18 °C during development, and switched to 29 °C 2-3 days after eclosion, to induce RNAi in adult flies.

Knockdown of SdhD in EBs did not result in a significant difference in the numbers of these cells after 6 days of RNAi expression (**Figure 11 A**; quantified in **A'**). To assess if a longer duration of RNAi expression would elicit a visible phenotype — which in the case where the *esg-gal4* driver was used resulted in a stronger phenotype (section 1.1, **Figure 8**) — the duration of RNAi expression was extended to 30 days. Once more, RNAi expression for 30 days did not result in any visible difference between RNAi and controls. At day 30, the number of EBs in both control and RNAi groups has increased when compared to day 6 in each group, which is expected during aging [56][111].

These results suggest that SdhD is not required in EBs for maintenance of their normal population numbers. One could argue that because EBs are short-lived in homeostatic conditions (it takes an EB on average 1 day between forming from an asymmetrical division of an ISC and differentiating to either an EE or an EC [72]), the expressed RNAi does not have enough time to induce a phenotype and these cells eventually differentiate to EEs or ECs, losing their EB identity and RNAi expression. However, in older flies such as the ones shown at day 30, is has been shown that EBs present delayed differentiation and get 'stuck' in an undifferentiated state [54][55][56], which would possibly give the RNAi enough time to induce a phenotype in these cells. As future experiments, to assess if the lack of a visible SdhD-RNAi phenotype in EBs is not caused by their short state as EBs, it is suggested to co-express RNAi against the Sox21a transcription factor, to block their differentiation [154] and determine if a longer expression of RNAi elicits a phenotype.

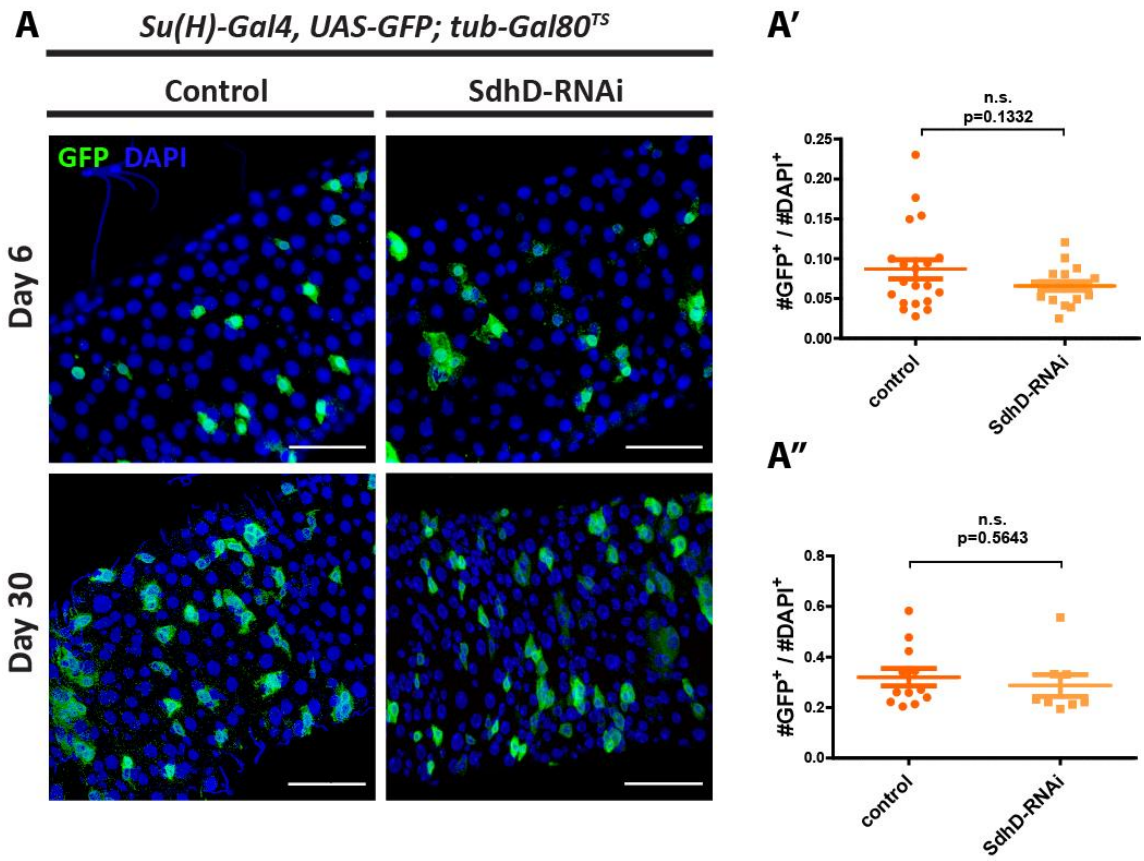


**Figure 11: Effects of EB-specific SdhD-knockdown in the abundance of EBs**
**A.** Knocking down SdhD specifically in EBs using the *SuH-Gal4,UAS-GFP; Gal80$^{TS}$* driver did not result in a significant decrease in the numbers of EBs (marked with GFP), after 6 days (upper panels) or 30 (lower panels) of RNAi induction. Scale bars = 50 µm. **A'.** Quantification of the results represented in the upper panels in A at day 6, indicating no significant difference in the number of EBs upon SdhD knockdown in these cells. n=22 in the control group and n=20 for SdhD-RNAi. **A''.** Quantification of the results exemplified in the lower panels in A at day 30. Statistical analysis showed no significant difference between control and SdhD-RNAi groups. n=12 in the control group and n=8 for SdhD-RNAi. Horizontal lines represent mean with SEM. Unpaired two-tailed Student's *t*-test.

## Remarks

The results presented in this section show that loss of SdhD in ISCs causes a depletion in the population of both ISCs and EBs. On the other hand, EB-specific knockdown of SdhD did not produce any discernible phenotype in this cell type, which suggests an ISC-specific requirement for SdhD. These data also suggest that the phenotypes previously obtained when using the progenitor cell-specific drivers 5961$^{GS}$ and *esg-Gal4* (section 1.1) result solely from the action of SdhD-RNAi in ISCs, with redundant expression in EBs. The following sections aim to characterize the functional aspects leading to loss of ISCs and EBs upon SdhD knockdown and possible mechanisms behind it.

## 2.2- SdhD is required for normal self-renewal rates in ISCs

Depletion of progenitor cells following SdhD knockdown as described in the previous section may happen due to a variety of factors acting independently or synergistically, such as cell death or inability to self-renew. To determine if the depletion of progenitor cells was caused by a decrease in self-renewal activity, intestines where SdhD was knocked down in progenitor cells using the *5961$^{GS}$* driver (previously used in the screening) were co-stained with an antibody against phosphorilated-histone-H3 (pHH3)— a method based on a post-translational phosphorylation of chromatin that occurs during mitosis [155]— and the number of cells undergoing division in each FOV was determined.

Stained intestines of 8-day-old control flies (no RNAi) revealed a very low frequency of cells undergoing mitosis (data not shown), which proved difficult to obtain statistically-significant data. To overcome this, RNAi and control flies were maintained for 45 days before dissections to obtain higher rates of ISC division induced by aging [56].

Maintaining the flies for 45 days before dissection has resulted in increased rates of ISC division in controls (**Figure 12**, panels on the left). Additionally, the number of ISCs undergoing division (pHH3-positive) in aged flies normalized to the total number of ISCs, is significantly reduced upon SdhD knockdown (quantified in **Figure 12 A**). Examples of these intestines are shown in **Figure 12 B**. In the control group (upper panel) an ISC is seen undergoing mitosis, marked by pHH3 (orange; pointed by an arrow); insets from the red square are shown in **B'** where the ISC undergoing division is seen in detail, with condensed chromatin (pHH3 and DAPI channels). The lower panels in **B** show that the number of progenitor cells under SdhD-RNAi is not completely depleted, as opposed to the case using the *esg-Gal4* driver for 30 days. This observation reinforces the idea that the 5961$^{GS}$ driver induces lower levels of expression than the *esg-Gal4*. Furthermore, knockdown of SdhD for 45 days appeared to reduce the aging-related phenotype of over-proliferation of GFP-positive cells, and the intestines look similar to the young control ones previously shown (**Figure 6**), suggesting that lower levels of SdhD-RNAi induced by a driver with weaker expression might be beneficial to the flies.

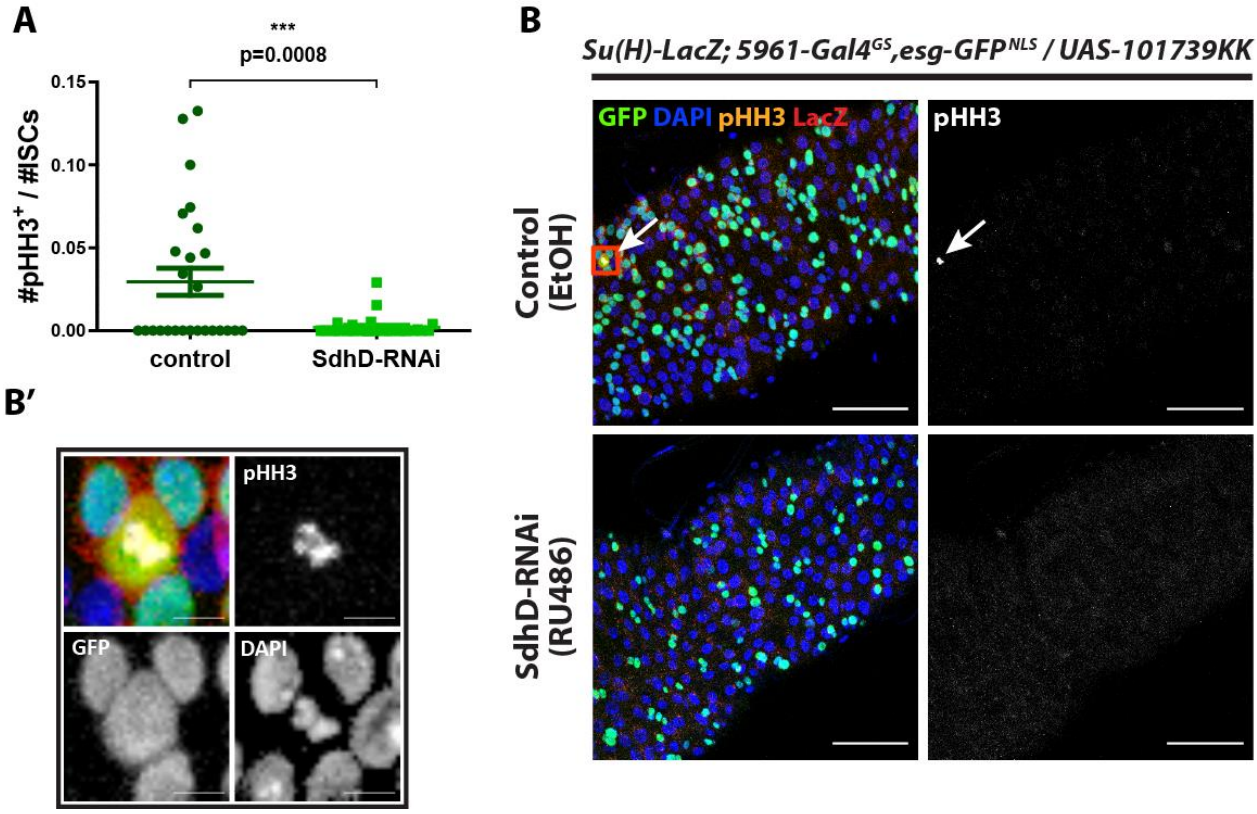


**Figure 12: Effects of SdhD knockdown in the rates of ISC division**
**A.** Numbers of ISCs undergoing mitosis (pHH3$^{+}$) normalized to the total number of ISCs in the same field of view in aged flies, revealing that knockdown of SdhD for 45 days causes a significant decrease in the rate of cell division in these cells (light green) compared to controls (dark green). **B.** Representative images of the data shown in A. depicting control (upper panels) vs knockdown of SdhD (lower panels) in progenitor cells (nuclear GFP, in green) using the *5961$^{GS}$* driver for 45 days. Enteroblasts are marked by LacZ (red) and the nuclei of all cells is marked with DAPI (blue). Cells undergoing mitosis are marked by pHH3 (orange; and panels on the right, in greyscale). In this example, an ISC in the control group is undergoing mitosis (pointed by the white arrows). Scale bars = 50 µm. **B´** Detailed images of the mitotic cell pointed in the red square in B (pHH3-positive) and surrounding cells. As expected, pHH3 staining colocalizes with DAPI in the chromatin, that is condensed. Scale bars = 5 µm. n=26 in the control group and n=30 in SdhD-RNAi. Unpaired two-tailed Student's *t*-test.

The results obtained indicate that SdhD is necessary for normal self-renewal in intestinal stem cells, at least in an aging context. These results challenge the general idea based on the reports described in the Introduction chapter (3.2), that inhibition of oxidative phosphorylation is associated with increased stem cell proliferation. Such observations extend to ISCs in *Drosophila* where knockdown of the mitochondrial pyruvate carrier causes decreased respiratory activity and induces proliferation, as described by Schell et al [109], suggesting that ISCs cells might be able to fulfill their energetic requirements via anaerobic glycolysis. Conversely, other authors have observed an inability of stem cells to progress through the cell cycle in the developing eye of *Drosophila*, and have attributed that to a depletion in ATP levels which in turn cause cell cycle arrest via AMPK/p53 elimination of cyclin E [118]. Perhaps stem cells in different organs have different metabolic requirements. If our ISCs were dividing less due to lack of ATP, one would think that RNAi against other

subunits would also cause a similar phenotype, which according to the initial screen, did not occur (**Figure 5**), although this can be attributed to differences in the strength of different RNAi lines, or a higher sensitivity of the ATP-generation process in ISCs to loss of SdhD. Further experiments should be performed to measure the levels of ATP and $O_2$ consumption, as well as lactate production and measurements of anaerobic/aerobic glycolysis.

The experiments here described with aged flies may not reflect normal homeostatic conditions. To overcome the use of phh3 and possibly get a statistical significant number of cycling cells in young guts, alternative experiments could include BrdU (5-bromo-2-deoxyuridine) or EdU (5-ethynyl-2'-deoxyuridine) feeding in young adult flies. These are thymidine analogues are incorporated in DNA during replication in the S phase and can be detected using specific antibodies. As these compounds are mixed in the fly food instead of used as immuno-labels, they could be incorporated for several days and as such, stain a higher number of cycling ISCs. As shown before, higher division rates correlate with higher numbers of BrdU-positive ISCs [156]; these assays, however, are less specific than anti-phh3 as they would also stain cells undergoing endoreduplication [157], rather than only cell division. As seen further in section 2.4, these ISCs show signs of endoreduplication which could render BrdU/EdU incorporation unfit for assessment of mitotic rates.

As the apparent reduction in mitosis in ISCs suggests a compromised cell cycle, future experiments should include an analysis of the cell cycle progression in these cells. The genetically-encoded fly FUCCI (fluorescent ubiquitination-based cell cycle indicator) is a valuable tool to assess cell cycle, that is based on fluorophore-tagged degrons from Cyclin B and E2F1 proteins that are degraded by the ubiquitin E3-ligases APC/C and CRL4Cdt2, during mitosis or at the onset of S phase, respectively. These degrons have attached different types of fluorophores (ex.: GFP or RFP), allowing for different phases of the cell cycle to be determined [158]. This tool could be co-expressed with SdhD-RNAi and control flies. Alternative methods include using anti-Cyclin antibodies to evaluate the cell cycle dynamics in these cells and try to pinpoint possible mechanisms resulting in decreased cell division rates upon SdhD knockdown. Cyclin D presence would indicate G1 phase, Cyclin E signal would indicate G1-S progression, Dacapo expression (an inhibitor of Cyclin E-CDK [159]) would show that the cells arrested in G1-S, Cyclin A would indicate S-G2 or G2-M phase progression, and Cyclin B would reveal G2-M progression [160].

## 2.3- SdhD is required for ISC survival

The intestines described in section 2.1 where SdhD-RNAi is expressed specifically in ISCs showed some of these cells presenting cytoplasmic rounding and shrinkage, YFP-positive protrusions and fragments around the cell body (**Figure 13 C'**), as well as chromatin fragmentation (**Figure 13 C''**), which were inexistent in controls where ISCs normally present a slightly elongated shape and no blebs or chromatin fragmentation (**Figure 13 A', A''**). These traits are associated with cell death across different organisms [161][162], including ISCs overexpressing the pro-apoptotic genes *reaper* (*rpr*) and *head involution defective* (*hid*) simultaneously [163] that were used as a positive control for apoptotic cells (**Figure 13 B', B''**). These data strongly suggest that SdhD-depleted ISCs might be undergoing cell death.

The cell death-associated protrusions, often named 'blebs', are believed to be formed by actin-myosin contractions or breaking of the cytoskeleton, causing the cell membrane to project outwards. In apoptosis, at later stages, they may contain intact organelles or fragments of the cell nucleus, which are enclosed within an intact plasma membrane. These protrusions may detach from the cell and be phagocytosed by macrophages and degraded within phagolysosomes [161][162][164][165]. In the following paragraphs, I introduce different forms of cell death to contextualize the observed phenotypes.

Apoptosis is a form of programmed cell death that occurs upon intrinsic or environmental cues such as cell damage or morphogenesis during development. It is characterized by nuclear condensation, DNA cleavage and nuclear fragmentation, loss of cell-cell contact, rounding of the cell, cell shrinkage due to loss of K+ and water, formation of blebs, and cytoplasmic fragmentation into apoptotic bodies [161][162][164][165][166]. At a molecular level, apoptosis is initiated by activation of Cysteinyl-aspartases (commonly known as caspases) — a type of proteases that contain cysteine in the active proteolytic center and are specific for aspartic acid. Caspases and constantly expressed in their inactive form, but upon stimuli, are activated to degrade cellular content. Both internal and external stimuli may initiate apoptosis. Internal stresses such as DNA damage or endoplasmic reticulum stress will initiate the *intrinsic pathway* which signals to mitochondria causing mitochondrial membrane permeabilization, triggering the release of pro-apoptotic factors such as Cytochrome c, which indirectly causes proteolytic maturation of caspase 9, an *initiator caspase*. Caspase 9 then cleaves *effector caspases* such as Caspase 3, Caspase 6 and Caspase 7, that degrade cellular proteins [167]. In contrast, external stimuli engage the *extrinsic pathway* via activation of death receptors on the cell surface such as the tumor necrosis factor-α (TNF) receptor, Fas ligand (FasL or CD95L) receptor or different GPRCs (G protein-coupled receptors) [168]. Activation of these receptors triggers the assembly of the death-

inducing signaling complex (DISC) in the cytoplasm which promotes the activation of the initiator Caspase 8, which in turn cleaves the aforementioned effector caspases. Caspase 8 may also activate other effectors such as Bid (H3 interacting-domain death agonist) which also causes mitochondrial membrane permeabilization.

Necrosis, in contrast to apoptosis, is a disorganized, irreversible and uncontrolled form of cell death, that occurs upon severe conditions unable to sustain normal physiology. These include extreme pH, insufficient ATP or ion imbalance, usually as a consequence of conditions such as infection, inflammation, or ischemia. Despite necrosis being traditionally thought of as an uncontrollable and chaotic form of cell death, studies have suggested that necrosis is also a regulated process that can be modulated. However, whether active signaling pathways for this form of death exist is uncertain. Necrosis is characterized by cytoplasmic swelling, early cellular membrane deformation and rupture, spill of cytoplasmic content to the extracellular space and cell lysis, swelling and rupture of mitochondria, organelle breakdown, accumulation of ROS and intracellular acidification [168][113]. Necrosis can be distinguished from apoptosis in that necrotic nuclei do not exhibit condensation, fragmentation or DNA cleavage (no DNA-ladder can be detected in a TUNEL assay), although DNA degradation occurs in late stages of necrosis [169]. Under very low ATP levels, cells programmed to die via apoptosis but unable to do so, may undergo necrosis [168].

Autophagy is a conserved catabolic process of degradation of cytoplasmic content in lysosomes. It is typically a protective, pro-survival response; however, if hyperactivated, it leads to cell death. It is a cellular response to a variety of internal and external stress stimuli such as nutrient deficiency, hypoxia, ER stress or oxidative stress. Autophagy is critical during starvation as self-digestion of non-essential and/or unwanted cellular components, providing essential nutrients during periods of stress. Autophagy also serves to remove damaged and dysfunctional organelles, misfolded proteins and foreign particles, including microorganisms, thus protecting cells against infections. Autophagy itself is not a form of cell death, but excessive autophagy may trigger cell death via apoptosis or necrosis [166]. Autophagy can facilitate apoptosis by maintaining ATP levels during starvation to promote ATP-dependent apoptotic processes such as formation of membrane blebs [168].

Cells can also die by a process called Caspase-independent cell death (CICD), that is defined as death occurring from pro-apoptotic signaling that leads to mitochondrial membrane permeabilization but fails to activate caspases. This may occur from damage induced by overwhelming generation of ROS, often by damaged mitochondria [168]. When induced by external stimuli, it is normally termed necroptosis. CICD is associated with partial

chromatin condensation, nuclear shrinking, abundancy of autophagosomes, but unlike apoptosis, no DNA laddering or formation of membrane blebs occurs [170].

In 'blebbing' SdhD-depleted ISCs, their compacted cytoplasm suggests that they may not be undergoing necrosis, since necrotic cells are usually swollen. Furthermore, necrotic ISCs shown in the study from Hou et al. do not appear to display blebs [113]. As cells dying by CICD cells do not display blebs, this form of cell death can perhaps be also ruled out. As SdhD-RNAi cells presented blebs, fragmented chromatin, and a shrunk, round cytoplasm, it suggests that they were undergoing apoptosis.

To test if SdhD-depleted ISCs were undergoing apoptosis, several detection assays were tested in intestines expressing SdhD-RNAi in ISCs and in intestines expressing *rpr* and *hid*, as a positive control for apoptotic ISCs. Intestines of *UAS-rpr,UAS-hid* flies displayed a reduced population of intestinal stem cells after 1 day of RNAi in adult flies. Unfortunately, immunofluorescent assays using antibodies against cleaved caspase 3 failed to detect apoptotic cells both in positive controls (*rpr,hid*) and SdhD-RNAi intestines (data not shown). The TUNEL assay (described in the Materials and methods chapter) was also used to look for fragmented DNA, but also failed to detect apoptosis in *rpr,hid* and SdhD-RNAi flies. The genetically-encoded *Apoliner* reporter that contains a caspase-sensitive site that upon cleavage initiates a fluorescent signal [171] was used in equivalent conditions but also failed to detect apoptosis in *rpr,hid* ISCs. It is not clear why these assays did not work in the intestine. Other researchers have also reported not being able to detect apoptosis in positive controls in the intestine of *Drosophila* ([172]; personal communications), although a recent report shows successful detection of apoptosis in ISCs in the intestine of *Drosopila* using anti-Cleaved Caspase 3 antibodies [173].

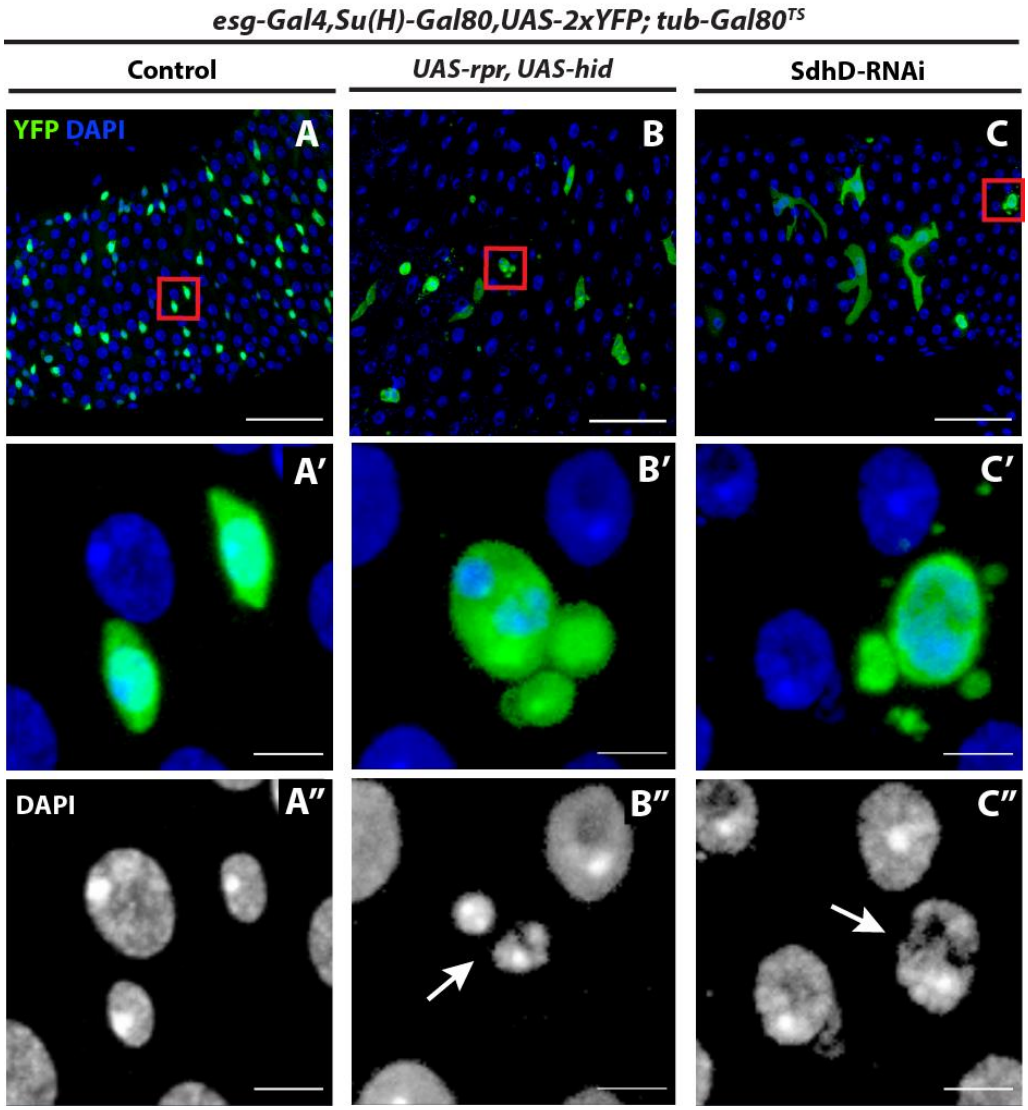


**Figure 13: ISCs depleted of SdhD show hallmarks of cell death**
SdhD knockdown (C) at day 13 causes ISCs to display phenotypes similar to those commonly observed during cellular death such as blebs and fragments around their main body, rounding of the cell (C′ inset) and apparent nuclear fragmentation (C′′; pointed by the arrow). These traits are also visible in positive-control apoptotic ISCs expressing the pro-apoptotic genes *rpr* and *hid* (B; B′; B′′), but not present in controls (A; A′; A′′). The nucleus of the cell shown in C′′ seems to be separating into two parts, similarly to the one in B′′. Scale bars = 50 µm. Scale bars of insets = 5 µm.

Suggested future experiments to confirm cell death in ISCs include the use of the fluorescent agent propidium iodide (PI) that stains necrotic cells, as these cells are unable to maintain an impermeable membrane and allow PI to infiltrate and stain RNA and DNA [174][113]. pGFP-Atg8a, a *Drosophila* reporter of autophagy would indicate the levels of autophagy in each cell [175]. Another test would be to use antibodies against cell death markers other than cleaved caspase 3, such as other caspases, bid, or cytochrome C. Co-expression of the anti-apoptotic gene p35 would rescue cell death if ISCs were dying by apoptosis, as previously observed in intestinal progenitor cells of *Drosophila* [148].

Electron microscopy (EM) is a powerful tool to indicate the state of the cell in respect to the different types of cell death. EM images show cell membrane integrity, mitochondrial membranes, chromatin and nuclear membrane, autophagosomes and autolysomes. During apoptosis, blebs with intact organelles could also be visualized by EM, while mitochondria would be damaged in necrosis. Excess autophagy would show several autophagosomes, as double-membraned vesicles that contain intact organelles [167].

As mitochondria are important modulators of apoptotic pathways (release of pro-, and anti-apoptotic factors), autophagy (under low ATP levels) and necrosis (due to generation of reactive oxygen species (ROS), but also under low ATP levels), it is not entirely surprising that knockdown of genes involved in metabolism induces cell death. Accordingly, previous studies have demonstrated that metabolic impairment leads to apoptosis, necrosis or autophagy [176][177], via inhibition of growth factors or unknown mechanisms.

These observations strongly suggest that SdhD-RNAi ISCs undergo cell death, which might contribute to the reduced population of ISCs observed upon SdhD knockdown in previous sections. It is unclear if ISCs undergo cell death due to general shutdown of cellular functions induced by SdhD knockdown, or if there is a specific pathway activated upon SdhD knockdown that triggers cell death. Both cases are discussed further later.

## 2.4- Loss of SdhD triggers hypertrophy in intestinal stem cells

Knockdown of SdhD specifically in ISCs using the driver *esg-Gal4,Su(H)-Gal80,UAS-2xYFP; tub-Gal80$^{TS}$* as described in the previous sections caused a drastic increase in the size of ISCs after 7 days (**Figure 14 A**). These cells display a visibly larger cytoplasmic size and increased nuclei area and apparent DNA content — obtained indirectly by integrating the fluorescent DAPI signal over the nucleus area, as previously described [1][131] (quantified in **Figure 14 B**; pointed out by arrows in **A**, lower right panel, vs controls, upper right panel). The cytoplasm of enlarged ISCs extends as a thin layer overlapping the membranes of ECs (stained with SSK, in orange), suggesting that these cells are growing basally through the space left between ECs, and thus maintain their basal ISC identity (**Figure 14**, lower left panel).

These observations suggest that SdhD-depleted ISCs undergo a hypertrophic/endoreduplication program. Endoreduplication, also referred as endocycling, occurs during normal development or in adult organisms in specific cell types. An increase in DNA content allows higher rates of gene expression, helping build larger cells, which can be advantageous in cases in which disruptions of the cytoskeleton or cell adhesion via mitosis would compromise tissue barrier function. This is the case of ECs in the *Drosophila* midgut, which can go up to 4 rounds of endoreduplication [158][50]. To achieve polyploidy, cells enter G1 and S phases. but skip different parts of the cell cycle, namely mitosis, depending on the cell type [50] (**Figure 15**; details in caption). Cellular hypertrophy refers to abnormal cell size commonly occurring as an adaptive response, and is usually accompanied by endoreduplication, although not all polyploid cells are necessarily considered hypertrophic [178][179].

To initiate endocycling, the cell cycle must be altered to skip mitosis while still allowing progression through G1 phase and DNA replication during S phase. G1 phase is necessary to assemble pre-replication complexes (PreRCs), which are used during S phase for proper DNA replication. To bypass mitosis, M-CDK (mitotic CDK; the cyclin-dependent kinase that drives G2-to-M phase progression) is downregulated, while S phase CDK (S-CDK; activated by expression of Cyclin E to drive G1-to-S progression) is periodically inactivated to allow the transition into G1 or G2 phase. In Drosophila, Notch signaling plays a major role in switching from a mitotic to an endocycle during differentiation in the midgut and follicle cells in the ovary [50]. Activation of Notch via Delta initiates a series of cascades that timely repress M-CDK, inhibiting mitosis, and promote entering G1 phase to allow formation of PreRCs and S phase for DNA replication [180].

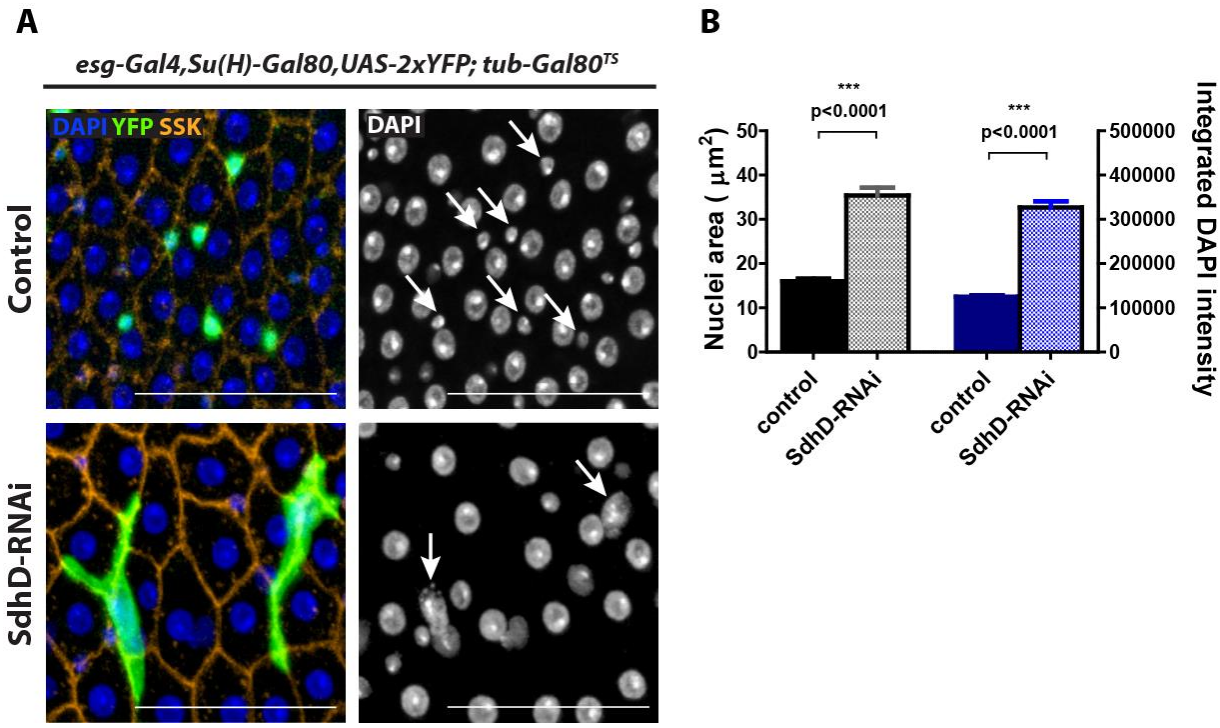


**Figure 14: Knockdown of SdhD causes hypertrophy in ISCs**

**A.** Knockdown of SdhD (lower panels) vs control (upper panels) in ISCs for 7 days. Knockdown of SdhD causes ISCs (YFP-positive) to become hypertrophic, evidenced by a clear increase in their cytoplasmic and nuclei size (pointed by the arrows in the panels on the right in both control and SdhD-RNAi). The overlap between the cytoplasm of ISCs and EC-membrane stain Snakeskin (SSK, in orange, lower left panel) suggests these cells are growing basally in the space left between the ECs. The size of ECs also appears increased in the SdhD-RNAi group. Scale bars = 50 µm. **B.** Quantification of nuclei area and DNA content in ISCs. Nuclei area was significantly increased in the SdhD-RNAi group, as represented in the plots on the left. The DNA content in the nuclei of ISCs was indirectly quantified by integrating the DAPI intensity over the area of each nuclei, revealing a significant increase in the SdhD-RNAi group, shown in the plots on the right, in arbitrary units. n=10 intestines in the control group and n=6 in SdhD-RNAi. Unpaired two-tailed Student's *t*-test.

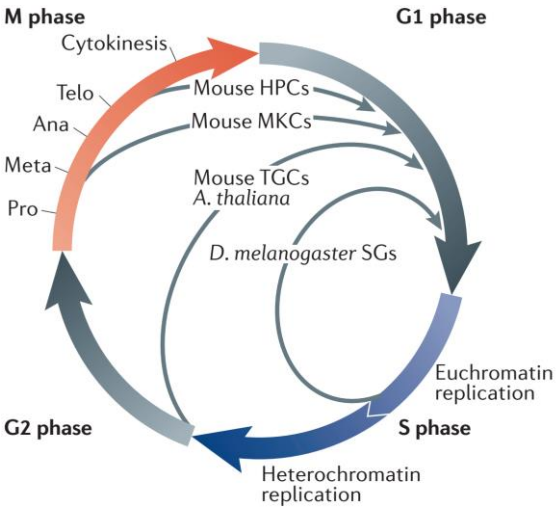


**Figure 15: Cell cycle abbreviations in different cell types**

To achieve polyploidy, cells must proceed through G1 and S phases but skip mitosis (M phase), or at least cytokinesis. As depicted in this diagram, different polyploid cells go through the cell cycle skipping different parts, as indicated by the thin arrows. *Drosophila* salivary glands (SGs) skip the heterochromatin replication part of the S phase and re-initiate the cycle proceeding through G1. Mouse trophoblast giant cells (TGCs) and *Arabidopsis thaliana* cells complete the S phase and briefly enter G2 to then proceed through G1. Mouse megakaryocytes (MKCs) go through G2 and initiate mitosis but exit before telophase (Telo) and re-enter G1, a variant called endomitosis. Mouse hepatocytes (HPCs) proceed through a normal cycle but skip only cytokinesis, a cell cycle variant known as acytokinetic mitosis, which produces multi-nucleated cells. Source: B. Edgar et al. [50].

Common pathways associated with hypertrophic growth/polyploidy during homeostasis or upon stress are the IGF pathway, with downstream effectors PI3K, AKT, FOXO, RAS and TOR [181][182][50]; c-Jun N-terminal kinase (JNK)-dependent Yorkie activation [182][183]; and EGFR/MAPK signaling [1][50]. In the midgut of *Drosophila*, Amcheslasvksy and colleagues observed that RNAi against tuberous sclerosis complex (TSC) in progenitor cells, that normally inhibits the GTPase Rheb and the TOR kinase, causes hypertrophy in ISCs. Mutants for TSC had defects in different steps of the cell cycle, and in strong similarity with SdhD-depleted ISCs, maintained stem cell identity, had lower division rates and were commonly found single instead of paired with another EB, suggesting that the population of EBs was also reduced. Feeding rapamycin to TSC-RNAi flies, or co-expressing TOR-RNAi or a dominant negative form of TOR, rescued the ISC hypertrophy phenotype, indicating a role for TOR in this phenotype [184]. Choi and colleagues observed that overexpression of insulin receptor in the fly midgut results in abnormally large ECs. However, overexpression of InR in progenitor cells did not result in any apparent increase in their size, and resulted in increased proliferation [72] as opposed to our results in ISCs, suggesting that InR signaling might not play a role in the hypertrophy phenotype in SdhD-depleted ISCs. At a downstream level, knockdown of genes involved in the regulation of mitosis such as *cycA* (cyclin A) also results in polyploid ISCs [185], which is consistent with the concept that inability to complete mitosis might result in the cells reentering the cell cycle, becoming polyploid.

Polyploidy does not always occur from programmed endocycling — different events such as cell fusion, endomitosis, acytokinetic mitosis and mitotic catastrophe also generate polypoid cells. Cell fusion and acytokinetic mitosis—caused by incomplete or no cell plate formation, skipping cytokinesis (exemplified in **Figure 15** as occurring in mouse hepatocytes)—result in multinucleated cells, which was not observed in SdhD-depleted ISCs. Endomitosis occurs when a cell enters mitosis but aborts during metaphase or anaphase, resulting in several copies of sister chromatids in the nucleus (exemplified in **Figure 15** as mouse megakaryocytes) [186]. Mitotic catastrophe (MC) occurs when a cell is unable to

proceed through mitosis in an unprogrammed manner, resulting in polyploidy; MC is discussed in more detail in section 4.2.

In SdhD-RNAi intestines, the cytoplasmic size of ECs also appears to be increased when compared to controls (**Figure 14 A**; delimited by SSK, in orange). Previous reports in different *Drosophila* and mammalian systems show that cells undergo hypertrophy to maintain organ size when mitotic cells are not available to replenish tissue [182]. Particularly, Jiang et al. observed that genetically-induced loss of *Drosophila* intestinal progenitor cells causes overall cell loss in the intestine and increased EC size [58]. On the other hand, different reports describing progenitor cell loss do not appear to show increased EC size [113][148]. It is unclear, however, if the ECs shown here are undergoing a hypertrophic program or have simply stretched following a likely loss of ECs due to lack of normal ISC function to replace the pool [182].

In the present case, it is unclear what mechanisms are behind the generation of hypertrophic ISCs. It is possible that one of the scenarios described above might result from failure to complete mitosis upon SdhD knockdown. To confirm the increase in DNA content in ISCs, FACS (fluorescence-activated cell sorting) is suggested as a future experiment [50][158]. Alternatively, FISH (Fluorescence in situ hybridization) staining of any specific gene, would show how many chromosome copies exist inside the nuclei. Although programmed polyploidy is normally an irreversible process and is linked to terminal cell differentiation [187], ISCs do not seem to be differentiating, since they still express the suppressor of differentiation Esg. The cell-cycle reporter line FUCCI [158] described in section 2.2 could be used to assess the cell cycle phase in ISCs. A higher percentage of ISCs in S phase would be expected when compared to controls, as it is where new DNA is synthesized. As alternative, BrdU or EdU incorporation could also be used to mark cells in the S cycle. The levels of proteins and transcription factors associated with hypertrophy should be assessed to help determine the mechanisms activated upon SdhD knockdown. Knocking down effectors of IIS, JNK or EGFR, such as TOR via RNAi could rescue the phenotype. It would remain to be determined how knockdown of SdhD led to activation of growth factors. Although Notch is not expected to be found in ISCs, because of its role in promoting endocycling in differentiating EBs, its levels and downstream mechanisms should also be assessed. Live visualization of chromatin dynamics and cell cycle progression expressing a fusion of histone 2A with green fluorescent protein [120] is also recommended. In section 4.4, the role of succinate as a possible trigger to hypertrophy is also explored.

# III- Effects of progenitor cell-specific SdhD knockdown in differentiated cells

## SdhD-RNAi in progenitor cells leads to an increased population of enteroendocrine cells

The requirement for SdhD in progenitor cells for differentiation choices and tissue homeostasis was tested by knocking down this gene in progenitor cells using the *esg*-Gal4 driver and staining EEs with an anti-Prospero (Pros) antibody, to assess whether loss of SdhD leads to changes in the numbers of differentiated cells (EEs and ECs) in the intestine.

Immunofluorescence images show that SdhD knockdown in progenitor cells led to a significant increase in the population of EEs after 6 days (**Figure 16 A, A'**). The number of ECs per field of view, calculated by subracting the number of progenitor (GFP-positive) and enteroendocrine (Pros-positive) cells from the total number of cells (DAPI-positive), remains unchanged upon SdhD knockdown in progenitor cells (**Figure 16 A, A'**).

These results suggest a that differentiation bias towards an enteroendocrine fate occurs upon SdhD knockdown in progenitor cells. To confirm these results, lineage-tracing was assessed using the *esg-FlipOut* tool [58][131] (*esg-Gal4,tub-Gal80$^{TS}$,UAS-GFP; UAS-flp,act>CD2>Gal4*; described in the Materials and Methods chapter). Expression of this construct in progenitor cells for 5 days revealed a slight differentiation preference towards EEs in the SdhD-RNAi group (**B**, lower panels, EE progeny is marked by both Pros and GFP, pointed by arrows), compared to controls where differentiation occurs mostly towards ECs (**B**, upper panels, large GFP-positive cells), although quantification of these occurrences showed no significant difference (**B'**). Experiments with a large sample size should be repeated to obtain more robust results.

The observed phenotypes are consistent with a loss of notch signaling in EBs [38][45], which is required at higher levels for differentiation into ECs. The loss of normal function in ISCs described in the previous chapters could lead to a depletion in the levels of Delta which in turn would result in lower Notch signaling in EBs. To test this hypothesis, it is recommended as a future experiment to express the Notch intracellular domain ($N^{intra}$) in EBs while expressing SdhD-RNAi in ISCs, to evaluate if it would rescue the phenotype. To confirm loss of Delta, anti-Delta antibodies should be used to co-stain these guts.

These data showed that loss of SdhD does not affect the capacity of EBs to differentiate, although they do not differentiate normally. It is unclear if the observed effect happens in ISCs or EBs as the *esg-Gal4* driver expresses Gal4 in both cell types.

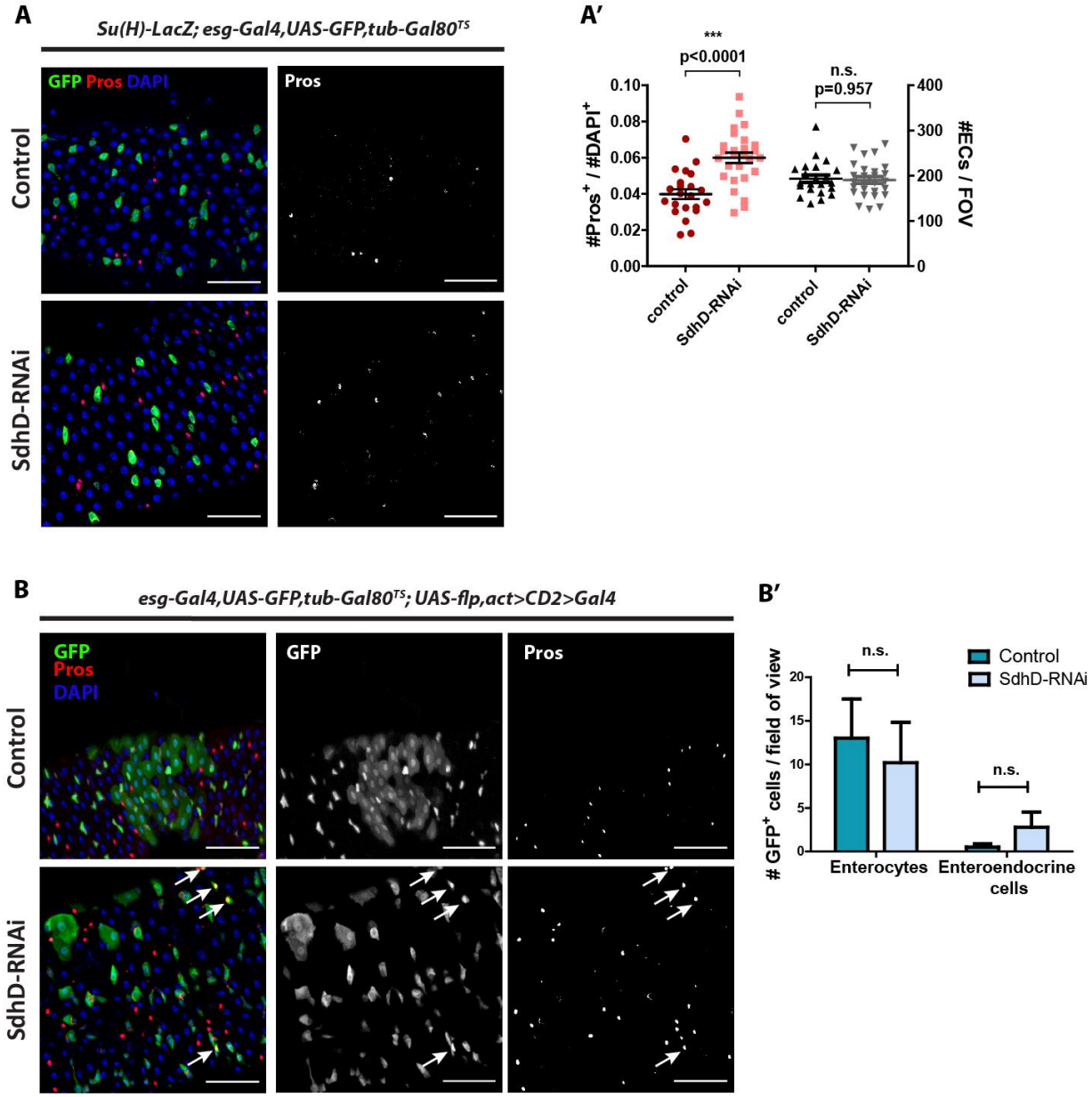


**Figure 16: Effects of SdhD knockdown in differentiation choices**
**A.** Images showing an increase in the numbers of EEs (marked by anti-Prospero, in red; isolated in the panels on the right) after 6 days of SdhD-RNAi in progenitor cells (lower panels) when compared to controls (upper panels). **A'.** Quantification of the number of EEs and ECs upon SdhD knockdown in progenitor cells, showing a significant increase in the number of EEs upon SdhD knockdown and no significant difference in the number of ECs. n=24 in controls and n=30 in the SdhD-RNAi group. **B.** Lineage tracing analysis in progenitor cells at day 5 using the *esg-FlipOut* tool, that marks progenitor cells and their lineage (EEs / ECs) with GFP (in green). In the controls (upper panels) it is shown that all progenitor cells differentiated into ECs (large, GFP-positive cells), while on the SdhD-RNAi group there are several marked EE progeny (small, GFP-positive, Pros-positive (red) cells) **B'.** Quantification of the results represented in B, indicating a preference for EE fate over ECs in SdhD-RNAi individuals when compared to controls, although not statistically significant. n=8 in controls and n=5 in the SdhD-RNAi group. Scale bars = 50 µm.

# IV- Mechanisms of action

In this section, I explore possible mechanisms of action mediating ISC death and hypertrophy upon SdhD knockdown, via experimental approaches and previously published results.

## 4.1- No evidence of ROS accumulation upon SdhD knockdown

Reactive oxygen species (ROS) play an important role in stem cell behavior. While high or uncontrolled levels of ROS may damage lipids, protein and DNA leading to cell death, homeostatic levels of ROS are required for proper stem cell function and proliferation [98][188][189].

The mitochondrial electron transport chain is a significant generator of ROS, including complex II [190], and SDH deficiencies are associated with elevated ROS levels within the cell [191]. To test if SdhD knockdown elicited an increase in ROS levels, the oxidative state in the mitochondria of SdhD-knockdown progenitor cells was assessed using the ROS-sensitive *mito-roGFP* reporter.

### 4.1.1 The *mito-roGFP* reporter reveals no changes in the oxidative state in mitochondria of SdhD-knockdown cells

The *mito-roGFP* reporter (described in the Materials and Methods chapter) was used to quantify the ratio of oxidative/reductive potential within the mitochondria of SdhD-RNAi and control progenitor cells. The SdhD-RNAi and pKC43 control lines were crossed to a line containing the $5961^{GS}$ driver promoting the expression of the *mito-roGFP* construct in progenitor cells. The flies were raised in normal food and 2-3 after eclosion, both groups were switched to RU-containing food to activate *mito-roGFP* expression, and the oxidative/reductive state in the mitochondria of these cells was assessed at day 8.

This experiment showed that no changes in the oxidative/reductive state of the modified GFP protein appear to occur, suggesting that mitochondria in progenitor cells depleted of SdhD are not in a more oxidative or reduced state than the ones in the control group (**Figure 17**). This experiment, however, was limited to the fact that ISCs were not distinguished from EBs, and as such the results refer to the oxidative state in mitochondria of both cell types, which could be different for both. To overcome this, it is suggested to add a *Su(H)-LacZ* reporter and co-stain samples with anti-β-Gal antibodies in the red channel to discard EBs in the analysis. Suggested future experiments include using the oxidant-sensitive dye dihydroethidium (DHE) that indicates intracellular ROS levels [113].

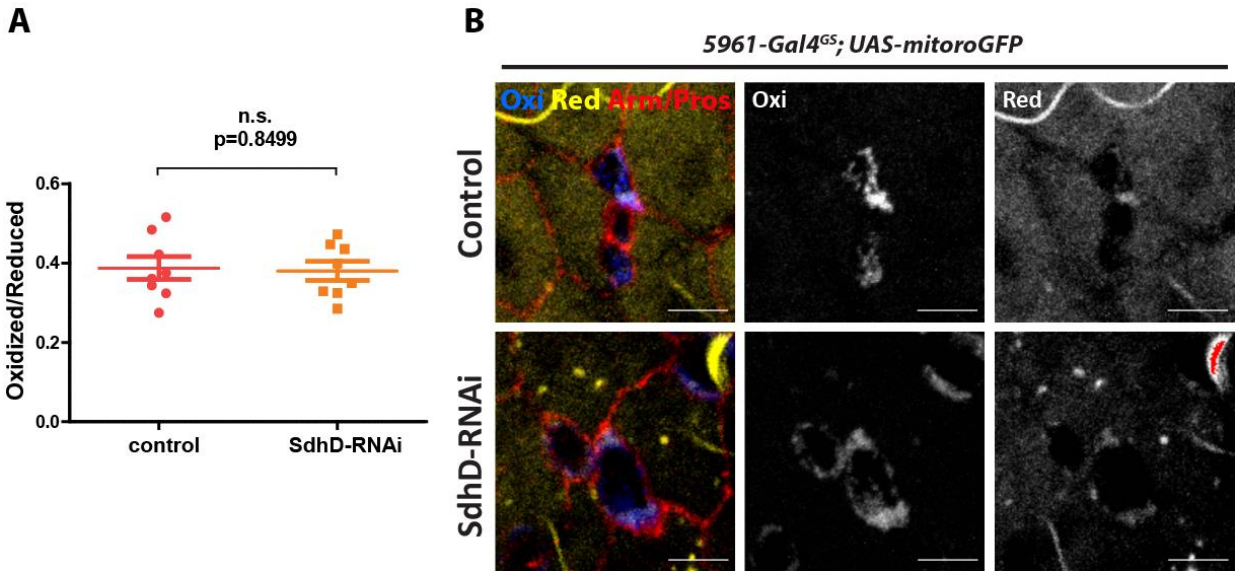


**Figure 17: Analysis of the oxidative environment in mitochondria using the *mito-roGFP* probe**
**A.** Quantification of the fluorescence-based redox indicator *mito-roGFP* showing that expression of SdhD-RNAi does not result in a significant change in the oxidative potential in the mitochondria of progenitor cells. Each circle/square represents the average ratio per intestine, obtained by integrating the *mito-roGFP* signal from 10 cells of each intestine. n=9 individuals in the control group (pKC43; in red) and n=9 in SdhD-RNAi (101739 KK; in orange). Unpaired two-tailed Student's *t*-test. **B.** Fluorescence images showing the *mito-roGFP* signal in mitochondria of progenitor cells. Oxidized probe (Oxi) in blue and middle panels. Fluorescent signal from probes in the reduced state (Red) in yellow and right panels. Cell membranes are marked with anti-Armadillo (red) and EEs marked with anti-Prospero (red; not shown). Scale bars = 5 µm.

### 4.1.2 Knockdown of ROS-scavenger Superoxide dismutase 2 does not replicate SdhD knockdown phenotypes

Superoxide dismutase 2 (SOD2) is a conserved ROS scavenger enzyme localized in the mitochondria that has an important role in preventing accumulation of ROS originating from the ETC [192]. Knockdown of SOD2 in *Drosophila* has been shown to lead to increased endogenous oxidative stress and reduced lifespan [193].

To test if SOD2 depletion in progenitor cells would replicate the SdhD-knockdown phenotypes, SOD2 was knocked down in these cells by means of RNAi using the *esg-Gal4* driver. The $w^{1118}$ line was used as control to match the genetic background of the UAS-SOD2-RNAi line. As seen in **Figure 18**, the progenitor cell population has increased slightly, although not significantly. Consistent with these findings, previous reports show that ROS are necessary for ISC replication in *Drosophila* and increased levels lead to a higher ISC population [194]. This SOD2-RNAi line was previously used successfully reducing SOD2 levels and causing phenotypes resulting from ROS accumulation [192][195].

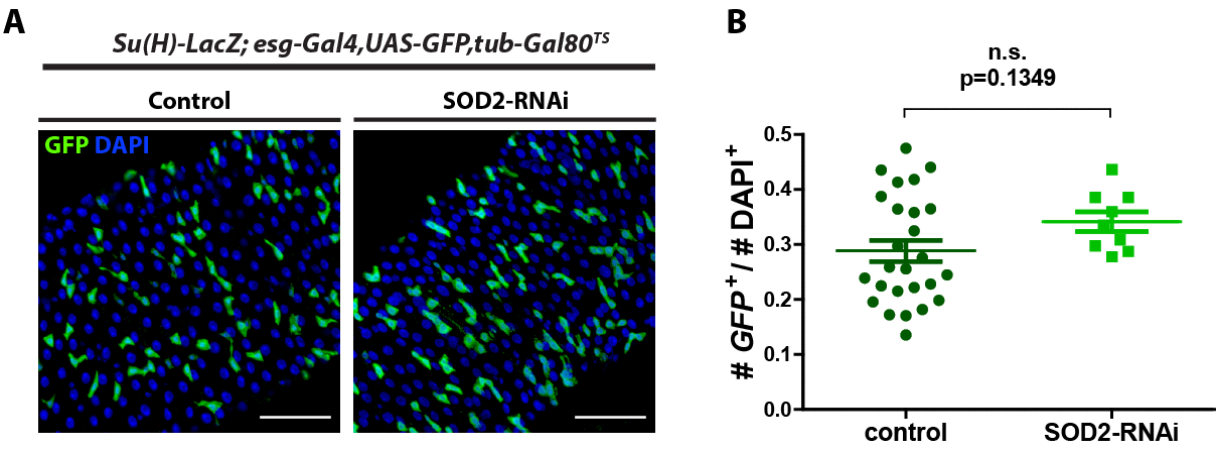


**Figure 18: Effects of SOD2-RNAi in the abundance of intestinal progenitor cells**
**A.** Immuno-fluorescent images comparing the effects of RNAi targeting the ROS-scavenger SOD2 (Superoxide dismutase 2) in progenitor cells ($GFP^+$) in controls (left) vs RNAi (right). Scale bars = 50 µm. **B.** Quantification of the results represented in A, showing that SOD2-RNAi does elicits only a small, non-significant change in the number of progenitor cells. n=10 in controls and n=5 in SdhD-RNAi. Unpaired two-tailed Student's *t*-test.

**Remarks:**

The data presented in this section together with previous reports suggest that ROS are not responsible for the phenotypes observed upon SdhD knockdown. While mutations in complex II genes are commonly associated with elevated ROS levels, other mechanisms resulting from SdhD knockdown might overcome the proliferative response normally caused by increased ROS levels. In the following sections, data is presented to elucidate other possible mechanisms elicited by SdhD knockdown in ISCs.

## 4.2- Mitotic catastrophe

Mitotic catastrophe (MC) is defined as inappropriate entry or progression through mitosis, resulting in polyploidy or cell death [196]. It may originate from chemical or physical stress or ionizing radiation, causing DNA damage and defective cell cycle checkpoints. It has also been associated with inhibition of complex I of the ETC [197]. MC is characterized by changes in nuclear morphology, polyploidy, cell fusion and often results in giant cells containing multiple micronuclei [198]. Rather than a form of cell death, MC is a trigger that often results in cell death via apoptosis, necrosis or CICD [169]. Although most cells die following MC, there is evidence that a small fraction of cells can survive this event [198][199]. Surviving cells can become senescent or stay viable, polyploid cells, which may or may not divide again generating daughter cells with different nuclei size [175]. Cell senescence is characterized by cell cycle arrest in the G1 phase and in some cases is associated with cellular hypertrophy [199][200]. Senescent ISCs, however, do not show increased cell size or polyploidy [111]. Moreover, SdhD-RNAi ISCs becoming polyploid is an indication that they are not arrested in the cell cycle.

Although SdhD-depleted ISCs share with MC cells such as polyploidy and cell death, they seem to lack other hallmarks such as the heterogenous nuclei signature or multinucleated cells. The nuclei of SdhD-RNAi ISCs (**Figure 13**), seem more homogeneous than the ones described following MC, also visualized via IF [198], suggesting that they are fragmenting as part of cell death instead of forming the micronuclei normally observed in MC. To test if the cells undergo MC, it is suggested as future experiment to obtain EM images where the nuclear membrane and chromatin are clearly shown to rule out the existence of these traits. Furthermore, the use of live imaging could provide clues as to the chromatin dynamics during the cell cycle. These experiments should be complemented by cell cycle analysis, to determine if the ISCs show signs of entering mitosis, namely by the presence of Cyclin B.

## 4.3- The importance of the enzymatic activity of succinate dehydrogenase

The results presented in the previous sections show that the knockdown of the subunit D of mitochondrial complex II of the respiratory chain in progenitor cells leads to a depletion in the population of these cells. In the initial screening presented in section I, the subunit C of complex II, SdhC, presented a similar phenotype, albeit less intense. The similarity in phenotypes resulting from knockdown of both complex II subunits C and D suggests that the results previously presented might be complex II-specific and possibly, resulting from a downregulation of its enzymatic activity.

### RNAi-targeting Complex II Subunit A in progenitor cells with the *esg*-Gal4 driver phenocopies Subunit D knockdown

The enzymatic activity of complex II is provided by SdhA. To test if a knockdown of SdhA in progenitor cells elicits an equivalent phenotype as the one observed with the SdhD-RNAi using the *esg-Gal4* driver, SdhA was knocked down in equivalent conditions.

Knockdown of SdhA using the *esg-Gal4* driver for 6 days has resulted in a significant depletion in the population of progenitor cells (**Figure 19**), similar to the phenotype caused by knockdown of SdhD in section 1.1 (**Figure 7**). These results strongly suggest that the phenotypes presented in sections 1 and 2 may be complex II-specific. Knockdown of SdhA with the $5961^{GS}$ driver in the initial screen did not result in a significant phenotype, which is attributed to a weaker activity of this driver when compared to *esg-Gal4* [45][147]. The differences between SdhA and SdhD in the screening could be explained by a weaker RNAi activity of the former.

Given that the observed phenotypes appear to be complex II-specific role in the depletion of progenitor cells upon RNAi, and complex II is also part of the Krebs cycle, a side experiment was performed to knockdown isocitrate dehydrogenase (Idh) — a component of the Krebs cycle that converts isocitrate to α-ketoglutarate. Upon Idh knockdown for 6 days using the *esg-Gal4* driver there was no observed phenotype (**Supplemental Figure 2**),suggesting that this Krebs cycle enzyme is not required at normal levels in progenitor cells.

Previous reports have shown that ablation of different subunits of complex II cause a decrease in the enzymatic activity of complex II (SDH). In humans, a specific mutation in SdhD causes a decrease in the enzymatic activity of SDH [153], while SdhA mutations cause the same effect in humans and yeast [152], as well as SdhB mutations in flies [191]. These

data suggest that knockdown of SdhD in ISCs might be related to decreased activity of SDH in these cells.

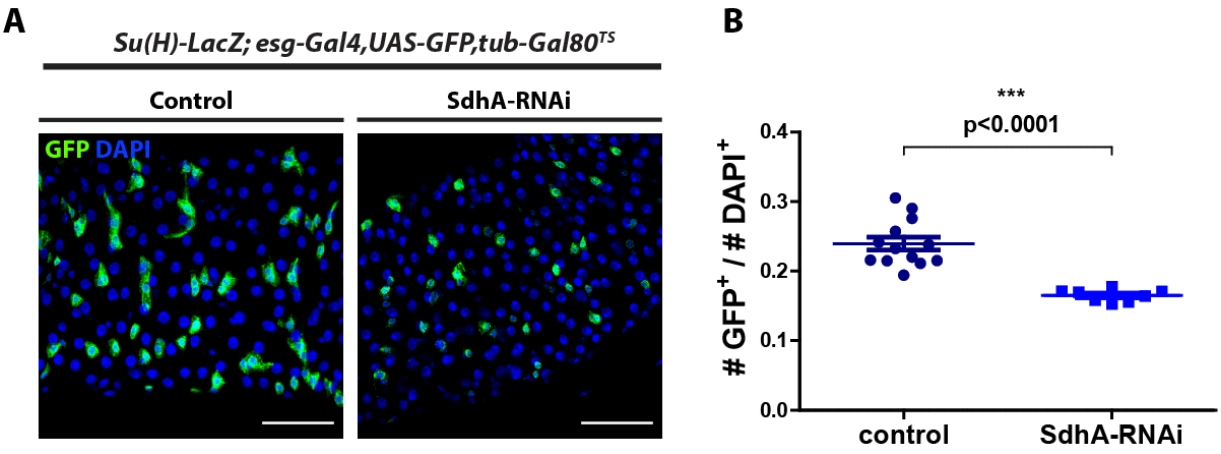


**Figure 19: Effects of SdhA knockdown in intestinal progenitor cells**
**A.** Knockdown of subunit A of complex II (right panel) replicated the phenotype of subunit D (SdHD) knockdown, in terms of reducing in the number of progenitor cells (green, GFP-positive) when compared to pKC43 controls (left panel). Accordingly, there also appears to be less progenitor cell pairs in the RNAi group. Scale bars = 50 µm. **B.** Quantification of progenitor cell numbers shows a significant decrease in the abundance of these cells upon SdhA-RNAi, replicating the SdhD-RNAi results. n=13 in the control group and n=8 in SdhA-RNAi. Statistics: unpaired two-tailed Student's t-test.

## 4.4– Succinate as a driver of hypertrophy and cellular death

The previous sectionss showed that a downregulation of subunits of complex II causes a reduction in the number of progenitor cells, suggesting a complex II-specific mechanism. Impaired enzymatic SDH activity caused by knockdown of complex II components has been shown to inhibit the conversion of succinate to fumarate in the Krebs cycle leading to accumulation of succinate [201][202][203]. Besides its role as a citric acid cycle intermediate, succinate also has a signaling function where it activates the cell-membrane G-protein-coupled-receptor GPR91 [204]. GPR91 has been shown to activate Gq protein signaling [205], which is involved in hypertrophy and cellular death via apoptosis [206][207][208][209][210].

Succinate is transported through the inner mitochondrial membrane via the mitochondrial dicarboxylate carrier (DIC) (encoded by the SLC25A10 gene (solute carrier family 25 member 10) in humans [211]) and Dic1 (CG8790) in *Drosophila* [212]. It is then transported across the outer mitochondrial membrane by the voltage-dependent anion channel VDAC [213], Porin in *Drosophila* [214]. Finally, it is transported extra-cellularly via sodium-dicarboxylate cotransporters, specifically SLC13A3 in mammals [215] and INDY in *Drosophila* [216][217]. These transporters are not specific for succinate and also transport small molecules and other Krebs cycle intermediates and dicarboxylates, such as pyruvate, fumarate, malate and citrate [217][218][219].

G-protein-coupled-receptors (GPCRs) are a group of transmembrane proteins that are conserved across species and exist in a variety of cell types with specific roles. These receptors are coupled to a heterodimer of G proteins (guanine nucleotide–binding regulatory proteins) consisting of subunits α, β and γ. When inactive, subunit α is bound to GDP; upon binding of an agonist to the receptor, an allosteric change takes place in the complex causing GDP to leave and be replaced by GTP, which in turn causes disassociation of subunit α from the other two subunits and allows it to target its effector molecules. Alpha subunits have several forms with distinct roles, the main ones being Gs, Gi, Gq and Gt [220].

Since the discovery in 2004 of succinate as a ligand for GPR91, this receptor has been extensively studied. GPR91, encoded by SUCNR1, in mammals is expressed in the kidney, liver, spleen, intestine, adipose tissue and cardiomyocytes [204][221][222][223]. Experiments using a library of 800 compounds and 200 carboxylic acids revealed that GPR91 binds exclusively with succinate; while succinate does not bind with any of the 30 other tested GPCRs [204]. Depending on the cell type, the GPR91 receptor associates with Gs, Gi or Gq alpha subunits, triggering a variety of signaling pathways [205][224].

Previous reports show that overexpression of Gq in cultured cardiomyocytes leads to hypertrophy and apoptosis depending on its expression levels: overexpression of Gq (4-fold normal levels) causeded hypertrophy while higher expression (8-fold) caused hypertrophy followed by apoptosis. This progression from hypertrophy to apoptosis was accompanied with activation of p38 and JNK MAPKs [225]. Other researchers have reported that succinate feeding in rats enhances the amount of artificially induced ventricular hypertrophy via PI3K/AKT signaling upon GPR91 activation [226]. Aguiar et al observed that administration of succinate to rats activates GPR91 in cardiomyocytes, causing hypertrophy via extracellular signal-regulated kinase 1/2 (ERK1/2), expression of calcium/calmodulin dependent protein kinase IIδ (CaMKIIδ) and translocation of histone deacetylase 5 (HDAC5) into the cytoplasm [227]. Furthermore, activation of GPR91 has also been associated with modulation of JNK signaling [228].

Succinate may also trigger other effects independent of GPR91 activation. Knockdown of SDHA in mice results in accumulation of succinate that competes with the Krebs Cycle intermediate α-ketoglutarate (α-KG) to inhibit α-KG-dependent dioxygenases—conserved enzymes that catalyze reactions on a diverse set of substrates, such as proteins, DNA/RNA and lipids. This leads to a cascade of events resulting in genome-wide histone methylations [203][229]. Further gene expression studies need to be performed to obtain a detailed map of the gene modulation arising from increased succinate. Mutations in complex II subunits in humans have been shown to lead to benign tumors that express high levels of succinate. It is though that these tumors arise from succinate-mediated hypermethylation of histones and DNA [230].

Succinate also inhibits prolyl hydroxylases (PHDs), stabilizing Hif1-α [153][201]. As such, high concentrations of succinate mimic the hypoxic state and induce the transcription of Hif1-α-dependent genes, that include genes involved cell survival or conversely, apoptosis [231].

In summary, succinate accumulation can trigger a variety of cellular events, either through GPR91 activation or other mechanisms such as epigenetic modulation or Hif1-α-mediated transcription of a variety of genes. Given the relation between mutations in complex II and increased succinate levels, we speculated that knockdown of SdhD would also increase the levels of succinate, which could have a possible role in inducing hypertrophy and death in ISCs. As such, the levels of succinate upon SdhD knockdown were quantified.

### 4.4.1- Knockdown of SdhD causes an accumulation of succinate

To test our hypothesis that SdhD knockdown in flies causes an increase in the levels of succinate, RNAi was delivered in adults flies for 13 days using the ubiquitous driver *tub-Gal4; Gal80$^{TS}$*, crossed to the 101739KK SdhD-RNAi line or pKC43 control. Extracts from whole individuals were then analyzed using gas chromatography tandem mass spectrometry (GC-MS) to detect and quantify the levels of succinate.

GC-MS analysis showed that knockdown of SdhD in whole flies resulted in a marked increase in the levels of succinate (**Figure 20**; corresponding chromatograms and mass spectra in **Supplemental Figure 3**). These data demonstrate that ubiquitous knockdown of SdhD (and possibly other subunits of complex II) causes an accumulation of succinate, likely originating from impaired SdhA activity in the conversion of succinate to fumarate.

To explore a possible role of succinate as an GPR ligand in *Drosophila*, the NCBI Gene database [232] was used to look for GPR91 homologues. Despite GRP91 being conserved across a number of mammals and chicken and frog, there is, no homolog reported for *Drosophila melanogaster*. To look for possible homologues with a similar sequence, a Basic Local Alignment Search Tool (BLAST) [233] query of human SUCNR1 (accession number NP_149039.2) over the *Drosophila* proteome was performed to find potential succinate receptors in the fly, which resulted in several alignments (**Supplemental Table 1**). The protein that produced the highest score is one of unknown function (accession number ABO52826.1), while others are known G protein-coupled receptors for allatostatins — a type of neuropeptide hormone commonly found in insects. The ABO52826.1 protein scored an identity of 26% over 84% of the sequence ('query cover'), with an E value of 1.00E-19. *Query cover* refers to the percentage of the sequence that was selected for its similarity to be analyzed; the *E value* corresponds to the number of alignments expected by chance (the lower this value, the more significant is the correspondence); *Identity* corresponds to the percentage of matches in the alignment. As comparison, the Lgr2 receptor in *Drosophila* (NP_476702.1), the homolog of the mammalian ISC marker Lgr5 (NP_003658.1 in humans) [234][235] generated an identity of 29% over 44% of the sequence with an E value of 1e-115 [233]. Overall, the *Drosophila* genome contains ~200 genes coding for (putative) GPCRs related to hormones, neurotransmitters, olfactory and taste receptors, of which several remain orphan [236].

Future work should include knocking down the succinate transporters Dic1, VDAC (aka porin, CG6647) or INDY (CG3979) while co-expressing SdhD-RNAi in the same cells, to observe if it rescues the phenotype. These experiments should be carefully controlled since these transporters are not specific for succinate and its knockdown could lead to effects

related to deficient transport of other metabolites such as citrate or malate, or even succinate playing other roles. Pharmacological inhibitors targeting the succinate transporters have the disadvantage of not being specific to ISCs.

Further experiments should be performed to test if any of the GPR candidates acts as a succinate receptor. The levels of activated G proteins in ISCs isolated by FACS could indicate if these were activated via GPR signaling upon SdhD knockdown. Alternatively, it is suggested to knockdown SdhD simultaneously with each of the candidate proteins. If a candidate protein has a role as succinate receptor to induce hypertrophy and cell death, these phenotypes would be rescued in a loss-of-function background. The same principle could be applied to G proteins, although given the ubiquitous nature of these proteins, one would expect undesired effects in ISCs from its action upon activation from other receptors.

The authors of the original study that revealed GPR91 as a succinate receptor, hypothesized that the carboxyl groups (-COOH) in succinate were responsible for its agonist effect in GPR91. As these groups are negatively charged at biological pH, they should bind to positive amino acid residues on GPR91. After identifying possible amino acids, the researchers used mutagenesis to identify Arg 99, His 103, Arg 252 and Arg 281 as being required for GPR91 activation by succinate, while mutations of other amino acids where not required for activation. A comparison of about 300 GPCRs revealed that GPR91 uniquely contains all four basic residues [204]. These same principles could be used to select candidate proteins as succinate receptors in the fruit fly.

To test the role of succinate in the observed phenotypes, another suggested experiment is to feed succinate to the flies. In similarity with RU, succinic acid is soluble in ethanol [237] and could be added to the fly meal. It is unclear if succinate would be able to reach ISCs without being metabolized before.

In conclusion, it was shown that ubiquitous knockdown of SdhD increases the levels of succinate in flies, which could elicit the phenotypes described in sections 1 and 2. These data refers only to accumulation of succinate in whole flies, and the effects on ISCs were not specifically tested. To assess the levels of succinate specifically in ISCs, fluorescence-activated cell sorting (FACS) of ISCs is recommended to separate these cells.

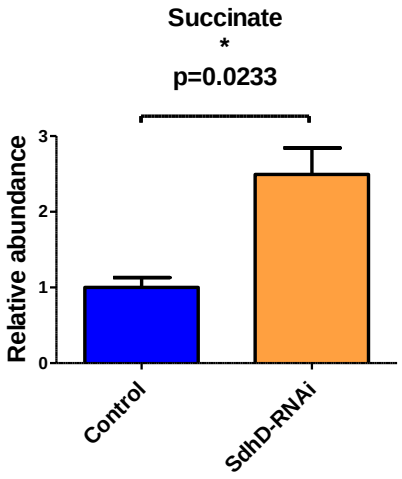


**Figure 20: Levels of succinate in whole flies upon ubiquitous SdhD knockdown**
Ubiquitous knockdown of SdhD resulted in an accumulation of succinate in whole flies (orange bar), when compared to controls (blue) after 13 days of RNAi expression, as quantified by GC-MS (details in Supplemental Figure 3). SdhD-RNAi (VDRC 101739 KK) was expressed in whole flies using the *tub-gal4* driver. As control, the pKC43 line was crossed to the same driver line. 3 biological replicates were used for each group, with 15 flies in each. Statistics: Unpaired two-tailed Student's t-test; p = 0.0233.

# General Discussion

**Characterization of the SdhD-RNAi phenotype in progenitor cells**

In this work, we performed a screen to explore the requirement for subunits of different ETC complexes in intestinal progenitor cells (ISCs and EBs) of *Drosophila*. Different subunits were individually knocked down via RNAi in intestinal progenitor cells of adult flies using the progenitor cell — and temporal — specific driver $5961^{GS}$. SdhD and SdhC of complex II emerged as strong candidates revealing both a similar phenotype in which the abundance of progenitor cells in the tissue was reduced (**Figure 5**). Knockdown of complex II subunit A (SdhA) did not result in a significant phenotype, but using the stronger *esg-Gal4* driver resulted in a significant decrease in the number of progenitor cells in the intestine, in similarity with SdhC and SdhD, which is attributed to a stronger expression of the *esg-Gal4* driver (see section 4.3). These results suggest a complex II-specific requirement in intestinal progenitor cells. Further experiments showed that knockdown of SdhD specifically in ISCs causes a significant reduction in the number of both ISCs and EBs, while EB-specific knockdown of SdhD did not result in changes in the abundance of these cells, indicating an ISC-specific requirement for SdhD (section 2.1). In addition, it was determined that ISCs depleted of SdhD display reduced rates of division (section 2.2). ISCs depleted of SdhD also display visible signs of cell death, such as cytoplasmic blebbing, shrinking and chromatin fragmentation (section 2.3). Further analysis showed that SdhD-depleted ISCs undergo hypertrophy, exhibiting a larger cytoplasmic and nuclear size, and higher nuclear content (2.4), suggesting that these cells become polyploid, which is a trait normally restricted to ECs or late EBs that are differentiating to ECs. To achieve polyploidy, cell must skip mitosis (or at least, cytokinesis) [50], which might explain the reduction in the rates of division observed in 2.2.

Additionally, preliminary data suggest that SdhD is required in progenitor cells for normal differentiation choices, as cells depleted of SdhD appear to present a differentiation bias towards an EE fate instead of EC, which is implied by an increased number of EEs upon SdhD knockdown in progenitor cells and an apparent increase in the numbers of EE-marked progeny observed in a lineage-tracing experiment, while the abundance of EC-marked progeny decreases (section 3). The differentiation bias towards an EE fate could be explained by lack of Delta-Notch signaling. As Notch signaling in EBs is dependent on the Delta ligand produced in ISCs, the loss (or malfunction) of ISCs could lead to a decreased Notch signaling in EBs, leading to a preference in differentiation towards EEs. Further experiments need to be performed to detect Delta and Notch levels in ISCs and EBs.

The phenotypes resulting from loss of SdhD in progenitor cells appear to occur in a progressive manner: during the first 6 days, most EBs are lost and fewer ISCs remain (see

section 1.1), after which ISCs become larger (more noticeable at days 7 and 13; see sections 2.3 and 2.4), and continue to disappear, likely through cell death (2.3), until complete depletion at day 30 (section 1.1, **Figure 8**). In light of the results obtained in sections 1, 2 and 3, the observed loss of EBs is attributed to differentiation of these cells into EEs and ECs (section 3), coupled to reduced division rates and death of ISCs (2.2 and 2.3), limiting their ability to generate EBs via asymmetric division. The loss of ISCs is attributed to cell death, as discussed in 2.3. The use of different drivers revealed the importance of the strength of GAL4 expression in generating the obtained phenotypes. SdhD knockdown in progenitor cells using the $5961^{GS}$ driver in flies fed 10 µg/ml RU did not result in hypertrophic ISCs that were seen using the ISC-specific driver based on *esg-Gal4*, neither a strong, cumulative reduction in their numbers, as visible in **Figure 12** where they still maintain a reasonable representation in the intestine after 45 days of SdhD-RNAi expression.

**Mechanisms behind hypertrophy and cell death in intestinal stem cells**

Many of the pathways that promote cell growth and polyploidy, such as the PI3K/AKT/TOR pathway, inhibit autophagy and apoptosis [176]. Accordingly, the authors who previously reported hypertrophy in ISCs via TOR activation, did not report cellular death [184]. This suggests that the observed results do not result from a typical hypertrophy/growth program, or that there are different mechanisms working in parallel that ultimately result in cell death. Despite many of the pathways that promote cell growth and polyploidy being associated with cell survival, two known processes are associated with polyploidy and cell death: mitotic catastrophe and succinate signaling via its receptor, GPR91 in mammals.

The observation of polyploidy and cell death in ISCs depleted of SdhD may indicate that these cells are unable to proceed through mitosis and become polyploid in a process named mitotic catastrophe (MC), which usually leads to cell death (described in 4.2). In this scenario, cells unable to proceed to mitosis would either die, or reenter the interphase of the cell cycle, increasing their DNA content and cell size. This hypothesis is in line with the observed results in that ISCs depleted of SdhD divide less (as seen in section 2.2) in the absence of a complete mitotic process, become polyploid and larger (2.4) and eventually die (2.3). It and also accounts for the specificity of the phenotype in ISCs and its absence in EBs (2.1), since it occurs from mitosis, which in principle does not occur in EBs. However, this does not account for the complex II specificity, since RNAi for subunits in other complexes did not elicit such phenotype, although this could be explained by differences in effectiveness of RNAi constructs or sensitivity of the OXPHOS process to loss of complex II components. If ISCs are very sensitive to loss of complex II subunits, perhaps they would not

have available energy to proceed through mitosis. Conversely, SdhD-RNAi ISCs are growing in size and DNA content, which is an energy-required process [82], and suggest a mechanism other than reduced ATP. Further experiments need to be performed to test this hypothesis, namely performing a complete metabolic profile of SdhD-depleted ISCs, including measuring ATP levels and AMPK activation, which occurs under low-energy conditions.

As knockdown of complex II subunits have been shown in other reports to cause a reduction in complex II activity (described in 4.3), leading an in increase in the levels of succinate, its levels were assessed in SdhD-depleted flies using the ubiquitous driver *tub-Gal4*. This experiment showed that knockdown of SdhD in flies results in an accumulation of succinate to levels more than two-fold higher than controls (4.4). The phenotypes of hypertrophy and cell death in ISCs could be explained by action of increased levels of succinate observed upon SdhD knockdown that trigger pathways responsible for hypertrophy and cell death. Previous reports exploring the role of succinate as a signaling molecule indicate these possibilities, as described in section 4.4. One possible pathway is the activation of the succinate receptor GPR91 that triggers the release of Gq proteins that have been previously associated with initiation of hypertrophy and apoptosis. This hypothesis accounts for the specificity of complex II observed in the screen, with SdhC-RNAi also causing a reduction in the number of progenitor cells (**Figure 5**) and SdhA-RNAi causing the same phenotype with the *esg-Gal4* driver (4.3). It does not explain, however, why there was an observed effect in ISCs but not in EBs. Perhaps ICSs have receptors that EBs do not have? Although the size of ECs around SdhD-depleted ISCs was not quantified, these cells appear to be larger than the ones in the control group (**Figure 10 A**, **Figure 14 A**). If succinate is responsible for increasing the size of ISCs, it could happen that excess succinate produced in ISCs could also trigger hypertrophy and cell death in ECs as an extracellular signaling molecule. However, the existence of a GPR91 homologue has not yet been confirmed in flies.

Under the “succinate receptor” hypothesis, it is expected that ISCs are dying by apoptosis. Determining the type of cell death in ISCs could provide important clues to the mechanisms behind the observed phenotypes, as mitotic catastrophe might result in cell death by either apoptosis or necrosis. Interestingly, HiF1-α, which is stabilized by succinate, is usually associated with cell survival, inhibiting apoptosis on a transcriptional level. In some cases, however, Hif1-α also triggers apoptosis via stabilization of p53 [176].

Manipulations resulting in reduction of aerobic respiration in ISCs has been shown to trigger increased proliferation in these cells [109] — the opposite of the phenotypes descibed here — indicating that ISCs should be able to rely on anaerobic respiration for survival and proliferation. Perhaps they are able to sustain small reductions in the levels of

OXPHOS activity, but not stronger changes. This could explain why SdhA-RNAi using the weaker $5961^{GS}$ driver caused a slight, non-significant, increase in the number of progenitor cells (section 1.1), but SdhA-RNAi using the *esg-Gal4* driver causes a visible reduction in their abundance (4.3). As ISCs rely on beta oxidation [113], it is expected that they require OXPHOS to some level, since Acetyl-CoA resulting from beta oxidation must be oxidized in the mitochondria for energy production.

It remains to be determined if ISCs are skipping mitosis (as strongly suggested from the data in 2.2 and 2.4) as part of a program, of simply because they are unable to complete it. More experiments are required to dissect the cell cycle dynamics and pathways leading to cell death. Live imaging of the midgut [238] would be of great importance in exposing the dynamics of the cell cycle in ISCs, namely via observation of chromatin, mitotic spindle and nuclear membrane transformations; determination of cyclin/CDK presence and their mediators should also be included, as discussed in more detail in section 2.2. EM would provide deep insights about the state of organelles such as mitochondria or phagosomes, the amount of lipid droplets and the morphology of the chromatin and nuclear membrane, giving crucial hints to the type of cell death and metabolic state of the cell [167]. ATP-depleted cells would likely present several autophagosomes containing organelles [167][168]. Finally, the state of pathways normally involved in hypertrophy and survival such as IGF, JNK, Hif1-α and Hippo should be assessed; and as described in 4.4, the possible role of succinate should be determined.

# Conclusion

The present work aimed at filling a gap in current knowledge regarding how individual subunits of the ETC play a role in stem cell behavior. In a knockdown screen in intestinal progenitor cells of *Drosophila melanogaster* with 18 tested ETC subunits, we identified subunits of complex II as being required for normal progenitor cell function, whose knockdown causes hypertrophy and cell death, a novel phenotype in this system [185], and to my knowledge the first report showing a direct cause-effect relation between knockdown/mutations in complex II, and cellular hypertrophy and death, although other reports have shown a correlation between these [239][240]. These observations also suggest a deviation from the current paradigm, in which inhibition of OXPHOS generally leads to stem cell proliferation and does not promote cell death [98][99].

Furthermore, these findings filled a gap in this field of research regarding the requirement for different complexes and subunits of the ETC in progenitor cells, and the differences between the ISCs and EBs in *Drosophila*, as SdhD-RNAi in EBs did not cause any discernible phenotype. The results here described also reinforce the importance of knockdown strength, cell type, and subunit specificity, for studies based on knockdown of metabolic genes. It remains to be exactly determined if in experiments to knockdown subunits of the ETC, the results are dependent simply of specific subunits; or the knockdown strength, that appears to cause a variety of effects; or the subunit itself having a higher importance in the associated complex, and at the end, downregulation of the complex itself being responsible for the phenotype.

Regretfully, there was no opportunity to obtain more insights regarding the mode of cell death, changes in the cell cycle, and metabolic state of ISCs. It remains to be determined whether the observed phenotypes are part of a hypertrophy/apoptosis program induced by succinate; a consequence of unsuccessful mitosis; or other undescribed pathway.

As ISCs share several similarities with their mammalian counterparts from a metabolic perspective [109], future work derived from these experiments might reveal conserved pathways important for mammalian ISCs. Strategies for drug development against cancer seek targets that affect only cells capable of dividing, such as ISCs but not EBs. Upon determination of the exact mechanisms behind the reduction in cell division rates (section 2.2) and cell death (section 2.3), these could be explored for possible. This study also provided a new model for the study of hypertrophy and cell death caused by metabolic impairment. Understanding the mechanisms of stem cell proliferation and hypertrophy is essential to the fields of regeneration and tissue repair, as both are involved in these processes [182]. Further understanding the mechanisms underlying cellular hypertrophy and death could support the development of therapies for diseases such as hypertrophic

cardiomyopathy — a disease of the myocardium commonly arising from mutations in myosin genes with unknown downstream mechanisms, in which cardiomyocytes display increased cytoplasmic and nuclear size, higher DNA content [241], and apoptosis [242], and has also been associated with mutations in SDHD and complex II defects [239][240].

# Supplementary data

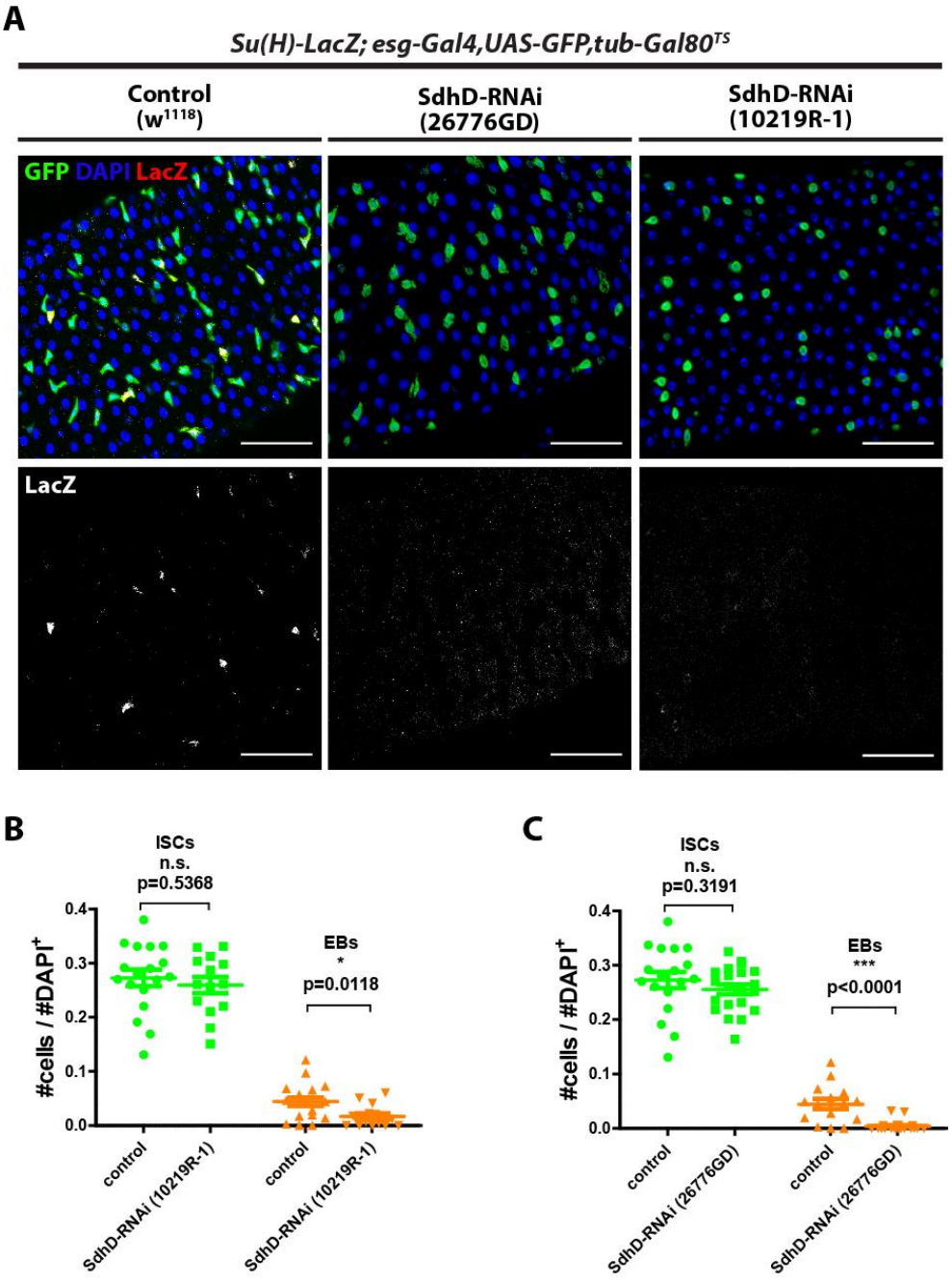


**Supplemental Figure 1: Effects of expression from different SdhD-RNAi lines in progenitor cells**
**A.** Knockdown of SdhD using the 26776GD and 10219R-1 RNAi lines partially replicates the phenotype previously obtained with the 101739KK line, with a significant decrease in the number of EBs (LacZ-positive). The reduction in the number of ISCs is not significant, which is attributed to a possible weaker RNAi activity of these lines. The line $w^{1118}$ was crossed to the *esg-gal4* driver and used as control. **B.** Quantification of the number of ISCs and EBs obtained upon SdhD-RNAi with the 26776 GD driver. n=18 in the control group and n=21 for RNAi **C.** Quantification for the 10219R-1 driver (n=14) vs controls (n=18). Unpaired two tailed Student's *t*-test.

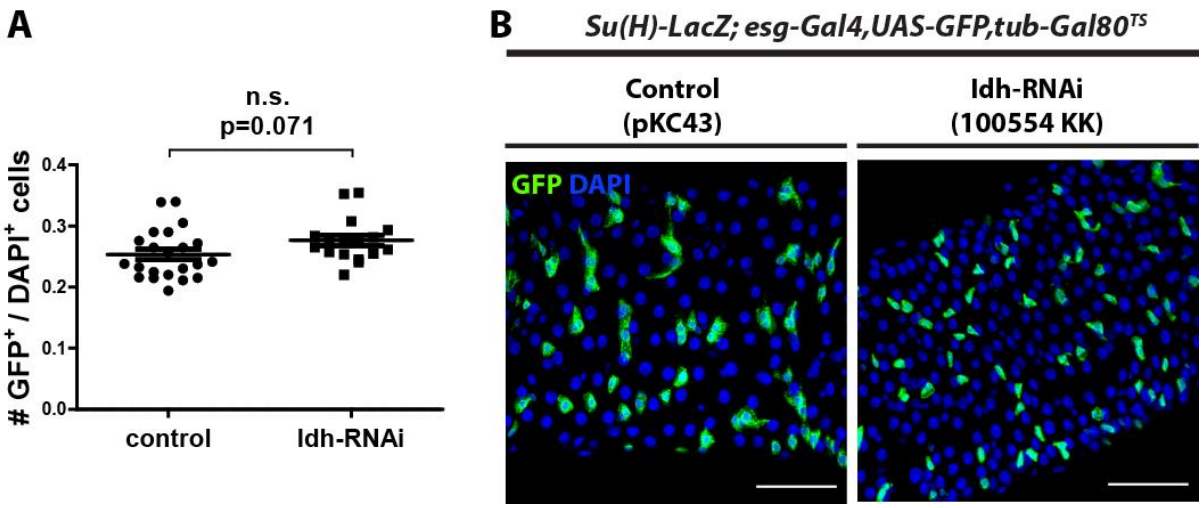


**Supplemental Figure 2: Isocitrate dehydrogenase knockdown in intestinal progenitor cells**
**A.** Quantification of the number of progenitor cells upon knockdown of isocitrate for 6 days reveals only a slight, non-significant increase in their numbers. **B.** Representative images of of Idh-RNAi (right) and control intestines (left), not showing any discernable phenotype. Scale bars = 50 µm. n=22 in controls and n=17 in Idh-RNAi. Statistics: unpaired two-tailed Student's *t*-test.

A

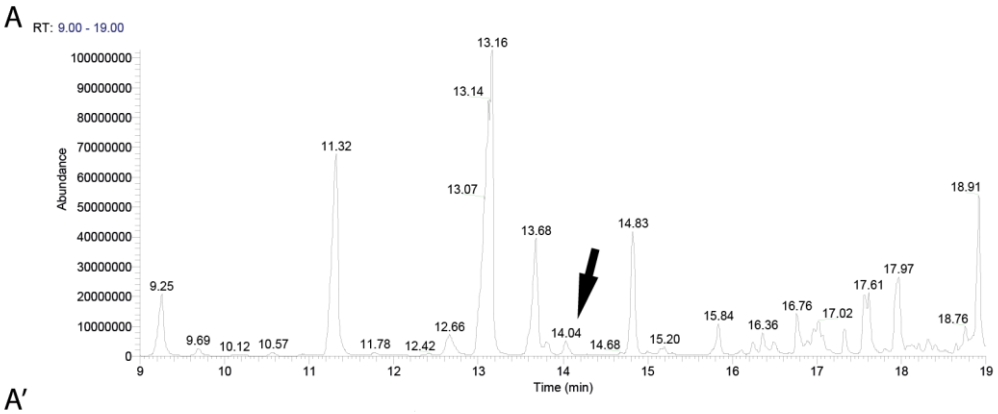
RT: 9.00 - 19.00
Abundance
Time (min)
13.16
13.14
11.32
13.07
18.91
13.68
14.83
17.97
17.61
9.25
16.76
17.02
15.84
16.36
18.76
12.66
14.04
9.69
10.12
10.57
11.78
12.42
14.68
15.20

A′

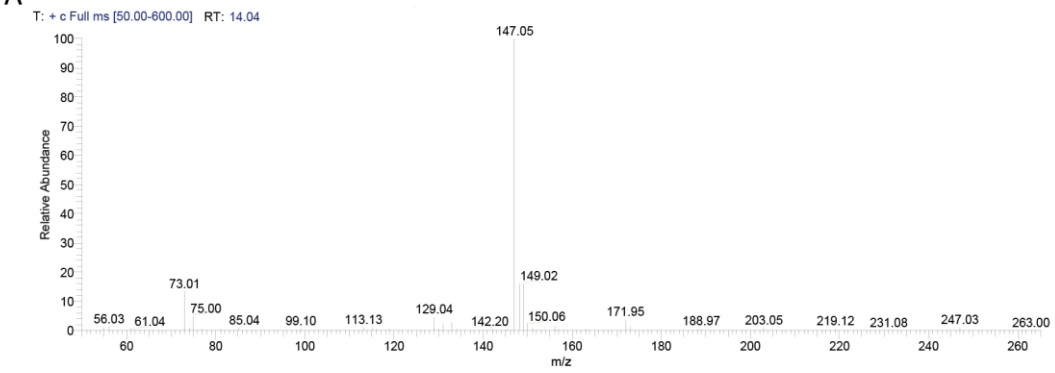
T: + c Full ms [50.00-600.00] RT: 14.04
Relative Abundance
m/z
147.05
149.02
73.01
75.00
129.04
56.03
61.04
85.04
99.10
113.13
142.20
150.06
171.95
188.97
203.05
219.12
231.08
247.03
263.00

B

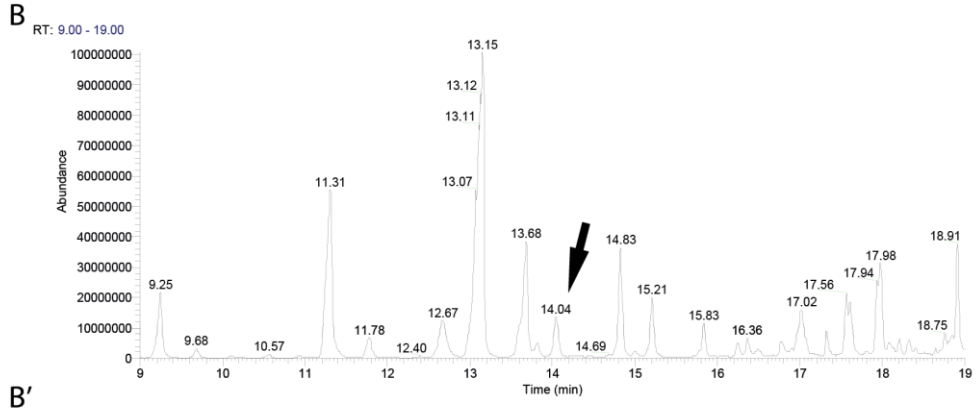
RT: 9.00 - 19.00
Abundance
Time (min)
13.15
13.12
13.11
11.31
13.07
13.68
14.83
18.91
17.98
9.25
17.94
15.21
17.56
12.67
14.04
17.02
15.83
11.78
16.36
18.75
9.68
10.57
12.40
14.69

B′

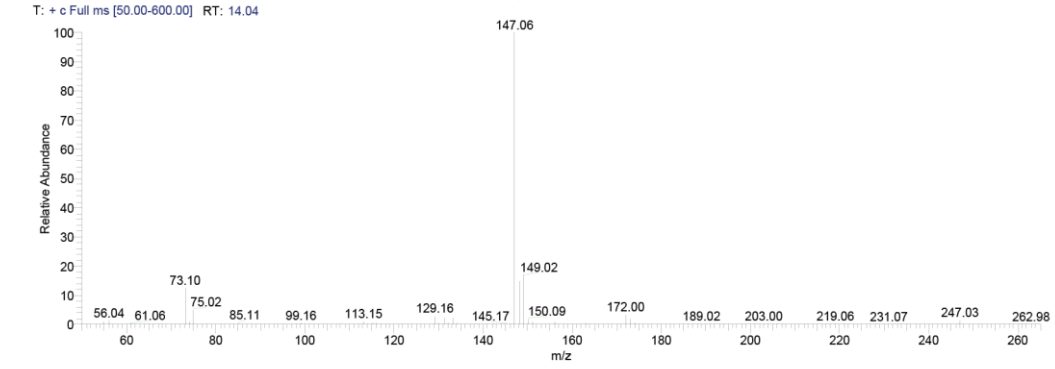
T: + c Full ms [50.00-600.00] RT: 14.04
Relative Abundance
m/z
147.06
149.02
73.10
75.02
56.04
61.06
85.11
99.16
113.15
129.16
145.17
150.09
172.00
189.02
203.00
219.06
231.07
247.03
262.98

C

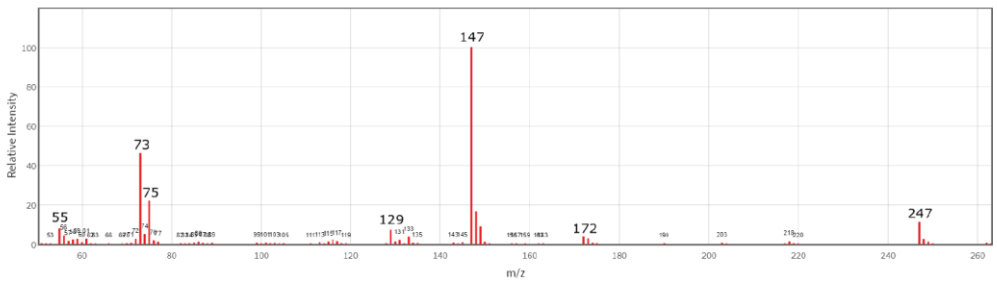
Relative Intensity
m/z
147
73
75
55
129
172
247

**Supplemental Figure 3: GC-MS analysis of SdhD-knockdown flies**

**A.** Chromatogram of pCK43 control extracts showing retention times (RT; x axis) between 9.00 and 19.00 minutes. In the y axis, 'abundance' refers to the absolute number of counts received at the detector which is proportional to the amount of each analyte in the sample. The peak at 14.04 min pointed by the arrow corresponds to succinate, confirmed by its mass spectrum. **A'.** Mass spectrum of the succinate 2TMS peak (RT=14.04) in controls, covering a molecular mass range of 50 to 265 m/z on the x axis (z corresponds to the charge of the particle which is usually +1). These peaks correspond with the ones from empirical data obtained from the NIST library (shown in C). **B**. Chromatogram of SdhD knockdown flies with the succinate 2TMS peak at 14.04 min showing a larger area than controls, corresponding to higher abundance of the metabolite. The other peaks in the chromatograms A and B correspond mostly to amino acids according to the NIST library (not shown) and do not appear to suffer major changes. **B'.** Mass spectrum of the succinate peak in SdhD-RNAi, similar to the one in A´, as expected. **C.** Empirical mass spectrum of succinate 2TMS obtained from the NIST library. The different peaks correspond to the different parts of the molecule that were broken apart, and may form new bonds with each other. A small peak is visible at 262 m/z which is the total mass of the derivatized succinate molecule.

Abundance in the mass spectra is relative to the maximum intensity obtained. Arbitrary units in the chromatogram reflect absolute abundance of the analytes. 3 biological replicates were used in each group, with 15 flies in each.

**Supplemental Table 1:** BLAST alignment results of human GPR91 and the *Drosophila melanogaster* proteome

| Description | Query cover | E value | Ident | Accession |
|---|---|---|---|---|
| IP03254p | 84% | 1.00E-19 | 26% | ABO52826.1 |
| allatostatin C/drostatin C receptor 1 | 84% | 2.00E-19 | 26% | AAL02125.1 |
| somatostatin receptor | 83% | 2.00E-19 | 26% | AAK31793.1 |
| allatostatin C receptor 2, isoform D | 83% | 2.00E-19 | 26% | NP_001262015.1 |
| allatostatin C receptor 2, isoform B | 83% | 2.00E-19 | 26% | NP_649039.4 |
| allatostatin C receptor 2, isoform F | 83% | 3.00E-19 | 26% | NP_001303398.1 |
| G protein-coupled neuropeptide pyrokinin-2 receptor (CG8795) - fruit fly | 86% | 2.00E-17 | 27% | JC8012 |
| putative PRXamide receptor | 86% | 2.00E-17 | 27% | AAN10043.1 |
| pyrokinin 2 receptor 2, isoform A | 86% | 2.00E-17 | 27% | NP_731788.1 |
| allatostatin A receptor 2, isoform B | 91% | 2.00E-17 | 24% | NP_001247352.1 |
| G protein-coupled neuropeptide pyrokinin-2 receptor (CG8784) | 92% | 5.00E-17 | 25% | JC8011 |

# References


[1] David L. Stocum. *Regenerative Biology and Medicine* (Second Edition) 2012, *Chapter 1 – An Overview of Regenerative Biology*, Pages 3–20

[2] Kristine P Krafts*. Tissue repair: The hidden drama.* Organogenesis. 2010 Oct-Dec; 6(4): 225–233. doi: 10.4161/org.6.4.12555

[3] Anderson DJ, Gage FH, Weissman IL. *Can stem cells cross lineage boundaries?* Nat Med. 2001 Apr;7(4):393-5

[4] Wagers AJ, Sherwood RI, Christensen JL, Weissman IL. *Little evidence for developmental plasticity of adult hematopoietic stem cells.* Science. 2002 Sep 27;297(5590):2256-9.

[5] Gurley KA, Sánchez Alvarado A. Stem cells in animal models of regeneration. 2008 Dec 31. In: StemBook [Internet]. Cambridge (MA): Harvard Stem Cell Institute; 2008-. Available from: https://www.ncbi.nlm.nih.gov/books/NBK27030/ doi: 10.3824/stembook.1.32.1

[6] Guasch G, Fuchs E. *Mice in the world of stem cell biology.* Nat Genet. 2005 Nov;37(11):1201-6.

[7] Brignier AC, Gewirtz AM. *Embryonic and adult stem cell therapy.* J Allergy Clin Immunol. 2010 Feb;125(2 Suppl 2):S336-44. doi: 10.1016/j.jaci.2009.09.032.

[8] Evans MJ, Kaufman MH. *Establishment in culture of pluripotential cells from mouse embryos.* Nature. 1981 Jul 9;292(5819):154-6.

[9] Martin GR. *Isolation of a pluripotent cell line from early mouse embryos cultured in medium conditioned by teratocarcinoma stem cells.* Proc Natl Acad Sci U S A. 1981 Dec;78(12):7634-8.

[10] Wong CW, Hou PS, Tseng SF, Chien CL, Wu KJ, Chen HF, Ho HN, Kyo S, Teng SC. *Krüppel-like transcription factor 4 contributes to maintenance of telomerase activity in stem cells.* Stem Cells. 2010 Sep;28(9):1510-7. doi: 10.1002/stem.477.

[11] Jen-Hua Chuang, Li-Chu Tung, and Yenshou Lin. *Neural differentiation from embryonic stem cells in vitro: An overview of the signaling pathways.* World J Stem Cells. 2015 Mar 26; 7(2): 437–447. doi: 10.4252/wjsc.v7.i2.437

[12] Kokkinopoulos I, Ishida H, Saba R, Coppen S, Suzuki K, Yashiro K. *Cardiomyocyte differentiation from mouse embryonic stem cells using a simple and defined protocol.* Dev Dyn. 2016 Feb;245(2):157-65. doi: 10.1002/dvdy.24366

[13] Ogaki S, Shiraki N, Kume K, Kume S. *Wnt and Notch signals guide embryonic stem cell differentiation into the intestinal lineages.* Stem Cells. 2013 Jun;31(6):1086-96. doi: 10.1002/stem.1344.

[14] Takahashi K, Yamanaka S. *Induction of pluripotent stem cells from mouse embryonic and adult fibroblast cultures by defined factors.* Cell. 2006 Aug 25;126(4):663-76

[15] Yu J, Vodyanik MA, Smuga-Otto K, Antosiewicz-Bourget J, Frane JL, Tian S, Nie J, Jonsdottir GA, Ruotti V, Stewart R, Slukvin II, Thomson JA. *Induced pluripotent stem cell lines derived from human somatic cells.* Science. 2007 Dec 21;318(5858):1917-20.

[16] Raya A, Rodríguez-Pizà I, Guenechea G, Vassena R, Navarro S, Barrero MJ, Consiglio A, Castellà M, Río P, Sleep E, González F, Tiscornia G, Garreta E, Aasen T, Veiga A, Verma IM, Surrallés J, Bueren J, Izpisúa Belmonte JC. *Disease-corrected haematopoietic progenitors from Fanconi anaemia induced pluripotent stem cells.* Nature. 2009 Jul 2;460(7251):53-9. doi: 10.1038/nature08129

[17] João V. Cordeiro & António Jacinto. *The role of transcription-independent damage signals in the initiation of epithelial wound healing.* Nature Reviews Molecular Cell Biology 14, 249–262 (2013) doi:10.1038/nrm3541
[18] Spangrude GJ, Heimfeld S, Weissman IL. *Purification and characterization of mouse hematopoietic stem cells.* Science. 1988 Jul 1;241(4861):58-62
[19] Seale P, Asakura A, Rudnicki MA. *The potential of muscle stem cells.* Dev Cell. 2001 Sep;1(3):333-42
[20] Cotsarelis G, Sun TT, Lavker RM. *Label-retaining cells reside in the bulge area of pilosebaceous unit: implications for follicular stem cells, hair cycle, and skin carcinogenesis.* Cell. 1990 Jun 29;61(7):1329-37
[21] Loeffler M, Birke A, Winton D, Potten C. *Somatic mutation, monoclonality and stochastic models of stem cell organization in the intestinal crypt.* J Theor Biol. 1993 Feb 21;160(4):471-91.
[22] Beltrami AP, Barlucchi L, Torella D, Baker M, Limana F, Chimenti S, Kasahara H, Rota M, Musso E, Urbanek K, Leri A, Kajstura J, Nadal-Ginard B, Anversa P. *Adult cardiac stem cells are multipotent and support myocardial regeneration.* Cell. 2003 Sep 19;114(6):763-76.
[23] Laugwitz KL, Moretti A, Lam J, Gruber P, Chen Y, Woodard S, Lin LZ, Cai CL, Lu MM, Reth M, Platoshyn O, Yuan JX, Evans S, Chien KR. *Postnatal isl1+ cardioblasts enter fully differentiated cardiomyocyte lineages.* Nature. 2005 Feb 10;433(7026):647-53
[24] Buchstaller J, Sommer L, Bodmer M, Hoffmann R, Suter U, Mantei N. *Efficient isolation and gene expression profiling of small numbers of neural crest stem cells and developing Schwann cells.* J Neurosci. 2004 Mar 10;24(10):2357-65
[25] Doetsch F, Caillé I, Lim DA, García-Verdugo JM, Alvarez-Buylla A. *Subventricular zone astrocytes are neural stem cells in the adult mammalian brain.* Cell. 1999 Jun 11;97(6):703-16.
[26] Kim CF, Jackson EL, Woolfenden AE, Lawrence S, Babar I, Vogel S, Crowley D, Bronson RT, Jacks T. *Identification of bronchioalveolar stem cells in normal lung and lung cancer.* Cell. 2005 Jun 17;121(6):823-35.
[27] Yamashita YM, Fuller MT, Jones DL. *Signaling in stem cell niches: lessons from the Drosophila* germline. J Cell Sci. 2005 Feb 15;118(Pt 4):665-72.
[28] Farbod Famili, Anna-Sophia Wiekmeijer, and Frank JT Staal. *The development of T cells from stem cells in mice and humans.* Future Sci OA. 2017 Aug; 3(3): FSO186. doi: 10.4155/fsoa-2016-0095
[29] Reya T, Morrison SJ, Clarke MF, Weissman IL. *Stem cells, cancer, and cancer stem cells.* Nature. 2001 Nov 1;414(6859):105-11.
[30] Mark A. Feitelson, Alla Arzumanyan, Rob J. Kulathinal, Stacy W. Blain, Randall F. Holcombe, Jamal Mahajna, Maria Marino, Maria L. Martinez-Chantar, Roman Nawroth, Isidro Sanchez-Garcia, Dipali Sharma, Neeraj K. Saxena, Neetu Singh, Panagiotis J. Vlachostergios, Shanchun Guom, Kanya Honokin, Hiromasa Fujiin, Alexandros G. Georgakilas, Alan Bilsland, Amedeo Amedei, Elena Niccolai, Amr Amin, S. Salman Ashraf, Chandra S. Boosanit, Gunjan Guhau, Maria Rosa Ciriolo, Katia Aquilanov, Sophie Chen, Sulma I. Mohammed, Asfar S. Azmi, Dipita Bhaktau, Dorota Halicka, W. Nicol Keith, Somaira Nowsheen. *Sustained proliferation in cancer: Mechanisms and novel therapeutic targets.* Seminars in Cancer Biology, Volume 35, Supplement, December 2015, Pages S25-S54

[31] Poss KD, Keating MT, Nechiporuk A. *Tales of regeneration in zebrafish.* Dev Dyn. 2003 Feb;226(2):202-10.
[32] Romanoff AL. *Cultivation of the early chick embryo in vitro*. The Anatomical Record. 1943;87:365–369
[33] Bjørnstad S, Austdal LP, Roald B, Glover JC, Paulsen RE. *Cracking the Egg: Potential of the Developing Chicken as a Model System for Nonclinical Safety Studies of Pharmaceuticals.* J Pharmacol Exp Ther. 2015 Dec;355(3):386-96. doi: 10.1124/jpet.115.227025
[34] Kain KH, Miller JW, Jones-Paris CR, Thomason RT, Lewis JD, Bader DM, Barnett JV, Zijlstra A. *The chick embryo as an expanding experimental model for cancer and cardiovascular research.* Dev Dyn. 2014 Feb;243(2):216-28. doi: 10.1002/dvdy.24093
[35] Duffy JB. *GAL4 system in Drosophila: a fly geneticist's Swiss army knife.* Genesis. 2002 Sep-Oct;34(1-2):1-15.
[36] Bharucha KN. *The epicurean fly: using Drosophila melanogaster to study metabolism.* Pediatr Res. 2009 Feb;65(2):132-7. doi: 10.1203/PDR.0b013e318191fc68.
[37] Craig A. Micchelli & Norbert Perrimon. *Evidence that stem cells reside in the adult Drosophila midgut epithelium.* Nature 439, 475-479 (26 January 2006) | doi:10.1038/nature04371
[38] Ohlstein B, Spradling A. *The adult Drosophila posterior midgut is maintained by pluripotent stem cells.* Nature. 2006 Jan 26;439(7075):470-4
[39] Elena M. Lucchetta and Benjamin Ohlstein. *The Drosophila midgut: a model for stem cell driven tissue regeneration.* Wiley Interdiscip Rev Dev Biol. 2012 Sep-Oct; 1(5): 781–788. doi: 10.1002/wdev.51
[40] Yiorgos Apidianakis and Laurence G. Rahme. *Drosophila melanogaster as a model for human intestinal infection and pathology.* Dis Model Mech. 2011 Jan; 4(1): 21–30. doi: 10.1242/dmm.003970
[41] Huaqi Jiang and Bruce A. Edgar. *Intestinal stem cell function in Drosophila and Mice.* Curr Opin Genet Dev. 2012 Aug; 22(4): 354–360.
[42] Zheng Guo, Elena Lucchetta, Neus Rafel, and Benjamin Ohlstein. *Maintenance of the Adult Drosophila Intestine: All Roads Lead to Homeostasis.* Curr Opin Genet Dev. 2016 Oct; 40: 81–86. doi: 10.1016/j.gde.2016.06.009
[43] Ji Chen, Seol-min Kim, and Jae Young Kwon. *A Systematic Analysis of Drosophila Regulatory Peptide Expression in Enteroendocrine Cells.* Mol Cells. 2016 Apr 30; 39(4): 358–366. doi: 10.14348/molcells.2016.0014
[44] Jinyi Xiang, Jennifer Bandura, Peng Zhang, Yinhua Jin, Hanna Reuter, and Bruce A. Edgar. *EGFR-dependent TOR-independent endocycles support Drosophila gut epithelial regeneration. Nat Commun. 2017; 8: 15125. doi: 10.1038/ncomms15125*
[45] Loza-Coll MA, Southall TD, Sandall SL, Brand AH, Jones DL. *Regulation of Drosophila intestinal stem cell maintenance and differentiation by the transcription factor Escargot.* EMBO J. 2014 Dec 17;33(24):2983-96. doi: 10.15252/embj.201489050
[46] Benoît Biteau and Heinrich Jasper. *Slit/Robo signaling regulates cell fate decisions in the intestinal stem cell lineage of Drosophila.* Cell Rep. 2014 Jun 26; 7(6): 1867–1875. doi: 10.1016/j.celrep.2014.05.024
[47] van der Flier LG, Clevers H. *Stem cells, self-renewal, and differentiation in the intestinal epithelium.* Annu Rev Physiol. 2009;71:241-60. doi: 10.1146/annurev.physiol.010908.163145.

[48] Bray S, Furriols M. *Notch pathway: making sense of suppressor of hairless.* Curr Biol. 2001 Mar 20;11(6):R217-21.
[49] Ute Koch, Rajwinder Lehal, Freddy Radtke*. Stem cells living with a Notch.* Development 2013 140: 689-704; doi: 10.1242/dev.080614
[50] Edgar BA, Zielke N, Gutierrez C. *Endocycles: a recurrent evolutionary innovation for post-mitotic cell growth.* Nat Rev Mol Cell Biol. 2014 Mar;15(3):197-210. doi: 10.1038/nrm3756
[51] Rachael L. Shaw, Alexander Kohlmaier, Cédric Polesello, Cornelia Veelken, Bruce A. Edgar, Nicolas Tapon. *The Hippo pathway regulates intestinal stem cell proliferation during Drosophila adult midgut regeneration.* Development 2010 137: 4147-4158; doi: 10.1242/dev.052506
[52] Horvay K, Casagranda F, Gany A, Hime GR, Abud HE. *Wnt signaling regulates Snai1 expression and cellular localization in the mouse intestinal epithelial stem cell niche.* Stem Cells Dev. 2011 Apr;20(4):737-45. doi: 10.1089/scd.2010.0188.
[53] Dutta D, Dobson AJ, Houtz PL, Gläßer C, Revah J, Korzelius J, Patel PH, Edgar BA, Buchon N. *Regional Cell-Specific Transcriptome Mapping Reveals Regulatory Complexity in the Adult Drosophila Midgut.* Cell Rep. 2015 Jul 14;12(2):346-58. doi: 10.1016/j.celrep.2015.06.009.
[54] Benoît Biteau, Christine E. Hochmuth, Heinrich Jasper. *JNK Activity in Somatic Stem Cells Causes Loss of Tissue Homeostasis in the Aging Drosophila Gut.* Cell Stem Cell. Volume 3, Issue 4, 9 October 2008, Pages 442-455
[55] Heinrich Jasper. *Exploring the physiology and pathology of aging in the intestine of Drosophila melanogaster.* Invertebr Reprod Dev. 2015 Jan 30; 59(sup1): 51–58. doi: 10.1080/07924259.2014.963713
[56] Hur JH, Bahadorani S, Graniel J, Koehler CL, Ulgherait M, Rera M, Jones DL, Walker DW. *Increased longevity mediated by yeast NDI1 expression in Drosophila intestinal stem and progenitor cells.* Aging (Albany NY). 2013 Sep;5(9):662-81.
[57] Jiang H, Edgar BA. *Intestinal stem cells in the adult Drosophila midgut.* Exp Cell Res. 2011 Nov 15;317(19):2780-8. doi: 10.1016/j.yexcr.2011.07.020.
[58] Jiang H, Patel PH, Kohlmaier A, Grenley MO, McEwen DG, Edgar BA. *Cytokine/Jak/Stat signaling mediates regeneration and homeostasis in the Drosophila midgut.* Cell. 2009 Jun 26;137(7):1343-55. doi: 10.1016/j.cell.2009.05.014.
[59] Jason S. Rawlings, Kristin M. Rosler, Douglas A. Harrison. *The JAK/STAT signaling pathway.* Journal of Cell Science 2004 117: 1281-1283; doi: 10.1242/jcs.00963
[60] Sharan Swarup and Esther M. Verheyen. *Wnt/Wingless Signaling in Drosophila.* Cold Spring Harb Perspect Biol. 2012 Jun; 4(6): a007930. doi: 10.1101/cshperspect.a007930
[61] Lin G, Xu N, Xi R. *Paracrine Wingless signalling controls self-renewal of Drosophila intestinal stem cells.* Nature. 2008 Oct 23;455(7216):1119-23. doi: 10.1038/nature07329.
[62] Julia B Cordero, Rhoda K Stefanatos, Alessandro Scopelliti, Marcos Vidal, and Owen J Sansomb. *Inducible progenitor-derived Wingless regulates adult midgut regeneration in Drosophila.* EMBO J. 2012 Oct 3; 31(19): 3901–3917. doi: 10.1038/emboj.2012.248
[63] Ai Tian, Hassina Benchabane, Zhenghan Wang, and Yashi Ahmed. *Regulation of Stem Cell Proliferation and Cell Fate Specification by Wingless/Wnt Signaling Gradients Enriched at Adult Intestinal Compartment Boundaries.* PLoS Genet. 2016 Feb; 12(2): e1005822. doi: 10.1371/journal.pgen.1005822

[64] Crosnier C, Stamataki D, Lewis J. *Organizing cell renewal in the intestine: stem cells, signals and combinatorial control.* Nat Rev Genet. 2006 May;7(5):349-59.
[65] Moon RT, Bowerman B, Boutros M, Perrimon N. *The promise and perils of Wnt signaling through beta-catenin.* Science. 2002 May 31; 296(5573):1644-6
[66] Davies C, Tournier C. *Exploring the function of the JNK (c-Jun N-terminal kinase) signalling pathway in physiological and pathological processes to design novel therapeutic strategies.* Biochem Soc Trans. 2012 Feb;40(1):85-9. doi: 10.1042/BST20110641.
[67] Rocio Sancho, Abdolrahman S Nateri, Amaya Garcia de Vinuesa, Cristina Aguilera, Emma Nye, Bradley Spencer-Dene, and Axel Behrens. *JNK signalling modulates intestinal homeostasis and tumourigenesis in mice.* EMBO J. 2009 Jul 8; 28(13): 1843–1854. doi: 10.1038/emboj.2009.153
[68] Ip YT, Davis RJ. *Signal transduction by the c-Jun N-terminal kinase (JNK)--from inflammation to development.* Curr Opin Cell Biol. 1998 Apr;10(2):205-19.
[69] Martin Resnik-Docampo, Christopher L. Koehler, Rebecca I. Clark, Joseph M. Schinaman, Vivien Sauer, Daniel M. Wong, Sophia Lewis, Cecilia D'Alterio, David W. Walker & D. Leanne Jones. *Tricellular junctions regulate intestinal stem cell behaviour to maintain homeostasis.* Nature Cell Biology volume 19, pages 52–59 (2017) doi:10.1038/ncb3454
[70] Xu N, Wang SQ, Tan D, Gao Y, Lin G, Xi R. *EGFR, Wingless and JAK/STAT signaling cooperatively maintain Drosophila intestinal stem cells.* Dev Biol. 2011 Jun 1;354(1):31-43. doi: 10.1016/j.ydbio.2011.03.018. Epub 2011 Apr 1.
[71] Yinhua Jin, Nati Ha, Marta Forés, Jinyi Xiang, Christine Gläßer, Julieta Maldera, Gerardo Jiménez and Bruce A. Edgar. *EGFR/Ras Signaling Controls Drosophila Intestinal Stem Cell Proliferation via Capicua-Regulated Genes.* PLoS Genet. 2015 Dec; 11(12): e1005634. doi: 10.1371/journal.pgen.1005634
[72] Choi NH, Lucchetta E, Ohlstein B. *Nonautonomous regulation of Drosophila midgut stem cell proliferation by the insulin-signaling pathway.* Proceedings of the National Academy of Sciences of the United States of America. 2011;108(46):18702-18707. doi:10.1073/pnas.1109348108.
[73] Meng C. Wang, Dirk Bohmann, Heinrich Jasper. *JNK Extends Life Span and Limits Growth by Antagonizing Cellular and Organism-Wide Responses to Insulin Signaling.* Cell, Volume 121, Issue 1, 8 April 2005, Pages 115-125
[74] Hongbing Zhang, James P. Stallock, Joyce C. Ng, Christoph Reinhard, and Thomas P. Neufeld. *Regulation of cellular growth by the Drosophila target of rapamycin dTOR*. Genes & Dev. 2000. 14: 2712-2724. doi: 10.1101/gad.835000
[75] Anyonya R Guntur, Clifford J Rosen. *IGF-1 regulation of key signaling pathways in bone.* BoneKEy Reports (2013) 2, Article number: 437 (2013) doi:10.1038/bonekey.2013.171
[76] Tian A, Shi Q, Jiang A, Li S, Wang B, *Jiang J. Injury-stimulated Hedgehog signaling promotes regenerative proliferation of Drosophila intestinal stem cells.* J Cell Biol. 2015 Mar 16;208(6):807-19. doi: 10.1083/jcb.201409025. Epub 2015 Mar 9.
[77] Duojia Pan. *The Hippo Signaling Pathway in Development and Cancer*. Dev Cell. 2010 Oct 19; 19(4): 491–505. doi: 10.1016/j.devcel.2010.09.011
[78] Zhipeng Meng, Toshiro Moroishi, and Kun-Liang Guan. *Mechanisms of Hippo pathway regulation*. Genes Dev. 2016 Jan 1; 30(1): 1–17. doi: 10.1101/gad.274027.115
[79] Bin Zhao, Karen Tumaneng and Kun-Liang Guan. *The Hippo pathway in organ size control, tissue regeneration and stem cell self-renewal.* Nature Cell Biology, Volume 13, Number 8, August 2011

[80] Camargo FD, Gokhale S, Johnnidis JB, Fu D, Bell GW, Jaenisch R, Brummelkamp TR. *YAP1 increases organ size and expands undifferentiated progenitor cells.* Curr Biol. 2007 Dec 4;17(23):2054-60. Epub 2007 Nov 1.
[81] Meng FW, Biteau B. *A Sox Transcription Factor Is a Critical Regulator of Adult Stem Cell Proliferation in the Drosophila Intestine.* Cell Rep. 2015 Nov 3;13(5):906-14. doi: 10.1016/j.celrep.2015.09.061.
[82] Alexei Vazquez, Jiangxia Liu, Yi Zhou, and Zoltán N Oltvai. *Catabolic efficiency of aerobic glycolysis: The Warburg effect revisited.* BMC Syst Biol. 2010; 4: 58. doi: 10.1186/1752-0509-4-58
[83] Pfeiffer T, Schuster S, Bonhoeffer S. *Cooperation and competition in the evolution of ATP-producing pathways.* Science. 2001 Apr 20;292(5516):504-7.
[84] Houten SM, Wanders RJ. *A general introduction to the biochemistry of mitochondrial fatty acid β-oxidation.* J Inherit Metab Dis. 2010 Oct;33(5):469-77. doi: 10.1007/s10545-010-9061-2
[85] B. Alberts, A. Johnson, J. Lewis, M. Raff, K. Roberts, and P. Walter. *Molecular biology of the cell, 5th edition.* New York: Garland Science; 2007. Chapter 14: Energy Conversion: Mitochondria and Chloroplasts. P813-878
[86] Berg JM, Tymoczko JL, Stryer L. *Biochemistry*. 5th edition. Chapter 23, Protein Turnover and Amino Acid Catabolism. New York: W H Freeman; 2002. Available from: https://www.ncbi.nlm.nih.gov/books/NBK21182
[87] Berg JM, Tymoczko JL, Stryer L. Biochemistry. 5th edition. New York: W H Freeman; 2002. Section 23.5, Carbon Atoms of Degraded Amino Acids Emerge as Major Metabolic Intermediates. Available from: https://www.ncbi.nlm.nih.gov/books/NBK22453/
[88] B. Alberts, A. Johnson, J. Lewis, M. Raff, K. Roberts, and P. Walter. *Molecular biology of the cell, 5th edition.* New York: Garland Science; 2007. Chapter 2: Cell Chemistry and Biosynthesis. P45-124
[89] Voet, Judith G.; Voet, Donald (2004). *Biochemistry (3rd ed.)*. New York: J. Wiley & Sons. P813–826
[90] Cho J, Hur JH, Graniel J, Benzer S, Walker DW. *Expression of yeast NDI1 rescues a Drosophila complex I assembly defect.* PLoS One. 2012;7(11):e50644. doi: 10.1371/journal.pone.0050644.
[91] Sazanov LA. *A giant molecular proton pump: structure and mechanism of respiratory complex I.* Nat Rev Mol Cell Biol. 2015 Jun;16(6):375-88. doi: 10.1038/nrm3997
[92] Hederstedt L. *Complex II is complex too.* Science. 2003 Jan 31;299(5607):671-2.
[93] Wanet A, Arnould T, Najimi M, Renard P. *Connecting Mitochondria, Metabolism, and Stem Cell Fate.* Stem Cells Dev. 2015 Sep 1;24(17):1957-71. doi: 10.1089/scd.2015.0117.St
[94] St John JC, Ramalho-Santos J, Gray HL, Petrosko P, Rawe VY, Navara CS, Simerly CR, Schatten GP. *The expression of mitochondrial DNA transcription factors during early cardiomyocyte in vitro differentiation from human embryonic stem cells.* Cloning Stem Cells. 2005;7(3):141-53.
[95] Prigione A, Fauler B, Lurz R, Lehrach H, Adjaye J. *The senescence-related mitochondrial/oxidative stress pathway is repressed in human induced pluripotent stem cells.* Stem Cells. 2010 Apr;28(4):721-33. doi: 10.1002/stem.404
[96] Sandra Varum, Ana S. Rodrigues, Michelle B. Moura, Olga Momcilovic, Charles A. Easley IV, João Ramalho-Santos, Bennett Van Houten, and Gerald Schatten. *Energy Metabolism*

*in Human Pluripotent Stem Cells and Their Differentiated Counterparts.* PLoS One. 2011; 6(6): e20914.bdoi: 10.1371/journal.pone.0020914

[97] Andrew B. J. Prowse, Fenny Chong, David A. Elliott, Andrew G. Elefanty, Edouard G. Stanley, Peter P. Gray, Trent P. Munro, and Geoffrey W. Osborne. *Analysis of Mitochondrial Function and Localisation during Human Embryonic Stem Cell Differentiation In Vitro.* PLoS One. 2012; 7(12): e52214. doi: 10.1371/journal.pone.0052214

[98] Joshua D. Ochocki and M. Celeste Simon. *Nutrient-sensing pathways and metabolic regulation in stem cells.* J Cell Biol. 2013 Oct 14; 203(1): 23–33. doi: 10.1083/jcb.201303110

[99] Rebecca J. Burgess, Michalis Agathocleous, and Sean J. Morrison. *Metabolic regulation of stem cell function.* J Intern Med. 2014 Jul; 276(1): 12–24. doi: 10.1111/joim.12247

[100] Prasad SM, Czepiel M, Cetinkaya C, Smigielska K, Weli SC, Lysdahl H, Gabrielsen A, Petersen K, Ehlers N, Fink T, Minger SL, Zachar V. *Continuous hypoxic culturing maintains activation of Notch and allows long-term propagation of human embryonic stem cells without spontaneous differentiation.* Cell Prolif. 2009 Feb;42(1):63-74. doi: 10.1111/j.1365-2184.2008.00571.x

[101] Zhang J, Khvorostov I, Hong JS, Oktay Y, Vergnes L, Nuebel E, Wahjudi PN, Setoguchi K, Wang G, Do A, Jung HJ, McCaffery JM, Kurland IJ, Reue K, Lee WN, Koehler CM, Teitell MA. *UCP2 regulates energy metabolism and differentiation potential of human pluripotent stem cells.* EMBO J. 2011 Nov 15;30(24):4860-73. doi: 10.1038/emboj.2011.401

[102] Tugba Simsek, Fatih Kocabas, Junke Zheng, Ralph J. DeBerardinis, Ahmed I. Mahmoud, Eric N. Olson, Jay W. Schneider, Cheng Cheng Zhang, and Hesham A. Sadek. *The Distinct Metabolic Profile of Hematopoietic Stem Cells Reflects Their Location in a Hypoxic Niche*. Cell Stem Cell. 2010 Sep 3; 7(3): 380–390. doi: 10.1016/j.stem.2010.07.011

[103] Takubo K, Nagamatsu G, Kobayashi CI, Nakamura-Ishizu A, Kobayashi H, Ikeda E, Goda N, Rahimi Y, Johnson RS, Soga T, Hirao A, Suematsu M, Suda T. *Regulation of glycolysis by Pdk functions as a metabolic checkpoint for cell cycle quiescence in hematopoietic stem cells.* Cell Stem Cell. 2013 Jan 3;12(1):49-61. doi: 10.1016/j.stem.2012.10.011

[104] Clifford D. L. Folmes, Timothy J. Nelson, Almudena Martinez-Fernandez, D. Kent Arrell, Jelena Zlatkovic Lindor, Petras P. Dzeja, Yasuhiro Ikeda, Carmen Perez-Terzic, and Andre Terzic. *Somatic oxidative bioenergetics transitions into pluripotency-dependent glycolysis to facilitate nuclear reprogramming.* Cell Metab. 2011 Aug 3; 14(2): 264–271. doi: 10.1016/j.cmet.2011.06.011

[105] Sharma NS, Wallenstein EJ, Novik E, Maguire T, Schloss R, Yarmush ML. *Enrichment of hepatocyte-like cells with upregulated metabolic and differentiated function derived from embryonic stem cells using S-NitrosoAcetylPenicillamine.* Tissue Eng Part C Methods. 2009 Jun;15(2):297-306. doi: 10.1089/ten.tec.2008.0303

[106] Kanno S, Kim PK, Sallam K, Lei J, Billiar TR, Shears LL 2nd. *Nitric oxide facilitates cardiomyogenesis in mouse embryonic stem cells.* Proc Natl Acad Sci U S A. 2004 Aug 17;101(33):12277-81

[107] Huang PI, Chou YC, Chang YL, Chien Y, Chen KH, Song WS, Peng CH, Chang CH, Lee SD, Lu KH, Chen YJ, Kuo CH, Hsu CC, Lee HC, Yung MC. *Enhanced differentiation of three-gene-reprogrammed induced pluripotent stem cells into adipocytes via adenoviral-mediated PGC-1α overexpression.* Int J Mol Sci. 2011;12(11):7554-68. doi: 10.3390/ijms12117554

[108] Sudip Mandal, Anne G. Lindgren, Anand S. Srivastava, Amander T. Clark, and Utpal Banerjee. *Mitochondrial function controls proliferation and early differentiation potential of embryonic stem cells.* Stem Cells. 2011 Mar; 29(3): 486–495. doi: 10.1002/stem.590

[109] Schell JC, Wisidagama DR, Bensard C, Zhao H, Wei P, Tanner J, Flores A, Mohlman J, Sorensen LK, Earl CS, Olson KA, Miao R, Waller TC, Delker D, Kanth P, Jiang L, DeBerardinis RJ, Bronner MP, Li DY, Cox JE, Christofk HR, Lowry WE, Thummel CS, Rutter J. *Control of intestinal stem cell function and proliferation by mitochondrial pyruvate metabolism.* Nat Cell Biol. 2017 Sep;19(9):1027-1036. doi: 10.1038/ncb3593.

[110] Pereira SL, Grãos M, Rodrigues AS, Anjo SI, Carvalho RA, Oliveira PJ, Arenas E, Ramalho-Santos J. *Inhibition of mitochondrial complex III blocks neuronal differentiation and maintains embryonic stem cell pluripotency.* PLoS One. 2013 Dec 2;8(12):e82095. doi: 10.1371/journal.pone.0082095

[111] C. L. Koehler, G. A. Perkins, M. H. Ellisman, and D. L. Jones. *Pink1 and Parkin regulate Drosophila intestinal stem cell proliferation during stress and aging*. The Journal of Cell Biology. 2017. doi: 10.1083/jcb.201610036

[112] Michael Rera, Sepehr Bahadorani, Jaehyoung Cho, Christopher L. Koehler, Matthew Ulgherait, Jae H. Hur, William S. Ansari, Thomas Lo, Jr., D. Leanne Jones, David W. Walker. *Modulation of longevity and tissue homeostasis by the Drosophila PGC-1 homolog.* Cell Metab. 2011 Nov 2; 14(5): 623–634. doi: 10.1016/j.cmet.2011.09.013

[113] Singh SR, Zeng X, Zhao J, Liu Y, Hou G, Liu H, Hou SX. *The lipolysis pathway sustains normal and transformed stem cells in adult Drosophila.* Nature. 2016 Oct 6;538(7623):109-113. doi: 10.1038/nature19788.

[114] Marlen Knobloch, Gregor-Alexander Pilz, Bart Ghesquière, Werner J. Kovacs, Thomas Wegleiter, Darcie L. Moore, Martina Hruzova, Nicola Zamboni, Peter Carmeliet, and Sebastian Jessberger. *A Fatty Acid Oxidation-Dependent Metabolic Shift Regulates Adult Neural Stem Cell Activity.* Cell Rep. 2017 Aug 29; 20(9): 2144–2155. doi: 10.1016/j.celrep.2017.08.029

[115] Knobloch M. *The Role of Lipid Metabolism for Neural Stem Cell Regulation.* Brain Plast. 2017 Nov 9;3(1):61-71. doi: 10.3233/BPL-160035.

[116] Larsson NG, Wang J, Wilhelmsson H, Oldfors A, Rustin P, Lewandoski M, Barsh GS, Clayton DA. *Mitochondrial transcription factor A is necessary for mtDNA maintenance and embryogenesis in mice.* Nat Genet. 1998 Mar;18(3):231-6

[117] Robert B. Hamanaka, Andrea Glasauer, Paul Hoover, Shuangni Yang, Hanz Blatt, Andrew R. Mullen, Spiro Getsios, Cara J. Gottardi, Ralph J. DeBerardinis, Robert M. Lavker, and Navdeep S. Chandel. *Mitochondrial Reactive Oxygen Species Promote Epidermal Differentiation and Hair Follicle Development.* Sci Signal. 2013 Feb 5; 6(261): ra8. doi: 10.1126/scisignal.2003638

[118] Mandal S, Guptan P, Owusu-Ansah E, Banerjee U. *Mitochondrial regulation of cell cycle progression during development as revealed by the tenured mutation in Drosophila.* Dev Cell. 2005 Dec;9(6):843-54

[119] Mandal S, Freije WA, Guptan P, Banerjee U. *Metabolic control of G1-S transition: cyclin E degradation by p53-induced activation of the ubiquitin-proteasome system.* J Cell Biol. 2010 Feb 22;188(4):473-9. doi: 10.1083/jcb.200912024.

[120] DiGregorio PJ, Ubersax JA, O'Farrell PH. *Hypoxia and nitric oxide induce a rapid, reversible cell cycle arrest of the Drosophila syncytial divisions.* J Biol Chem. 2001 Jan 19;276(3):1930-7

[121] Copeland JM, Cho J, Lo T Jr, Hur JH, Bahadorani S, Arabyan T, Rabie J, Soh J, Walker DW. *Extension of Drosophila life span by RNAi of the mitochondrial respiratory chain. Curr Biol. 2009 Oct 13;19(19):1591-8. doi: 10.1016/j.cub.2009.08.016.*
[122] Marianes A, Spradling AC. *Physiological and stem cell compartmentalization within the Drosophila midgut.* Elife. 2013 Aug 27;2:e00886. doi: 10.7554/eLife.00886.
[123] Brand AH, Perrimon N. *Targeted gene expression as a means of altering cell fates and generating dominant phenotypes.* Development. 1993 Jun;118(2):401-15.
[124] Gregg Roman, Keita Endo, Lin Zong, and Ronald L. Davis. *P{Switch}, a system for spatial and temporal control of gene expression in Drosophila melanogaster.* PNAS October 23, 2001. 98 (22) 12602-12607; https://doi.org/10.1073/pnas.221303998
[125] McGuire SE, Le PT, Osborn AJ, Matsumoto K, Davis RL. *Spatiotemporal rescue of memory dysfunction in Drosophila.* Science. 2003 Dec 5;302(5651):1765-8.
[126] Louise Nicholson, Gunisha K. Singh, Thomas Osterwalder, Gregg W. Roman, Ronald L. Davis, and Haig Keshishian. *Spatial and Temporal Control of Gene Expression in Drosophila Using the Inducible GeneSwitch GAL4 System. I. Screen for Larval Nervous System Drivers.* Genetics. 2008 Jan; 178(1): 215–234. doi: 10.1534/genetics.107.081968
[127] Divya Mathur, Alyssa Bost, Ian Driver, and Benjamin Ohlstein. *A Transient Niche Regulates the Specification of Drosophila Intestinal Stem Cells.* Science. 2010 Jan 8; 327(5962): 210–213. doi: 10.1126/science.1181958
[128] Thomas Osterwalder, Kenneth S. Yoon, Benjamin H. White, and Haig Keshishian. *A conditional tissue-specific transgene expression system using inducible GAL4.* Proc Natl Acad Sci U S A. 2001 Oct 23; 98(22): 12596–12601. doi: 10.1073/pnas.221303298
[129] Wang L, Zeng X, Ryoo HD, Jasper H. *Integration of UPRER and oxidative stress signaling in the control of intestinal stem cell proliferation.* PLoS Genet. 2014 Aug 28;10(8):e1004568. doi: 10.1371/journal.pgen
[130] Lee T, Luo L. *Mosaic analysis with a repressible cell marker for studies of gene function in neuronal morphogenesis.* Neuron. 1999 Mar;22(3):451-61.
[131] Jerome Korzelius, Svenja K Naumann, Mariano A Loza-Coll, Jessica SK Chan, Devanjali Dutta, Jessica Oberheim, Christine Gläßer, Tony D Southall, Andrea H Brand, D Leanne Jones, and Bruce A Edgar. *Escargot maintains stemness and suppresses differentiation in Drosophila intestinal stem cells.* EMBO J. 2014 Dec 17; 33(24): 2967–2982. Published online 2014 Oct 8. doi: 10.15252/embj.201489072
[132] Vienna Drosophila Resource Center (VDRC) [cited 2017 Sep 25]. Available from: http://stockcenter.vdrc.at/control/targets/~productId=101739/~targetType=OFF
[133] NIG-Fly Stock Center. Japanese National Institute of Genetics. [cited 2017 Sep 25]. Available from: https://shigen.nig.ac.jp/fly/nigfly/
[134] Green EW, Fedele G, Giorgini F, Kyriacou CP. *A Drosophila RNAi collection is subject to dominant phenotypic effects.* Nat Methods. 2014 Mar;11(3):222-3. doi: 10.1038/nmeth.2856.
[135] Craig A. Micchelli. *Whole-mount immunostaining of the adult Drosophila gastrointestinal tract.* Methods. 2014 Jun 15; 68(1): 273–279. doi: 10.1016/j.ymeth.2014.03.022
[136] Hanson GT, Aggeler R, Oglesbee D, Cannon M, Capaldi RA, Tsien RY, Remington SJ. *Investigating mitochondrial redox potential with redox-sensitive green fluorescent protein indicators. J Biol Chem. 2004 Mar 26;279(13):13044-53.*
[137] Schindelin, J.; Arganda-Carreras, I. & Frise, E. et al. (2012), *Fiji: an open-source platform for biological-image analysis*, Nature methods 9(7): 676-682, PMID 22743772

[138] Jones TR, Kang IH, Wheeler DB, Lindquist RA, Papallo A, Sabatini DM, Golland P, Carpenter AE (2008) *CellProfiler Analyst: data exploration and analysis software for complex image-based screens.* BMC Bioinformatics 9(1):482/doi: 10.1186/1471-2105-9-482. PMID: 19014601 PMCID: PMC2614436

[139] Gavrieli, Y., Y. Sherman, and S.A. Ben-Sasson. Identification of programmed cell death in situ via specific labeling of nuclear DNA fragmentation. J. Cell Biol. 1992. 119: 493-501.

[140] Deepika Vasudevan and Hyung Don Ryoo. *Detection of Cell Death in Drosophila Tissues.* Methods Mol Biol. *2016; 1419: 131–144. doi: 10.1007/978-1-4939-3581-9_11*

[141] Grob, Robert L., Barry, Eugene F. *Modern Practice of Gas Chromatography (4th Ed.)* 2004. John Wiley & Sons. ISBN 0-471-22983-0

[142] Francis Orata. *Advanced Gas Chromatography - Progress in Agricultural, Biomedical and Industrial Applications.* Chapter 5: *Derivatization Reactions and Reagents for Gas Chromatography Analysis.* 2012. ISBN 978-953-51-0298-4

[143] NIST Chemistry WebBook, NIST Standard Reference Database Number 69, Eds. National Institute of Standards and Technology, Gaithersburg MD, 20899, doi:10.18434/T4D303, (Mass spectrum retrieved Dec 4, 2017 from https://webbook.nist.gov/cgi/inchi?ID=C40309577&Mask=200#Mass-Spec)

[144] Bricker DK, Taylor EB, Schell JC, Orsak T, Boutron A, Chen YC, Cox JE, Cardon CM, Van Vranken JG, Dephoure N, Redin C, Boudina S, Gygi SP, Brivet M, Thummel CS, Rutter J. *A mitochondrial pyruvate carrier required for pyruvate uptake in yeast, Drosophila, and humans.* Science. 2012 Jul 6;337(6090):96-100. doi: 10.1126/science.1218099

[145] Tennessen JM, Bertagnolli NM, Evans J, Sieber MH, Cox J, Thummel CS. *Coordinated metabolic transitions during Drosophila embryogenesis and the onset of aerobic glycolysis.* G3 (Bethesda). 2014 Mar 12;4(5):839-50. doi: 10.1534/g3.114.010652

[146] Gramates LS, Marygold SJ, dos Santos G, Urbano J-M, Antonazzo G, Matthews BB, Rey AJ, Tabone CJ, Crosby MA, Emmert DB, Falls K, Goodman JL, Hu Y, Ponting L, Schroeder AJ, Strelets VB, Thurmond J, Zhou P and the FlyBase Consortium. (2017) *FlyBase at 25: looking to the future*. Nucleic Acids Res. 45(D1):D663-D671 www.flybase.org

[147] Benoît Biteau, Jason Karpac, Stephen Supoyo, Matthew DeGennaro, Ruth Lehmann, and Heinrich Jasper. *Lifespan Extension by Preserving Proliferative Homeostasis in Drosophila.* PLoS Genet. 2010 Oct; 6(10): e1001159. Published online 2010 Oct 14. doi: 10.1371/journal.pgen.1001159

[148] Resende LP, Truong ME, Gomez A, Jones DL. *Intestinal stem cell ablation reveals differential requirements for survival in response to chemical challenge.* Dev Biol. 2017 Apr 1;424(1):10-17. doi: 10.1016/j.ydbio.2017.01.004.

[149] Amcheslavsky A, Song W, Li Q, Nie Y, Bragatto I, Ferrandon D, Perrimon N, Ip YT. *Enteroendocrine cells support intestinal stem-cell-mediated homeostasis in Drosophila.* Cell Rep. 2014 Oct 9;9(1):32-39. doi: 10.1016/j.celrep.2014.08.052

[150] Zhang J, Guan Z, Murphy AN, Wiley SE, Perkins GA, Worby CA, Engel JL, Heacock P, Nguyen OK, Wang JH, Raetz CR, Dowhan W, Dixon JE. *Mitochondrial phosphatase PTPMT1 is essential for cardiolipin biosynthesis.* Cell Metab. 2011 Jun 8;13(6):690-700. doi: 10.1016

[151] Nath AK, Ryu JH, Jin YN, Roberts LD, Dejam A, Gerszten RE, Peterson RT. *PTPMT1 Inhibition Lowers Glucose through Succinate Dehydrogenase Phosphorylation.* Cell Rep. 2015 Feb 4. pii: S2211-1247(15)00023-6. doi: 10.1016/j.celrep.2015.01.010.

[152] Bourgeron T, Rustin P, Chretien D, Birch-Machin M, Bourgeois M, Viegas-Péquignot E, Munnich A, Rötig A. *Mutation of a nuclear succinate dehydrogenase gene results in mitochondrial respiratory chain deficiency.* Nat Genet. 1995 Oct;11(2):144-9.

[153] Gimenez-Roqueplo AP, Favier J, Rustin P, Mourad JJ, Plouin PF, Corvol P, Rötig A, Jeunemaitre X. The R22X mutation of the SDHD gene in hereditary paraganglioma abolishes the enzymatic activity of complex II in the mitochondrial respiratory chain and activates the hypoxia pathway. Am J Hum Genet. 2001 Dec;69(6):1186-97

[154] Zongzhao Zhai, Shu Kondo, Nati Ha, Jean-Philippe Boquete, Michael Brunner, Ryu Ueda & Bruno Lemaitre. *Accumulation of differentiating intestinal stem cell progenies drives tumorigenesis.* Nature Communications volume 6, Article number: 10219 (2015)

[155] Anna Sawicka and Christian Seiser. *Histone H3 phosphorylation – A versatile chromatin modification for different occasions.* Biochimie. 2012 Nov; 94(11): 2193–2201. doi: 10.1016/j.biochi.2012.04.018

[156] Mojca Adlesic, Christian Frei, and Ian J. Frew. *Cdk4 functions in multiple cell types to control Drosophila intestinal stem cell proliferation and differentiation.* Biol Open. 2016 Mar 15; 5(3): 237–251. doi: 10.1242/bio.016584

[157] Jakob W von Trotha, Boris Egger, and Andrea H Brand. *Cell proliferation in the Drosophila adult brain revealed by clonal analysis and bromodeoxyuridine labelling.* Neural Dev. 2009; 4: 9. doi: 10.1186/1749-8104-4-9

[158] Zielke N, Korzelius J, van Straaten M, Bender K, Schuhknecht GF, Dutta D, Xiang J, Edgar BA. Fly-FUCCI: A versatile tool for studying cell proliferation in complex tissues. Cell Rep. 2014 Apr 24;7(2):588-98. doi: 10.1016/j.celrep.2014.03.020

[159] Swanson CI, Meserve JH, McCarter PC, Thieme A, Mathew T, Elston TC, Duronio RJ. *Expression of an S phase-stabilized version of the CDK inhibitor Dacapo can alter endoreplication.* Development. 2015 Dec 15;142(24):4288-98. doi: 10.1242/dev.115006

[160] Mike Boxem. *Cyclin-dependent kinases in C. elegans.* Cell Div. 2006; 1: 6. doi: 10.1186/1747-1028-1-6

[161] L F Barros, T Kanaseki, R Sabirov, S Morishima, J Castro, C X Bittner, E Maeno, Y Ando-Akatsuka & Y Okada. Apoptotic and necrotic blebs in epithelial cells display similar neck diameters but different kinase dependency. Cell Death and Differentiation (2003) 10, 687–697 (2003) doi:10.1038/sj.cdd.4401236

[162] Bovellan M, Fritzsche M, Stevens C, Charras G. *Death-associated protein kinase (DAPK) and signal transduction: blebbing in programmed cell death.* FEBS J. 2010 Jan;277(1):58-65. doi: 10.1111/j.1742-4658.2009.07412.x

[163] Meifang Ma, Hang Zhao, Hanfei Zhao, Richard Binari, Norbert Perrimon, and Zhouhua Li. *Wildtype adult stem cells, unlike tumor cells, are resistant to cellular damages in Drosophila.* Dev Biol. 2016 Mar 15; 411(2): 207–216. doi: 10.1016/j.ydbio.2016.01.040

[164] Vermeulen K, Van Bockstaele DR, Berneman ZN. *Apoptosis: mechanisms and relevance in cancer.* Ann Hematol. 2005 Oct;84(10):627-39

[165] Elmore S. *Apoptosis: a review of programmed cell death.* Toxicol Pathol. 2007 Jun;35(4):495-516.

[166] Guido Kroemer and Beth Levine. *Autophagic cell death: the story of a misnomer.* Nat Rev Mol Cell Biol. 2008 Dec; 9(12): 1004–1010. doi: 10.1038/nrm2527

[167] Kroemer G, Galluzzi L, Brenner C. *Mitochondrial membrane permeabilization in cell death.* Physiol Rev. 2007 Jan;87(1):99-163. http://sci-hub.tw/10.1152/physrev.00013.2006

[168] Mayur V Jain, Anna M Paczulla, Thomas Klonisch, Florence N Dimgba, Sahana B Rao, Karin Roberg, Frank Schweizer, Claudia Lengerke, Padideh Davoodpour, Vivek R Palicharla, Subbareddy Maddika, and Marek Łos. *Interconnections between apoptotic, autophagic and necrotic pathways: implications for cancer therapy development*. J Cell Mol Med. 2013 Jan; 17(1): 12–29. Published online 2013 Jan 10. doi: 10.1111/jcmm.12001

[169] David Gewirtz, Shawn E. Holt, Steven Grant. *Apoptosis, Senescence and Cancer.* Chapter 4. 2nd Edition. Humana Press. 2007. ISBN 978-1-59745-221-2. doi: 10.1007/978-1-59745-221-2

[170] Tait SW, Green DR. *Caspase-independent cell death: leaving the set without the final cut.* Oncogene. 2008 Oct 27;27(50):6452-61. doi: 10.1038/onc.2008.311

[171] Pierre-Luc Bardet, Golnar Kolahgar, Anita Mynett, Irene Miguel-Aliaga, James Briscoe, Pascal Meier, and Jean-Paul Vincent. *A fluorescent reporter of caspase activity for live imaging.* Proc Natl Acad Sci U S A. 2008 Sep 16; 105(37): 13901–13905. doi: 10.1073/pnas.0806983105

[172] Shaw, RL. *Regulation of Drosophila intestinal regeneration by the Hippo pathway.* Doctoral Thesis. 2012, University College London and Cancer Research UK London Research Institute, UK. Available online as of Sep 2017 at http://discovery.ucl.ac.uk/1366711/1/RShaw_thesis_041012_small.pdf

[173] Péter Nagy, Gyöngyvér O. Sándor & Gábor Juhász. *Autophagy maintains stem cells and intestinal homeostasis in Drosophila.* Nature Scientific Reports. 2018. Volume 8, Article number: 4644

[174] Fumiaki Obata, Shiho Tanaka, Soshiro Kashio, Hidenobu Tsujimura, Ryoichi Sato, and Masayuki Miura. *Induction of rapid and selective cell necrosis in Drosophila using Bacillus thuringiensis Cry toxin and its silkworm receptor.* BMC Biol. 2015; 13: 48. doi: 10.1186/s12915-015-0160-2

[175] Kepp O, Galluzzi L, Lipinski M, Yuan J, Kroemer G. *Cell death assays for drug discovery.* Nat Rev Drug Discov. 2011 Mar;10(3):221-37. doi: 10.1038/nrd3373.

[176] Altman BJ, Rathmell JC. *Metabolic stress in autophagy and cell death pathways.* Cold Spring Harb Perspect Biol. 2012 Sep 1;4(9):a008763. doi: 10.1101/cshperspect.a008763

[177] Douglas R. Green, Lorenzo Galluzzi, and Guido Kroemer. *Metabolic control of cell death. Science.* 2014 Sep 19; 345(6203): 1250256. doi: 10.1126/science.1250256

[178] Daniel J. Lips Leon J. deWindt Dave J.W. van Kraaij Pieter A. Doevendans. *Molecular determinants of myocardial hypertrophy and failure: alternative pathways for beneficial and maladaptive hypertrophy.* European Heart Journal, Volume 24, Issue 10, 1 May 2003, Pages 883–896, https://doi.org/10.1016/S0195-668X(02)00829-1

[179] Russell B, Motlagh D, Ashley WW. *Form follows function: how muscle shape is regulated by work.* J Appl Physiol (1985). 2000 Mar;88(3):1127-32.

[180] Deng, W. M., Althauser, C. & Ruohola-Baker, H. *Notch–Delta signaling induces a transition from mitotic cell cycle to endocycle in Drosophila follicle cells*. *Development* 128, 4737–4746 (2001)

[181] Demontis, F. & Perrimon, N. Integration of Insulin receptor/Foxo signaling and dMyc activity during muscle growth regulates body size in Drosophila. Development 136, 983–993 (2009).

[182] Yoichiro Tamori and Wu-Min Deng. *Compensatory Cellular Hypertrophy: The Other Strategy for Tissue Homeostasis.* Trends Cell Biol. 2014 Apr; 24(4): 230–237

[183] Vicki P. Losick, Donald T. Fox, and Allan C. Spradling. *Polyploidization and cell fusion contribute to wound healing in the adult Drosophila epithelium*. Curr Biol. 2013 Nov 18; 23(22): 2224–2232. doi: 10.1016/j.cub.2013.09.029

[184] Amcheslavsky A, Ito N, Jiang J, Ip YT. *Tuberous sclerosis complex and Myc coordinate the growth and division of Drosophila intestinal stem cells.* J Cell Biol. 2011 May 16;193(4):695-710. doi: 10.1083/jcb.201103018

[185] Xiankun Zeng, Lili Han, Shree Ram Singh, Hanhan Liu, Ralph A. Neumüller, Dong Yan, Yanhui Hu, Ying Liu, Wei Liu, Xinhua Lin, and Steven X. Hou. *Genome-wide RNAi Screen Identifies Networks Involved in Intestinal Stem Cell Regulation in Drosophila.* Cell Rep. 2015 Feb 24; 10(7): 1226–1238. doi: 10.1016/j.celrep.2015.01.051

[186] Zakir Ullah, Chrissie Y Lee, and Melvin L DePamphilis. *Cip/Kip cyclin-dependent protein kinase inhibitors and the road to polyploidy.* Cell Div. 2009; 4: 10. doi: 10.1186/1747-1028-4-10

[187] Trakala M, Rodríguez-Acebes S, Maroto M, Symonds CE, Santamaría D, Ortega S, Barbacid M, Méndez J, Malumbres M. *Functional reprogramming of polyploidization in megakaryocytes.* Dev Cell. 2015 Jan 26;32(2):155-67. doi: 10.1016/j.devcel.2014.12.015.

[188] Janel E. Le Belle, Nicolas M. Orozco, Andres A. Paucar, Jonathan P. Saxe, Jack Mottahedeh, April D. Pyle, Hong Wu, and Harley I. Kornblum. *Proliferative Neural Stem Cells Have High Endogenous ROS Levels that Regulate Self-Renewal and Neurogenesis in a PI3K/Akt-Dependant Manner.* Cell Stem Cell. 2011 Jan 7; 8(1): 59–71. doi: 10.1016/j.stem.2010.11.028

[189] Marisa M. Juntilla, Vineet D. Patil, Marco Calamito, Rohan P. Joshi, Morris J. Birnbaum, and Gary A. Koretzky. *AKT1 and AKT2 maintain hematopoietic stem cell function by regulating reactive oxygen species.* Blood. 2010 May 20; 115(20): 4030–4038. doi: 10.1182/blood-2009-09-241000

[190] Qun Chen, Edwin J. Vazquez, Shadi Moghaddas, Charles L. Hoppe, and Edward J. Lesnefsky. *Production of Reactive Oxygen Species by Mitochondria.* The Journal of Biological Chemistry, 2003, 278, 36027-36031., doi: 10.1074/jbc.M304854200

[191] Walker DW, Hájek P, Muffat J, Knoepfle D, Cornelison S, Attardi G, Benzer S. *Hypersensitivity to oxygen and shortened lifespan in a Drosophila mitochondrial complex II mutant.* Proc Natl Acad Sci U S A. 2006 Oct 31;103(44):16382-7

[192] Roberta Filograna, Vinay K. Godena, Alvaro Sanchez-Martinez, Emanuele Ferrari, Luigi Casella, Mariano Beltramini, Luigi Bubacco, Alexander J. Whitworth, and Marco Bisaglia. *Superoxide Dismutase (SOD)-mimetic M40403 Is Protective in Cell and Fly Models of Paraquat Toxicity.* J Biol Chem. 2016 Apr 22; 291(17): 9257–9267. doi: 10.1074/jbc.M115.708057

[193] Kirby K, Hu J, Hilliker AJ, Phillips JP. *RNA interference-mediated silencing of Sod2 in Drosophila leads to early adult-onset mortality and elevated endogenous oxidative stress.* Proc Natl Acad Sci USA. 2002 Dec 10;99(25):16162-7.

[194] Hochmuth CE, Biteau B, Bohmann D, Jasper H. *Redox regulation by Keap1 and Nrf2 controls intestinal stem cell proliferation in Drosophila.* Cell Stem Cell. 2011 Feb 4;8(2):188-99. doi: 10.1016/j.stem.2010.12.006.

[195] Hussain A, Pooryasin A, Zhang M, Loschek LF, La Fortezza M, Friedrich AB, Blais CM, Üçpunar HK, Yépez VA, Lehmann M, Gompel N, Gagneur J, Sigrist SJ, Grunwald Kadow IC. *Inhibition of oxidative stress in cholinergic projection neurons fully rescues aging-associated olfactory circuit degeneration in Drosophila.* Elife. 2018 Jan 18;7. pii: e32018. doi: 10.7554/eLife.32018.

[196] H L Lanz, R M E Zimmerman, J Brouwer, M H M Noteborn, and C Backendorf. *Mitotic catastrophe triggered in human cancer cells by the viral protein apoptin.* Cell Death Dis. 2013 Feb; 4(2): e487. doi: 10.1038/cddis.2013.2

[197] Gonçalves AP, Máximo V, Lima J, Singh KK, Soares P, Videira A. *Involvement of p53 in cell death following cell cycle arrest and mitotic catastrophe induced by rotenone.* Biochim Biophys Acta. 2011 Mar;1813(3):492-9. doi: 10.1016/j.bbamcr.2011.01.006

[198] Vakifahmetoglu H, Olsson M, Zhivotovsky B. *Death through a tragedy: mitotic catastrophe.* Cell Death Differ. 2008 Jul;15(7):1153-62. doi: 10.1038/cdd.2008.47

[199] Vitale I, Galluzzi L, Castedo M, Kroemer G. *Mitotic catastrophe: a mechanism for avoiding genomic instability.* Nat Rev Mol Cell Biol. 2011 Jun;12(6):385-92. doi: 10.1038/nrm3115

[200] Takao Ito and Tatsushi Igaki. *Dissecting cellular senescence and SASP in Drosophila.* Inflamm Regen. 2016; 36: 25. doi: 10.1186/s41232-016-0031-4

[201] Selak MA, Armour SM, MacKenzie ED, Boulahbel H, Watson DG, Mansfield KD, Pan Y, Simon MC, Thompson CB, Gottlieb E. *Succinate links TCA cycle dysfunction to oncogenesis by inhibiting HIF-alpha prolyl hydroxylase.* Cancer Cell. 2005 Jan;7(1):77-85.

[202] Judith A. Hobert, Jessica L. Mester, Jessica Moline, Charis Eng, *Elevated plasma succinate in PTEN, SDHB, and SDHD mutation–positive individuals*. Genetics in Medicine (2012) 14, 616–619 doi:10.1038/gim.2011.63

[203] Mengtao Xiao, Hui Yang, Wei Xu, Shenghong Ma, Huaipeng Lin, Honguang Zhu, Lixia Liu, Ying Liu, Chen Yang, Yanhui Xu, Shimin Zhao, Dan Ye, Yue Xiong, and Kun-Liang Guan. *Inhibition of α-KG-dependent histone and DNA demethylases by fumarate and succinate that are accumulated in mutations of FH and SDH tumor suppressors.* Genes Dev. 2012 Jun 15; 26(12): 1326–1338. doi: 10.1101/gad.191056.112

[204] He W, Miao FJ, Lin DC, Schwandner RT, Wang Z, Gao J, Chen JL, Tian H, Ling L. *Citric acid cycle intermediates as ligands for orphan G-protein-coupled receptors.* Nature. 2004 May 13;429(6988):188-93.

[205] Mossa AH, Velasquez Flores M, Cammisotto PG, Campeau L. *Succinate, increased in metabolic syndrome, activates GPR91 receptor signaling in urothelial cells.* Cell Signal. 2017 Sep;37:31-39. doi: 10.1016/j.cellsig.2017.05.014

[206] Yoshihito Sakata, Brian D. Hoit, Stephen B. Liggett, Richard A. Walsh, Gerald W. Dorn. *Decompensation of Pressure-Overload Hypertrophy in Gαq-Overexpressing Mice.* Circulation. 1998;97:1488-1495 https://doi.org/10.1161/01.CIR.97.15.1488

[207] U. Mende, A. Kagen, A. Cohen, J. Aramburu, F. J. Schoen, and E. J. Neer. *Transient cardiac expression of constitutively active Gαq leads to hypertrophy and dilated cardiomyopathy by calcineurin-dependent and independent pathways.* Proc Natl Acad Sci U S A. 1998 Nov 10; 95(23): 13893–13898.

[208] Adams JW, Pagel AL, Means CK, Oksenberg D, Armstrong RC, Brown JH. *Cardiomyocyte apoptosis induced by Galphaq signaling is mediated by permeability transition pore formation and activation of the mitochondrial death pathway.* Circ Res. 2000 Dec 8;87(12):1180-7.

[209] Yussman MG, Toyokawa T, Odley A, Lynch RA, Wu G, Colbert MC, Aronow BJ, Lorenz JN, Dorn GW 2nd. *Mitochondrial death protein Nix is induced in cardiac hypertrophy and triggers apoptotic cardiomyopathy.* Nat Med. 2002 Jul;8(7):725-30

[210] Vanessa P.M van Empel and Leon J De Windt. *Myocyte hypertrophy and apoptosis: a balancing act.* Cardiovascular Research, Volume 63, Issue 3, 15 August 2004, Pages 487–499.

[211] Mizuarai S, Miki S, Araki H, Takahashi K, Kotani H. *Identification of dicarboxylate carrier Slc25a10 as malate transporter in de novo fatty acid synthesis. J Biol Chem. 2005 Sep 16;280(37):32434-41.*

[212] Iacopetta D, Madeo M, Tasco G, Carrisi C, Curcio R, Martello E, Casadio R, Capobianco L, Dolce. *A novel subfamily of mitochondrial dicarboxylate carriers from Drosophila melanogaster: biochemical and computational studies.* Biochim Biophys Acta. 2011 Mar;1807(3):251-61. doi: 10.1016/j.bbabio.2010.11.013.

[213] Hodge T, Colombini M. *Regulation of metabolite flux through voltage-gating of VDAC channels.* J Membr Biol. 1997 Jun 1;157(3):271-9.

[214] Aiello R, Messina A, Schiffler B, Benz R, Tasco G, Casadio R, De Pinto V. *Functional characterization of a second porin isoform in Drosophila melanogaster.* DmPorin2 forms voltage-independent cation-selective pores. J Biol Chem. 2004 Jun 11;279(24):25364-73. Epub 2004 Mar 30.

[215] Inoue K, Zhuang L, Maddox DM, Smith SB, Ganapathy V. *Structure, function, and expression pattern of a novel sodium-coupled citrate transporter (NaCT) cloned from mammalian brain.* J Biol Chem. 2002 Oct 18;277(42):39469-76.

[216] Knauf F, Rogina B, Jiang Z, Aronson PS, Helfand SL. *Functional characterization and immunolocalization of the transporter encoded by the life-extending gene Indy.* Proc Natl Acad Sci U S A. 2002 Oct 29;99(22):14315-9.

[217] Inoue K, Fei YJ, Huang W, Zhuang L, Chen Z, Ganapathy V. *Functional identity of Drosophila melanogaster Indy as a cation-independent, electroneutral transporter for tricarboxylic acid-cycle intermediates.* Biochem J. 2002 Oct 15;367(Pt 2):313-9.

[218] Felix Knauf, Blanka Rogina, Zhirong Jiang, Peter S. Aronson, and Stephen L. Helfand. *Functional characterization and immunolocalization of the transporter encoded by the life-extending gene Indy.* Proc Natl Acad Sci U S A. 2002 Oct 29; 99(22): 14315–14319.

[219] de Castro Fonseca M, Aguiar CJ, da Rocha Franco JA, Gingold RN, Leite MF. *GPR91: expanding the frontiers of Krebs cycle intermediates.* Cell Commun Signal. 2016 Jan 12;14:3. doi: 10.1186/s12964-016-0126-1.

[220] Neves SR, Ram PT, Iyengar R. *G protein pathways. Science. 2002 May 31;296(5573):1636-9.*

[221] Ariza AC, Deen PM, Robben JH. *The succinate receptor as a novel therapeutic target for oxidative and metabolic stress-related conditions.* Front Endocrinol (Lausanne). 2012 Feb 16;3:22. doi: 10.3389/fendo.2012.00022. eCollection 2012.

[222] Bhuniya D, Umrani D, Dave B, Salunke D, Kukreja G, Gundu J, Naykodi M, Shaikh NS, Shitole P, Kurhade S, De S, Majumdar S, Reddy SB, Tambe S, Shejul Y, Chugh A, Palle VP, Mookhtiar KA, Cully D, Vacca J, Chakravarty PK, Nargund RP, Wright SD, Graziano MP, Singh SB, Roy S, Cai TQ. *Discovery of a potent and selective small molecule hGPR91 antagonist.* Bioorg Med Chem Lett. 2011 Jun 15;21(12):3596-602. doi: 10.1016/j.bmcl.2011.04.091. Epub 2011 Apr 28.

[223] Weiwei Lei, Wenwen Ren, Makoto Ohmoto, Joseph F. Urban Jr., Ichiro Matsumoto, Robert F. Margolskee, and Peihua Jiang. *Activation of intestinal tuft cell-expressed Sucnr1 triggers type 2 immunity in the mouse small intestine.* PNAS May 7, 2018. 201720758; https://doi.org/10.1073/pnas.1720758115

[224] Sundström L, Greasley PJ, Engberg S, Wallander M, Ryberg E. *Succinate receptor GPR91, a Gα(i) coupled receptor that increases intracellular calcium concentrations through PLCβ.* FEBS Lett. 2013 Aug 2;587(15):2399-404. doi: 10.1016/j.febslet.2013.05.067.

[225] John W. Adams, Yoshihito Sakata, Michael G. Davis, Valerie P. Sah, Yibin Wang, Stephen B. Liggett, Kenneth R. Chien, Joan Heller Brown, and Gerald W. Dorn. *Enhanced Gαq signaling: A common pathway mediates cardiac hypertrophy and apoptotic heart failure*. Proc Natl Acad Sci U S A. 1998 Aug 18; 95(17): 10140–10145.

[226] Lei Yang, Di Yu, Huan-Huan Fan, Yu Feng, Liang Hu, Wei-Yan Zhang, Kai Zhou, Xu-Ming Mo, *Triggering the succinate receptor GPR91 enhances pressure overload-induced right ventricular hypertrophy*. Int J Clin Exp Pathol. 2014; 7(9): 5415–5428.

[227] Carla J Aguiar, João A Rocha-Franco, Pedro A Sousa, Anderson K Santos, Marina Ladeira, Cibele Rocha-Resende, Luiz O Ladeira, Rodrigo R Resende, Fernando A Botoni, Marcos Barrouin Melo, Cristiano X Lima, José M Carballido, Thiago M Cunha, Gustavo B Menezes, Silvia Guatimosim, M Fatima Leite. *Succinate causes pathological cardiomyocyte hypertrophy through GPR91 activation.* Cell Communication and Signaling 2014 12:78 DOI: 10.1186/s12964-014-0078-2

[228] Hu J, Wu Q, Li T, Chen Y, Wang S. *Inhibition of high glucose-induced VEGF release in retinal ganglion cells by RNA interference targeting G protein-coupled receptor 91.* Exp Eye Res. 2013 Apr;109:31-9. doi: 10.1016/j.exer.2013.01.011

[229] Laukka T, Mariani CJ, Ihantola T, Cao JZ, Hokkanen J, Kaelin WG Jr, Godley LA, Koivunen P. *Fumarate and Succinate Regulate Expression of Hypoxia-inducible Genes via TET Enzymes.* J Biol Chem. 2016 Feb 19;291(8):4256-65. doi: 10.1074/jbc.M115.688762

[230] Tretter L, Patocs A, Chinopoulos C. *Succinate, an intermediate in metabolism, signal transduction, ROS, hypoxia, and tumorigenesis.* Biochim Biophys Acta. 2016 Aug;1857(8):1086-1101. doi: 10.1016/j.bbabio.2016.03.012

[231] Koivunen P, Hirsilä M, Remes AM, Hassinen IE, Kivirikko KI, Myllyharju J. *Inhibition of hypoxia-inducible factor (HIF) hydroxylases by citric acid cycle intermediates: possible links between cell metabolism and stabilization of HIF*. J Biol Chem. 2007 Feb 16;282(7):4524-32

[232] Gene [Internet]. Bethesda (MD): National Library of Medicine (US), National Center for Biotechnology Information; 2004 – [cited 2018 Apr 20]. Available from: https://www.ncbi.nlm.nih.gov/gene/

[233] BLAST [Internet]. Bethesda (MD): National Library of Medicine (US), National Center for Biotechnology Information; 2004 – [cited 2017 Sep 25]. Available from: https://blast.ncbi.nlm.nih.gov/

[234] Shinya Nishi, Sheau Yu Hsu, Karen Zell, Aaron J. W. Hsueh. *Characterization of Two Fly LGR (Leucine-Rich Repeat-Containing, G Protein-Coupled Receptor) Proteins Homologous to Vertebrate Glycoprotein Hormone Receptors: Constitutive Activation of Wild-Type Fly LGR1 But Not LGR2 in Transfected Mammalian Cells.* Endocrinology, Volume 141, Issue 11, 1 November 2000, Pages 4081–4090, https://doi.org/10.1210/endo.141.11.7744

[235] Scopelliti A, Cordero JB, Diao F, Strathdee K, White BH, Sansom OJ, Vidal M. *Local control of intestinal stem cell homeostasis by enteroendocrine cells in the adult Drosophila midgut.* Curr Biol. 2014 Jun 2;24(11):1199-211. doi: 10.1016/j.cub.2014.04.007

[236] Thomas Brody and Anibal Cravchikb. *Drosophila melanogaster G Protein–Coupled Receptors.* J Cell Biol. 2000 Jul 24; 150(2): 83–88.

[237] O'Neil, M.J. (ed.). The Merck Index - An Encyclopedia of Chemicals, Drugs, and Biologicals. 13th Edition, Whitehouse Station, NJ: Merck and Co., Inc., 2001., p. 1580

[238] Judy Martin, Erin Nicole Sanders, Paola Moreno-Roman, Shruthi Balachandra, XinXin Du, Leslie Ann Jaramillo Koyama, Lucy Erin O'Brien. *Long-term live imaging of the*

*Drosophila adult midgut reveals real-time dynamics of cell division, differentiation, and loss* (Preprint). BioRxiv. February 26, 2018. doi: https://doi.org/10.1101/271742

[239] Alston CL, Ceccatelli Berti C, Blakely EL, Oláhová M, He L, McMahon CJ, Olpin SE, Hargreaves IP, Nolli C, McFarland R, Goffrini P, O'Sullivan MJ, Taylor RW. *A recessive homozygous p.Asp92Gly SDHD mutation causes prenatal cardiomyopathy and a severe mitochondrial complex II deficiency.* Hum Genet. 2015 Aug;134(8):869-79. doi: 10.1007/s00439-015-1568-z.

[240] Angelini C, Melacini P, Valente ML, Reichmann H, Carrozzo R, Fanin M, Vergani L, Boffa GM, Martinuzzi A, Fasoli G. *Hypertrophic cardiomyopathy with mitochondrial myopathy. A new phenotype of complex II defect.* Jpn Heart J. 1993 Jan;34(1):63-77.

[241] Hughes SE. *The pathology of hypertrophic cardiomyopathy.* Histopathology. 2004 May;44(5):412-27.

[242] Kavantzas NG, Lazaris AC, Agapitos EV, Nanas J, Davaris PS. *Histological assessment of apoptotic cell death in cardiomyopathies.* Pathology. 2000 Aug;32(3):176-80.